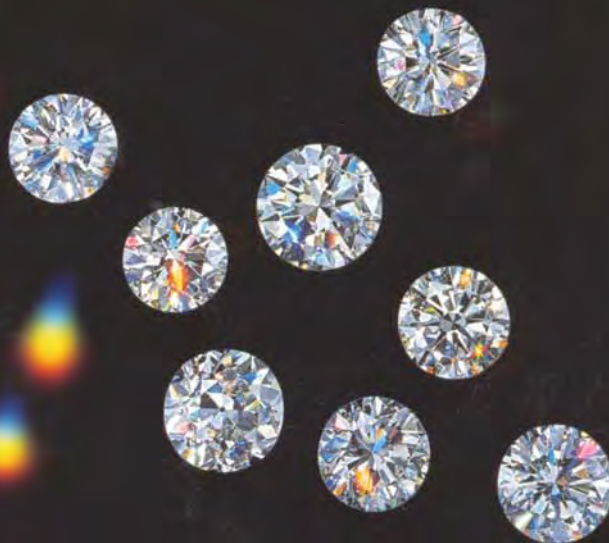


VOLUME XXXVII

# GEMS & GEMOLOGY

FALL 2001

*More on  
Diamond Cut:  
Analysis of Fire*



THE QUARTERLY JOURNAL OF THE GEMOLOGICAL INSTITUTE OF AMERICA



pg. 175

## EDITORIAL

173 **Shedding Light on "Fire"***William E. Boyajian*

## FEATURE ARTICLE

174 **Modeling the Appearance of the Round Brilliant Cut Diamond: An Analysis of Fire, and More About Brilliance***Ilene M. Reinitz, Mary L. Johnson, T. Scott Hemphill, Al M. Gilbertson, Ron H. Geurts, Barak D. Green, and James E. Shigley*

GIA's latest research on diamond cut introduces a metric for fire, DCLR, and reveals that all facets of a round brilliant affect its fire and brilliance.

## NOTES AND NEW TECHNIQUES

198 **Pyrope from the Dora Maira Massif, Italy***Alessandro Guastoni, Federico Pezzotta, Margherita Superchi, and Francesco Demartin*

A report on the unusual pale purple to purplish pink garnets from the Western Alps of Italy.

206 **Jeremejevite: A Gemological Update***Kenneth Scarratt, Donna Beaton, and Garry DuToit*

A detailed examination of this rare gemstone, using both standard and advanced testing methods.



pg. 207

## REGULAR FEATURES

212 **Gem Trade Lab Notes**

- Gem baddeleyite •Conch "pearls" •13 ct datolite •Carved "Hamsa" diamond •Heat-treated black diamonds •Update on blue and pink HPHT-annealed diamonds •Fracture-filled "bloodshot" iolite •Maw-sit-sit beads •Two unusual opals •Unusual star sapphire

220 **2001 Challenge Winners**222 **Gem News International**

- 2nd World Diamond Conference •Diamonds from Copeton, Australia •Maxixe-type beryls •Gems from Pala, California •Vanadium-colored green beryl from China •Statuette with a large natural blister pearl •Carpet shell pearl •Tahitian "keshi" cultured pearls •Pearl culturing in northwest Australia •Chilean powellite •Anhydrite inclusion in ruby •Ruby and sapphire from Australia and northern Myanmar •"Spider" quartz •Nigerian tourmaline •Langasite and a related material •Synthetic ruby "crystal" from Sri Lanka •Medieval sapphire imitations

246 **Book Reviews**249 **Gemological Abstracts**

pg. 216



pg. 239

# Shedding Light on “Fire”

Most of us would like to see the assessment of cut in round brilliants (or any shape, for that matter) simplified into a neat, easily explained package. Unfortunately, this probably will not be the case for some time to come. The lead article in this issue sheds more light on the cut question, but it also underscores its complexity. Only with careful review will our astute readers fully understand the authors' research and, as importantly, their results.

GIA's landmark brilliance study, published in the Fall 1998 issue of *Gems & Gemology*, was the first major breakthrough in the scientific analysis of cut in decades. It introduced a metric for brilliance, WLR (weighted light return), and demonstrated that many different proportion combinations can yield equally bright round brilliant cut diamonds. The article in this issue presents a metric for fire, DCLR (dispersed colored light return). With the results of these two major segments of GIA's cut research project now published, we are very close to answering the key questions involved in proportion evaluation for round brilliants.

The authors conclude that there is no easy way to characterize the “best” cut in round brilliants for either brilliance or fire. Rather, it is the complex interaction of multiple proportions, involving all of a diamond's facets, that must be considered in the assessment of these key appearance aspects. Furthermore, there is now even more evidence to support the conclusion that there is no one “best” cut for a round brilliant diamond.

Some generalizations can be made about DCLR, as they were for WLR. The authors clearly point this out. However, as we learn more about the complex interactions of different proportions with light, we also see the limitations under which most current cut grading systems are operating. These systems typically use small ranges of individual proportions, often with long-held historical parameters as target points. Although these well-respected parameters can produce beautiful diamonds, there are many other proportion combinations that produce diamonds of equal attractiveness. Further, the authors' research—which also includes observations of actual diamonds—shows that the lengths of star and lower-girdle facets are critical to cut assessment in round brilliants, although no current grading systems incorporate these factors in their analysis of cut.

As the authors acknowledge, it is difficult to say whether brilliance or fire has more impact on diamond appearance in round brilliants. It is also premature at this point to combine WLR and DCLR into a single overall proportion evaluation system or cut grade. As

more results are obtained from this project, however, a single cut grading system may become feasible.

In the meantime, you may ask, what does all this research mean to the gem and jewelry trade? And how will GIA use this information to serve the industry and the consuming public?

First and foremost, GIA is a non-profit public benefit corporation with an educational mission. Thus, like any college or university, we seek to better understand problems and provide solutions for the trade and the public. We have already placed a great deal of information about cut research on the GIA Web site ([www.gia.edu/giaresearch](http://www.gia.edu/giaresearch)). In addition, the knowledge we have gathered will be incorporated into our education courses with the all-new Graduate Gemologist program to be introduced in 2002. Also, next year we will adapt and apply knowledge gained through this research to our Gem Trade Laboratory reports.

The inclusion of this new cut information on our diamond grading reports, while revolutionary in some sense, will be largely transitional. We plan to introduce it in a way that will neither disrupt the current commercial flow of goods in the pipeline, nor require major adjustments in the use of our reports. It is likely that, as research continues, further insights on cut will be adapted to both our education program and our laboratory reports in the years to come. We also hope to develop cut-evaluation instrumentation, thus completing the circle of service. The insights gained through this cut research will be available to everyone in a variety of formats.

While we laud the efforts taken in past decades to uncover the secrets of diamond proportions and fine cutting, we know that assumptions were made that now can be either verified or corrected through modern scientific means. Marcel Tolokowsky accomplished a great deal with the limited technology and information available in the early 20th century, but the analytical power provided by modern computers and the access to literally tens of thousands of actual diamonds have given GIA the tools to propel cut research well into the 21st century.



*William E. Boyajian*

William E. Boyajian, President  
Gemological Institute of America

# MODELING THE APPEARANCE OF THE ROUND BRILLIANT CUT DIAMOND: AN ANALYSIS OF FIRE, AND MORE ABOUT BRILLIANCE

By Ilene M. Reinitz, Mary L. Johnson, T. Scott Hemphill, Al M. Gilbertson, Ron H. Geurts, Barak D. Green, and James E. Shigley

This article presents the latest results of GIA's research on the interaction of light with fully faceted colorless symmetrical round brilliant cut diamonds of various proportions. The second major article in this three-dimensional modeling study, it deals with fire—the visible extent of light dispersed into spectral colors. As fire is best seen with directed (spot) lighting, the metric for fire presented (dispersed colored light return, or DCLR) uses this lighting condition. DCLR values were computed for more than 26,000 combinations of round brilliant proportions. In general, different sets of proportions maximize DCLR and WLR (weighted light return, our metric for brilliance), but there are some proportion combinations that produce above-average values of both metrics. Analysis of these metric values with variations of five proportion parameters demonstrated that every facet contributes to the appearance of a round brilliant diamond. In particular, star and lower-girdle facet lengths—which are ignored by most cut-evaluation systems—could have a noticeable effect on WLR and DCLR. Observations of actual diamonds corroborate these results.

For more than 80 years, the diamond trade has debated which proportions produce the best-looking round brilliant (see, e.g., Ware, 1936; "Demand for ideal proportions . . .," 1939; Dake, 1953; Liddicoat, 1957; Dengenhard, 1974; Eulitz, 1974), with discussions growing quite animated in the last decade (see, e.g., Boyajian, 1996; Kaplan, 1996; Gilbertson and Walters, 1996; Bates and Shor, 1999; Nestlebaum, 1999; Holloway, 2000). Many methods of evaluating cut have been presented, including several grading systems (see box A; also see table 3 in Hemphill et al., 1998). Although interest at GIA in how diamond cut relates to appearance extends back more than 50 years, we have been researching the topic using modern computer technology since 1989 (Manson, 1991; again, see Hemphill et al., 1998). Our overall research goal is to understand why a round brilliant cut diamond looks the way it does. Its appearance is a complex mixture of the effects of various lighting and observing conditions, the specific characteristics of each diamond, and the interpretation by the human visu-

al system of the overall pattern of light shown by the diamond (figure 1). Traditionally, the appearance of the round brilliant diamond has been described using three aspects: brilliance, fire, and scintillation.

A method that scientists use to address a complicated problem is: (1) break it into simpler aspects, examining each aspect separately; and then (2) make sure that solutions for each small piece of the problem also hold true for the larger problem as a whole. We have applied this approach to our study of polished diamond appearance by examining each appearance aspect separately. In our report on the first of these (Hemphill et al., 1998), we used a mathematical expression for brilliance, called weighted light return or WLR, which we developed from the definition of *brilliance* given in the *GIA*

---

See end of article for About the Authors and Acknowledgments.  
GEMS & GEMOLOGY, Vol. 37, No. 3, pp. 174–197  
© 2001 Gemological Institute of America

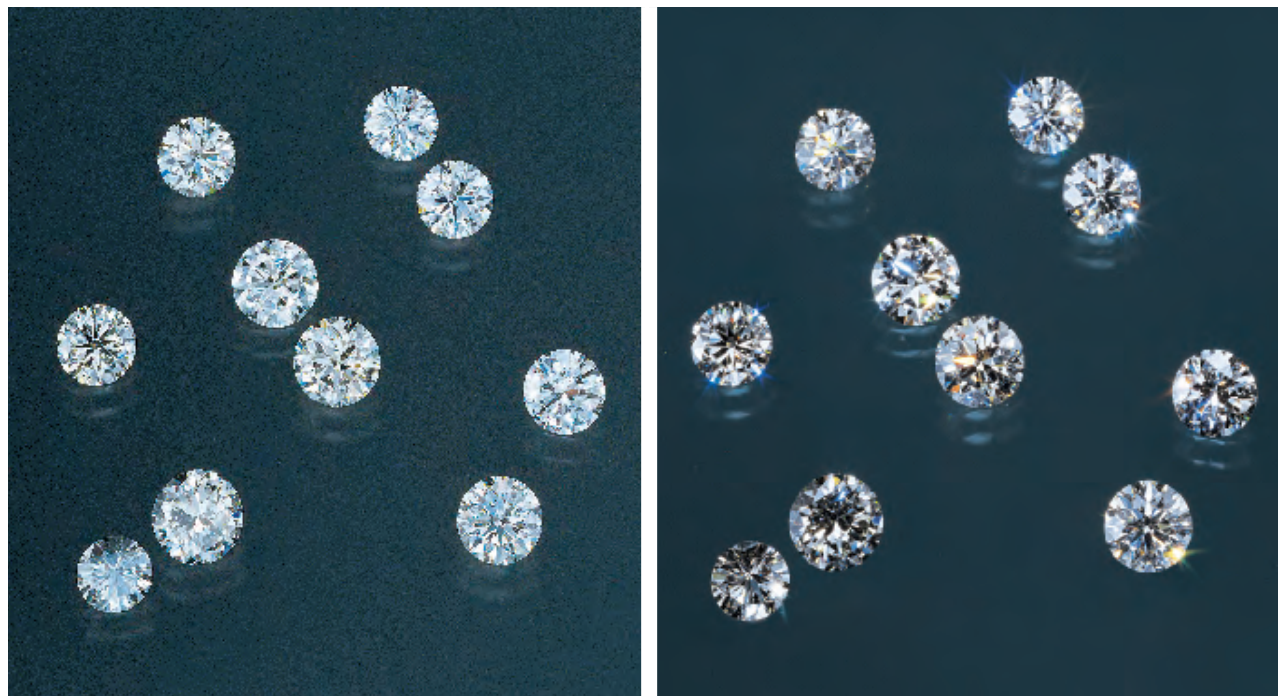


Figure 1. These 10 diamonds were selected to show a range of values for brilliance (as weighted light return, WLR) and fire (as dispersed colored light return, DCLR). They are, clockwise from the top right: RD13, 1, 6, 10, 25, 27, 24, and 23, with RD19 above RD21 in the center. Diffuse lighting, used for the photo on the left, emphasizes brilliance, represented by WLR; spot lighting, used to produce the image on the right, emphasizes fire, modeled as DCLR. The diamonds have been positioned so that WLR increases from left to right, and DCLR from bottom to top. For proportions and other information about these diamonds, see table 2. Photos by Harold & Erica Van Pelt.

*Diamond Dictionary* (1993)—that is, the intensity of the internal and external reflections of white light from the crown. (Note, however, that WLR does not include external reflections, i.e., glare.) The present installment of our research on the appearance of round brilliant diamonds addresses the effects of various proportions on fire. However, in the same dictionary, the definition for *fire* states merely “see Dispersion.” Since all diamonds have the same dispersion value (0.044), this definition is not adequate. Rather, fire is the result of dispersion. Thus, we suggest a more direct definition: *fire is the visible extent of light dispersed into spectral colors*. As with WLR to express brilliance, we have developed a metric, or number, to express how well a round brilliant can disperse—or spread—light into colors (dispersed colored light return, or DCLR, as defined on p. 181 below).

In the present article, we discuss how dispersion creates the appearance of fire in a polished round brilliant diamond, present our metric for fire, and describe how this metric varies with changes in the proportion parameters. We also extend our earlier analysis of brilliance (WLR) over variations in two additional proportion parameters: star- and lower-girdle-facet lengths. Last, we compare the results

from our exploration of fire to those from our earlier analysis of brilliance. We plan to address practical applications of our research to date in our next article, and to report on scintillation (the flashes of light reflected from the crown) in the future.

## BACKGROUND

In Hemphill et al. (1998), we introduced our computer model for tracing light rays through a “virtual” diamond—a mathematical representation of a standard, 58-facet, round brilliant cut with a fully faceted girdle. The virtual diamond has perfect symmetry, so its exact shape can be described with eight parameters: crown angle, pavilion angle, table size, star facet length, lower-girdle facet length, culet size, girdle thickness, and number of girdle facets (figure 2). We scaled the values of most parameters (e.g., table percentage) to the diameter at the girdle, so the virtual diamond model applies to diamonds of any size. In addition, the virtual diamond has no inclusions, is perfectly polished, and is completely colorless. The model results include the power, position, exit angle, and color (i.e., wavelength) of all traced light rays; these results can be expressed both numerically and graphically.

## BOX A: CURRENT PROPORTION GRADING SYSTEMS AND OTHER EVALUATIONS OF CUT

Trade debate on cut issues moved from the theoretical to the practical in the 1990s. The American Gem Society (AGS) opened a diamond grading laboratory in 1996 ("New AGS lab...", 1996), offering a cut grade for round brilliants that was modified from the conclusions set forth by Marcel Tolkowsky in *Diamond Design* (1919), as described and defined in the AGS Manual (American Gem Society, 1975). This system compares the proportions of the diamond to fixed ranges of crown angle, pavilion depth percentage, table percentage, girdle thickness, and culet size; it then assigns grades from 0 (best) to 10 (worst), for diamonds with good (or better) symmetry and finish. Several other organizations (for example, the Accredited Gemologists Association [AGA]; the Association of Gemological Laboratories, Japan [AGJ]; the International Gemological Institute [IGI]; and the Hoge Raad voor Diamant [HRD]) have their own grading systems that use different ranges of these proportions, as well as values of total depth percentage, to evaluate cut (Federman, 1997; Attrino, 1999). In each of these systems, the final grade is determined on the basis of the individual proportions, which are considered independently of one another. In addition, only small ranges of these individual proportions are assigned the highest grade, and deviations from these small ranges receive lower grades in each of these systems.

While the above laboratories use proportion measurements to evaluate diamond cut, others in the industry have used different approaches. Diamond Profile Laboratory pioneered a report with three types of photographic images that display cut information regarding the symmetry, dispersion, and light leakage of a polished diamond, independent of its proportions (Gilbertson, 1998). GemEx Systems produces a cut analysis report based on measurements taken with an imaging spectrophotometer using five light source positions (Roskin, 1999).

As branding has become more widely used for round brilliant cut diamonds, some manufacturing and retail firms have placed great emphasis on the proportions to which their diamonds are cut, while others have stressed the concept of light performance (see, e.g., "Hearts on Fire debuts...", 1997; "Perfectly cut...", 1997; Weldon, 1998). In addition, consumer- and trade-oriented Internet sites have hosted free-wheeling discussions about the many aspects of cut and its relationship to the appearance of a polished diamond (see, e.g., "Diamonds discussion forum," 2001). Despite all this interest and effort, substantial differences of opinion continue to be expressed with regard to (1) whether there is a single set of proportions that produces the best appearance in a round brilliant diamond, and (2) how the proportions of a diamond affect the different aspects of its appearance.

In our analysis of brilliance, we chose a diffuse hemisphere of theoretical daylight (D65; see, e.g., Commission Internationale de L'Éclairage [C.I.E.], 1963) to illuminate this virtual diamond, and a hemisphere located at infinity for our observing surface, with a weighting function (cosine squared) that counted light rays that exit vertically more heavily than those that exit at shallow angles. We introduced the WLR metric for brilliance, and analyzed the values of this metric for about 20,000 combinations of crown angle, pavilion angle, and table size (see, e.g., table 1). The results showed that WLR depends on the *combination* of these three proportion parameters, rather than on the value of any one of them. They also showed that many diverse combinations of proportions produced similar WLR values.

We stated in 1998 that those results constituted only one part of the appearance of a round brilliant diamond, and that our virtual diamond would continue to be useful for exploring other appearance aspects. Within a computer model, we can control—and vary—the lighting and observing conditions, as well as work with large numbers of exact propor-

tions that would be prohibitively expensive (or perhaps impossible) to manufacture as real diamonds. In addition, three important physical aspects of light interaction with a round brilliant cut diamond—three-dimensionality (3D), dispersivity, and polarization—can be readily incorporated into a computer model, although these aspects were omitted from earlier analyses of cut (see, e.g., Tolkowsky, 1919; Eulitz, 1974). More details on these physical aspects in diamond and other transparent materials can be found in Newton ([1730] 1959), Phillips (1971), Ditchburn (1976), and Born and Wolf (1980). A brief summary of the application of these aspects to diamond in particular can be found on the Internet (*GIA on diamond cut...*, 2001).

In short, diamond is a dispersive material: Its refractive index (R.I.) varies for different wavelengths (colors) of light. The dispersion value, 0.044, is the difference between diamond's R.I. for blue light (431 nm) and that for red light (687 nm). When a beam of white light enters a diamond at any angle other than perpendicular to the surface, it refracts, and the differences in R.I. among all the different

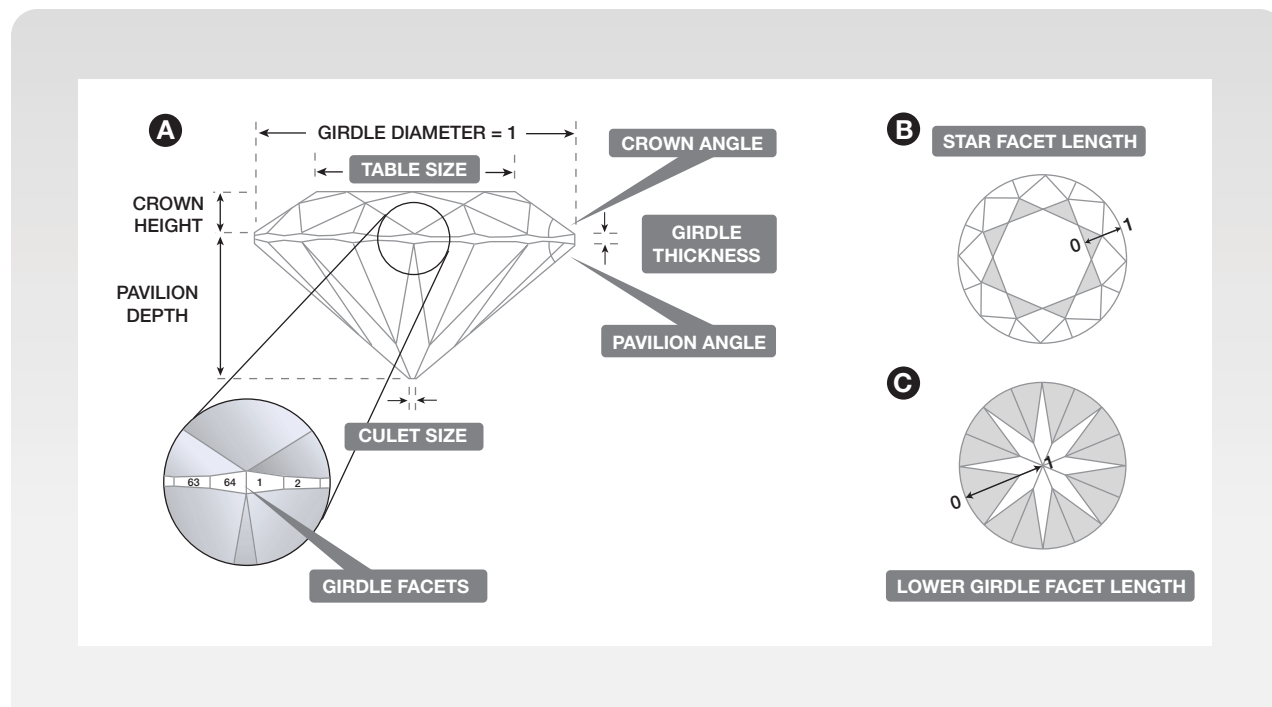


Figure 2. We used eight parameters—varied across the range given in table 1—to define our geometric model of the round brilliant shape. (A) All linear distances in this profile view can be described as a percentage of the girdle diameter. The enlarged view of the girdle is centered on the position where we measured the girdle thickness. (B) In this face-up view of the crown, the star facet length is shown at 50% so that the star facets extend half the distance from the table to the girdle (indicated here by 0–1). (C) In this face-down view of the pavilion, the lower-girdle facet length is shown at 75%, so that the lower-girdle facets extend three-fourths of the distance from the girdle to the culet (0–1). Adapted from Hemphill et al. (1998).

wavelengths cause the light to disperse, or spread, into its component colors. Although the initial spread of colors is less than  $0.5^\circ$ , these light rays of different wavelengths spread out further each time

the light interacts with a facet; consequently, light rays of different colors that enter the diamond at the same spot, with the same orientation, can take totally different paths inside the diamond. The fire

**TABLE 1.** The eight proportion parameters that define the virtual diamond’s shape, our reference proportions, and values used for calculations of DCLR and WLR.

Parameters	Reference proportions <sup>a</sup>	Values for DCLR	Increment for DCLR	Previous values for WLR	Values for new WLR results	Increment for WLR
Crown angle	34°	10°–46°	2°	19°–50°	20°–40° <sup>b</sup>	1°
Pavilion angle	40.5°	36°–45°	0.5°	38°–43°	38°–43° <sup>b</sup>	0.25°
Table size	56%	54%–68%	2%	50%–75%	53%–65% <sup>b</sup>	1%
Star facet length	50%	30%–74%; 50%–70% <sup>b</sup>	2%; 10%	5%–95%	30%–74% <sup>b</sup>	2%
Lower-girdle facet length	75%	45%–95%; 50%, 75%, 85% <sup>b</sup>	5%; N/A	50%–95%	50%, 75%, 85% <sup>b</sup>	N/A
Girdle thickness	3%	1.8%–4.4%	0.2%	1.8%–4%	Not varied	Not varied
Culet size	0.5%	0% <sup>c</sup> –20%	1%	0% <sup>c</sup> –20%	Not varied	Not varied
Number of girdle facets	64	Not varied	Not varied	16–144	Not varied	Not varied

<sup>a</sup> The reference value of a proportion is the default value chosen for that proportion in the cases for which it is not varied in the computer calculations.

<sup>b</sup> These proportions were used for the five-parameter simultaneous variation.

<sup>c</sup> A culet of 0% is also called no culet (or a pointed culet or pointed pavilion).

one observes in a polished diamond is the net result of this dispersion of light.

In addition, because a round brilliant is made up of flat facets, light becomes partially polarized when it enters the diamond, and the polarization state then changes as the light moves within the diamond and interacts with several facets. This is important because the polarization state of a ray of light governs how much of its energy is reflected at various angles of incidence, for both internal and external reflections. The fraction of light that refracts and the fraction that reflects internally can be calculated accurately only by keeping track of the light's polarization state.

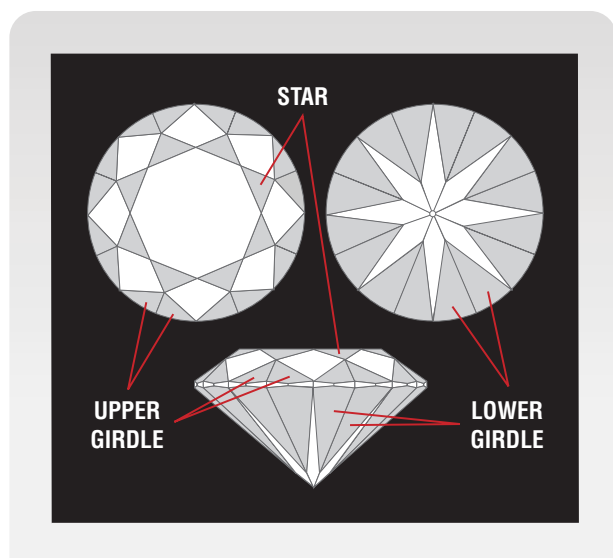
Three-dimensional light movement makes one aspect of diamond faceting obvious: For most commercially available proportions, star facets and upper- and lower-girdle facets together cover more than half the surface area of the round brilliant (figure 3). Although most cut analyses to date have focused on crown angle, pavilion angle, and table size, we cannot ignore the role that the star, upper-girdle, and lower-girdle facets play in the appearance of a typical round brilliant (our model does not

require a separate parameter for upper-girdle facet length, because this parameter is determined by the combination of star length, crown angle, and table size). If the star length is approximately 50%, the star and upper-girdle facets make up about 40% of the surface area of the crown. Similarly, if the lower-girdle length is approximately 80%, the lower-girdle facets cover about 80% of the pavilion surface. The amount of light that refracts through and reflects from these facets is likely to be significant, but the two-dimensional analyses of cut found in the literature do not account for their contributions to appearance.

Four teams of investigators (including the present authors) have modeled three-dimensional light movement in round brilliant cut diamonds, using a wavelength-dependent refractive index. The other three are: J. S. Dodson (1978, 1979); P. Shannon and S. Wilson, of Diamond Technologies Inc. (Shor, 1998; Shannon and Wilson, 1999); and a group at the Gemological Center in Lomonosov Moscow State University (abbreviated here as MSU) and OctoNus Software Ltd., headed by Y. Shelementiev and S. Sivovolenko ("Diamond cut study," 2001). Dodson kept track of the polarization component of each light ray so that its exact intensity could be calculated. The published literature does not indicate whether Shannon and Wilson included polarization in their model. The MSU group uses a "fixed polarization" approach, in which half the light energy is calculated in one polarization state and the other half is calculated in the state that is polarized perpendicular to the first. There are also some differences from one model to the next regarding the extent to which light rays are followed. The MSU group follows rays until they have interacted with at most 20 virtual facets, discounting any remaining energy a ray might have after this point. Our model follows all rays until at least 99% of their energy has been accounted for; some rays interact with more than 100 facets to reach this level.

Of course, real diamonds are subject to many more variations than are presently included in any of these models. For instance, inclusions and asymmetries may affect the appearance of a round brilliant as much as, or more than, variations in proportions. Color and fluorescence may also interact with a diamond's proportions to alter its appearance. In addition, it is well known among manufacturers that poor polish has a detrimental effect on diamond appearance regardless of the proportions. Last, grease and dirt on a diamond significantly degrade its appearance.

*Figure 3. For most commercially available proportions, more than half the total surface area of the round brilliant is covered by star facets and upper- and lower-girdle facets. Because these facets also interact with light rays that enter the diamond and reflect within it, they must be considered in modeling the brilliance and fire of a diamond. However, most existing cut grading systems do not include evaluation of these facets.*





## MATERIALS AND METHODS

**Computation.** For this work, we began with the same proprietary computer programs we used previously, and wrote several more computer routines to represent additional light sources and to calculate results relevant to the dispersion of light. As we did in 1998, we verified these new programs by running a test program for which the solution was found manually. Our programs run on any computer that accepts programs written in C; we used 16 Pentium III and four Pentium II processors in conventional desktop computers to carry out the calculations presented here. With these programs, we calculated the fire metric (DCLR) for more than 26,000 round brilliant proportion combinations (again, see table 1). On average, these calculations took 1.5–2 processor hours each.

Starting with 5,733 typical combinations of

crown angle, pavilion angle, and table size (from the ranges used in Hemphill et al., 1998), we also calculated WLR values with various star and lower-girdle facet lengths, keeping girdle thickness, culet size, and the number of girdle facets fixed at our reference proportions (again, see table 1). This resulted in 395,577 additional WLR values, using 23 star facet lengths (from 30%–74%, in increments of 2%), and three lower-girdle facet lengths (short—50%, medium—75%, and long—85%). The medium and long lower facet lengths were chosen as typical values seen in the trade today, while the short (50%) value was chosen because this is the lower-girdle length Tolokowsky (1919) used (see also Green et al., 2001).

**Diamonds.** We obtained (or had manufactured) 28 round brilliant diamonds (0.44–0.89 ct), some with unconventional proportions (see table 2). The 45 “view from infinity” (VFI) diagrams described below

**TABLE 2.** Proportions and calculated metric values for 28 diamonds examined for this study.<sup>a</sup>

Sample no.	Weight (ct)	Clarity grade	Color grade	Crown angle (°)	Pavilion angle (°)	Table size (%)	Star facet length (%)	Lower-girdle facet length (%)	Girdle thickness (%)	Culet size (%)	WLR	DCLR
RD01	0.61	VS <sub>1</sub>	E	34.3	40.6	54	53.8	81	2.9	0.91	0.283	3.97
RD02	0.64	SI <sub>2</sub>	E	32.9	41.5	59	54.7	77	4.5	1.09	0.277	3.41
RD03	0.55	VS <sub>2</sub>	H	32.0	40.9	63	60.3	80	3.7	0.75	0.272	3.39
RD04	0.70	VVS <sub>2</sub>	E	36.2	41.9	58	57.7	79	5.6	0.73	0.261	3.10
RD05	0.66	VS <sub>2</sub>	F	24.1	42.2	58	56.5	83	3.6	0.69	0.294	2.86
RD06	0.59	VVS <sub>2</sub>	F	23.1	41.9	57	60.6	78	3.2	1.07	0.301	2.87
RD07	0.76	SI <sub>1</sub>	F	36.4	41.5	53	59.4	89	3.1	1.72	0.271	3.46
RD08	0.50	VVS <sub>1</sub>	H	33.4	41.2	58	54.0	84	3.9	0.97	0.279	3.79
RD09	0.66	IF	F	23.6	42.1	56	58.8	80	4.5	1.04	0.300	2.92
RD10	0.68	VS <sub>2</sub>	G	34.9	40.9	54	54.7	76	3.0	0.70	0.281	3.89
RD11	0.71	VS <sub>2</sub>	D	37.2	41.9	58	49.1	87	4.3	0.89	0.262	3.21
RD12	0.71	SI <sub>1</sub>	F	35.0	41.0	57	58.5	76	4.6	0.71	0.274	3.52
RD13	0.59	VVS <sub>2</sub>	E	33.7	41.1	52	63.0	80	3.3	1.11	0.281	4.01
RD14	0.71	SI <sub>1</sub>	G	34.5	42.1	59	60.9	80	3.5	1.05	0.276	2.87
RD15	0.67	VS <sub>1</sub>	H	25.7	40.6	59	54.2	76	3.4	0.68	0.291	3.37
RD16	0.82	VS <sub>1</sub>	G	33.8	40.4	54	51.9	76	3.3	0.82	0.281	3.77
RD17	0.75	VS <sub>2</sub>	F	26.0	38.4	60	51.3	75	3.5	0.97	0.283	3.08
RD18	0.62	VVS <sub>2</sub>	H	29.1	41.2	61	46.9	75	3.3	0.88	0.281	3.16
RD19	0.72	VS <sub>1</sub>	H	29.2	39.5	63	51.7	76	3.3	0.83	0.276	3.41
RD20	0.62	VVS <sub>1</sub>	I	34.3	40.7	61	55.1	79	3.2	1.26	0.279	3.63
RD21	0.82	VVS <sub>1</sub>	I	35.8	41.2	57	57.3	76	3.7	0.83	0.275	3.14
RD22	0.81	VS <sub>1</sub>	K	35.9	39.2	55	54.2	77	3.3	0.83	0.274	3.75
RD23	0.72	VVS <sub>2</sub>	I	36.6	40.5	54	55.9	79	4.0	1.23	0.269	3.92
RD24	0.58	VVS <sub>1</sub>	H	35.8	38.8	66	58.9	79	4.0	0.91	0.259	3.23
RD25	0.82	VVS <sub>2</sub>	H	39.9	41.8	70	53.2	76	3.0	0.82	0.253	2.18
RD26	0.89	VS <sub>1</sub>	I	38.0	42.0	61	56.9	74	3.6	0.98	0.261	2.66
RD27	0.44	VS <sub>2</sub>	G	11.1	50.7	63	51.8	77	3.4	1.00	0.213	1.06
RD29 <sup>b</sup>	0.69	SI <sub>1</sub>	F	37.7	41.9	61	50.5	76	3.0	1.07	0.267	2.76

<sup>a</sup>All samples showed good or very good symmetry.

<sup>b</sup>Sample RD28 was not included in this study because it has a modified facet arrangement.

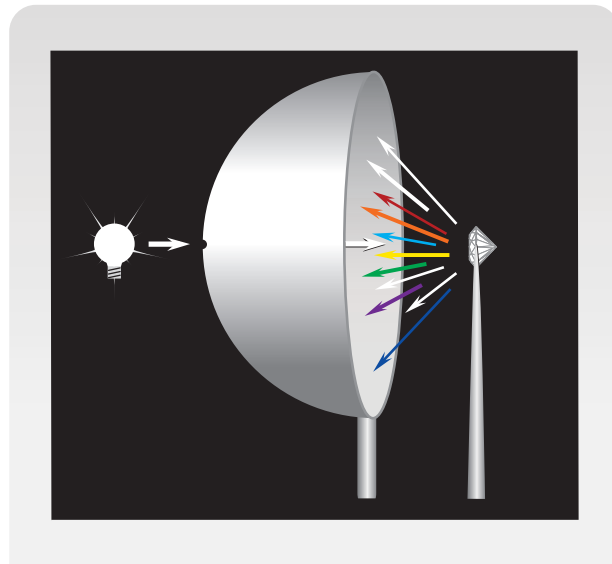


Figure 4. This experimental design allowed us to observe dispersed light from actual diamonds. A white hemisphere 40.6 cm (16 inches) in diameter is used as the observing surface, and a 0.95 cm hole at the center allows light from behind the hemisphere to shine on a diamond. The round brilliant is centered in the beam of light, with its girdle as close as feasible to the plane of the hemisphere's rim and its table oriented perpendicular to the beam. The light source is located about 20 cm behind the hole, so that light shining on the diamond is largely composed of parallel rays. Sizes and distances in this diagram are not to scale.

were calculated for these 28 diamonds and for another 17 diamonds (in the same weight range) with very good or excellent symmetry and polish that were chosen at random from those graded at the GIA Gem Trade Laboratory (GIA GTL). We examined and recorded dispersed patterns of colored light (see next section) for these diamonds and for more than 400 round brilliants chosen from the same GIA GTL population using the same symmetry and polish criteria.

**Conditions for Observing Fire.** To analyze brilliance, we chose the diffuse lighting condition we reported on in 1998, specifically because it maximized the effects of white light return while minimizing the impact of fire and contrast. However, because this lighting condition suppresses fire, it would not be appropriate for exploring the effect of proportion combinations on this appearance aspect. Again, fire in a round brilliant is the display of pure spectral hues that arise because the diamond is behaving like a prism, dispersing white light into its color components. Fire is not seen as a uniform color across the entire crown of the diamond at

once, or as a single rainbow, but as localized flashes of various colors that change depending on the position from which the diamond is viewed.

Keeping these aspects in mind, we began our search for a suitable lighting condition with the observation that diamonds look fiery under both sunlight and spot lights (such as the halogen lights found in many retail stores). This lighting is *directed*, that is, it comes from a very small area (relatively speaking), in contrast to diffuse lighting, which comes from all directions (such as outdoors on a foggy day, or fluorescent lighting reflected off white ceilings). These impressions were further supported by our experience photographing polished diamonds to capture their displays of fire. With either film or a digital camera, we found that a source of directed light was needed (in combination with diffused tungsten photography lights) to see fire in a photographic image (again, see figure 1).

Tolkowsky (1919) suggested a way to view fire from a diamond, that is, by using a sheet of paper with a pinhole. Light shining through the hole in the paper falls on the table of the diamond, and dispersed light that returns through the crown can be observed on the side of the paper facing the diamond. In such an illumination geometry, however, angular relationships are distorted, and the distance between the diamond and the paper strongly affects how much of the light returning through the crown is visible.

Using the same general idea, we created an apparatus to view and capture images of dispersed light from actual diamonds. As shown in figure 4, we introduced light through a 0.95 cm hole in a white plastic hemisphere (40.6 cm [16 inches] in diameter), which was the observing surface. We used a Lumina fiber-optic light, model Fo-150, which has a color temperature of 2920 K, and placed it approximately 20 cm from the hole, so that a preponderance of the light rays falling on the diamond were parallel to one another. The beam of light was centered on the diamond's table, and perpendicular to it. The diameter of this hemisphere was about 70 times larger than that of the diamonds we examined. The light emerging from the diamond could be viewed on the hemisphere, or recorded as a photograph, such as the one shown in figure 5.

We call the colored patches on the surface of the hemisphere *chromatic flares*. (In contrast, *fire* is seen when we observe the diamond directly.) Observation of chromatic flares requires an edge to the light source, specifically, a strong difference between light and dark: The dark portion contributes no color, so dispersion is emphasized.

Many of the flares are quite small, but some are wide, or long, or both (again, see figure 5). Any particular chromatic flare may include the whole spectrum of colors or only a few of them. Furthermore, if the dome is increased in size, most flares may spread out. The overall light level in the room strongly affects how many chromatic flares an observer sees; we saw many more flares in the dome in a darkened room than with the room lights on.

We used a Minolta X700 camera with a 45-mm lens, ASA 100 film, and an f-stop of 18 to take photographs of light dispersed from real diamonds. Exposure times varied from 45 to 150 seconds. We examined and recorded dispersed patterns of colored light for the more than 400 round brilliants mentioned earlier, to gain an understanding of the range of appearances of chromatic flares, and thus of fire in polished diamonds.

**Model Conditions for Fire.** We chose to model directed lighting as a bright point source of D65 illumination (a common model for average daylight; see again C.I.E., 1963), located very far from the diamond (at infinite distance) and centered over the diamond's table. With this condition, the unpolarized light rays entering the crown facets are parallel to one another and perpendicular to the table (figure 6, left). The entire crown is illuminated.

An observer position also needed to be determined. As the distance between the observer and the diamond increases, the observer sees less white light and more dispersed colors, but he or she can see only some of the colors at one time (figure 6, right). Conversely, when a round brilliant is viewed close up, the fire is less discernable since various colors viewed close together appear as white light. (This effect also was demonstrated in our apparatus for observing chromatic flares from actual diamonds, where some of the dispersed light output from the diamonds appeared as white light.) Therefore, to observe maximum fire, the observer must be as far away from the diamond as possible. In addition, the assessment of fire requires multiple views of the diamond, from different viewing angles. (The fact that these multiple views cannot be made simultaneously, but must be made sequentially from various positions, may complicate the assessment of fire in a diamond by an "actual" observer, but can be incorporated relatively easily in a model.) Our "observer" for WLR was a hemisphere at infinity (with a cosine squared weighting function for the returned light), and we found that this observer was a good choice for viewing fire as

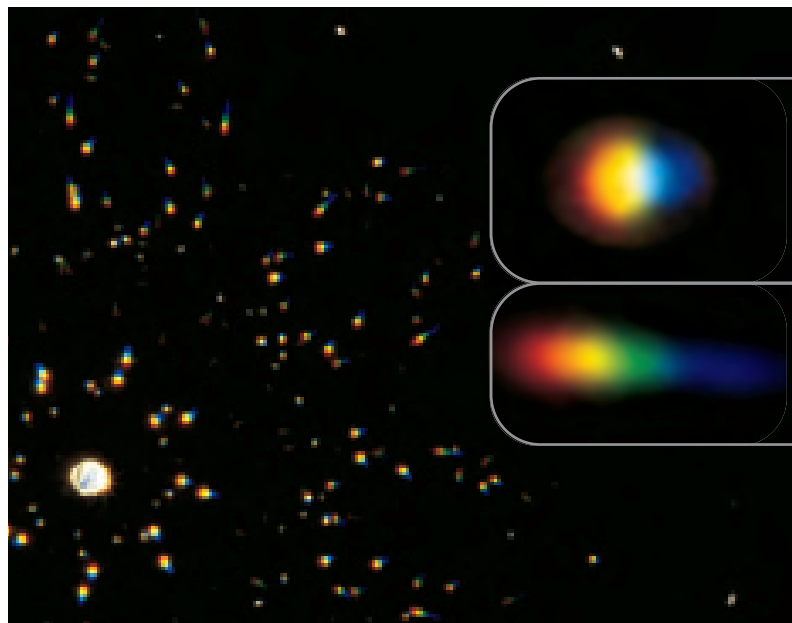


Figure 5. This image shows a variety of chromatic flares (colored light patterns) that were produced by a round brilliant diamond on our observation hemisphere. Larger images of two chromatic flares, shown as insets, illustrate some of the variety seen in these patterns. Photo by Al Gilbertson.

well. This model observer "views" the virtual diamond from all angles, while the weighting factor incorporates the importance of the face-up position. This combination of lighting and observing conditions tests the *maximum extent* to which a round brilliant with a particular choice of proportions can disperse light into its component colors.

**A Metric for Fire: DCLR.** To analyze the fire from a virtual diamond graphically, we plotted the model output of our observing hemisphere, projected onto a flat plane, using a polar projection in which the distance of any plotted point from the center of the diagram is proportional to the exit angle of that ray. We call this graphic result a *view from infinity* (VFI) diagram. The combination of point light source and infinite viewing distance yields only dispersed light on the observing hemisphere; that is, the result appears as various colored streaks (with no white centers). These streaks are composed of colored spots showing the final exit directions of individual rays. The *colored streaks* on a VFI diagram for a virtual diamond correspond to the chromatic flares on the hemisphere for an actual diamond of the same proportions.

Figure 7 shows a complete VFI diagram for a virtual round brilliant cut diamond of our reference proportions. For a diamond with perfect symmetry (such as our virtual diamond), all of this information

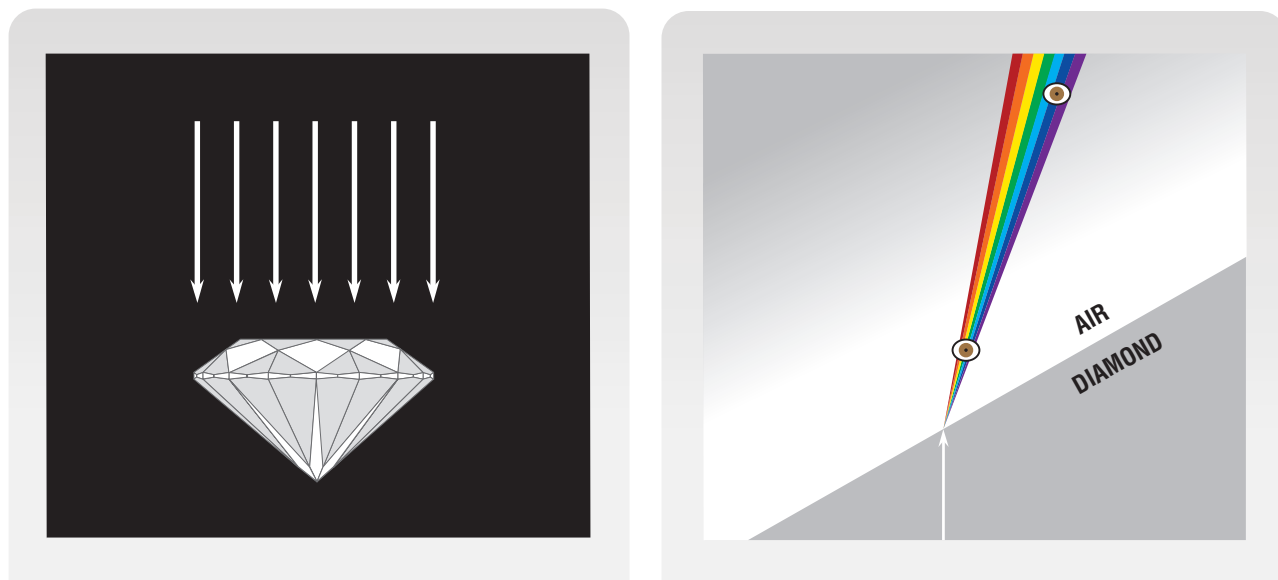
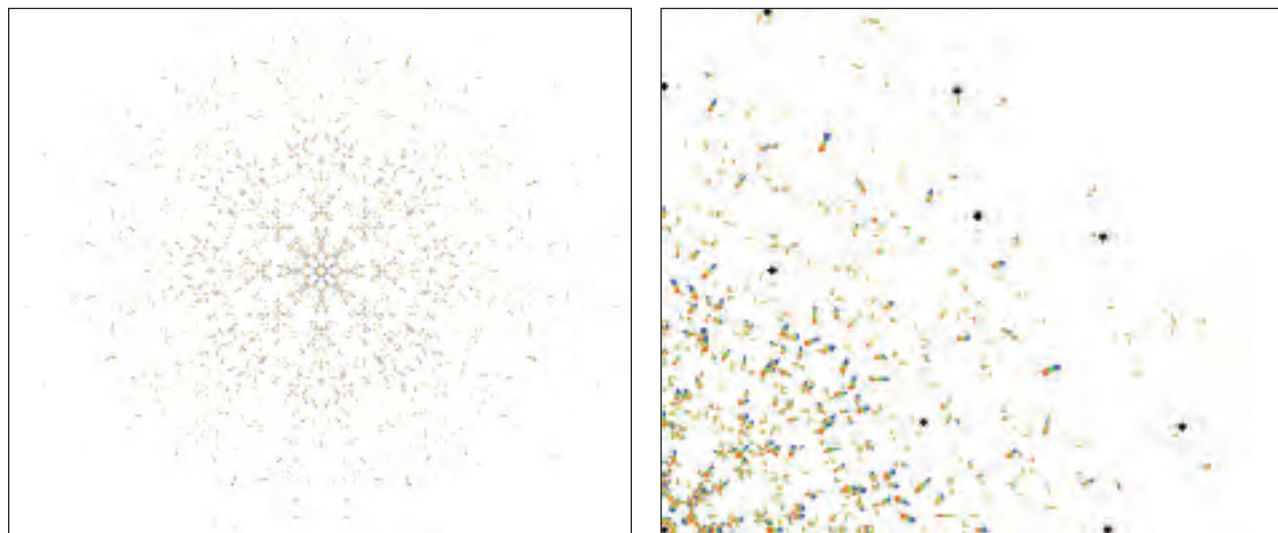


Figure 6. Left: In our model lighting condition for fire, a point source located at infinity produces parallel rays entering the crown of the diamond, perpendicular to the table. Right: As dispersing light moves away from its source (here, the surface of a diamond), the different wavelengths spread out in space. When a small detector, such as a human eye, is far enough away (shown as the upper oval), only some of the colors can be seen from any one view-point, so movement of the diamond (or observer) is necessary to see the other colors. When the detector (lower oval) is close enough to the surface of the diamond, all the colors are present, so it “sees” predominantly white light.

is in fact contained in a one-eighth “pie slice” of the diagram. The angle at which rays exit from the crown is shown by their position; rays that exit perpendicular to the table are displayed in the center of

the diagram, while those that exit close to the horizontal appear around the circumference of the circle. We can take advantage of the symmetry and plot only one-fourth of this diagram on a sheet of paper,

Figure 7. This “view from infinity” (VFI) diagram is calculated for a virtual round brilliant cut diamond of our reference proportions (34° crown angle, 40.5° pavilion angle, 56% table, 50% star facet length, 75% lower-girdle facet length, thin to medium girdle, 0.5% culet, and 64 girdle facets). Rays of dispersed light that emerge straight up from the round brilliant are displayed in the center of the diagram, whereas rays that emerge close to the horizontal are shown near the edge of the circle. The perfect eight-fold symmetry of the virtual diamond allows us to portray all the information for the diamond using a small part of such a diagram. For example, on the right, a quarter of the diagram is shown with each ray’s line width proportional to its brightness.



with the different intensities of the rays appearing as different plotted thicknesses (figure 7, right).

We calculated VFI diagrams for proportion combinations taken from 45 actual diamonds, to compare with their observed dispersion patterns. (The detailed measurements of each round brilliant were averaged to produce a symmetrical proportion combination for that diamond.) Figure 8 shows three actual diamonds with different proportions as well as the VFI diagrams calculated for them. Although these color-streak patterns look different, we had no way to evaluate these VFI images quantitatively: the diamonds appear to show comparable fire. We needed a numerical value—that is, a metric—that could be used to evaluate fire for thousands of proportion combinations. It was important that the metric incorporate factors that matter to people when they observe fire in round brilliants; it also had to produce numerical values that differentiate a very fiery diamond from one with little fire.

The VFI diagrams display a variety of properties that can be combined into a metric, such as the total number and relative brightness of colored spots, and the lengths and angular distribution of the colored streaks made up of these spots. The metric we derived—*dispersed colored light return*, or *DCLR*—describes the potential of a round brilliant diamond with given proportions to display dispersed light when viewed face-up. Mathematically, DCLR is defined as:

$$\text{DCLR} = \sum_{\text{streaks}} \sum_{\text{colors}} (\text{Area} \times \text{Smoothed Intensity} \times \text{Weighting Factor})$$

That is, DCLR is the sum over all colored streaks, of the sum over all colors (sampled every 10 nm; see again C.I.E., 1963), of the size (area) of each colored streak multiplied times the “smoothed”<sup>\*</sup> brightness (intensity) of each spot along the streak, times an exit-angle weighting factor (the square of the cosine of the ray’s exit angle, which we also used for WLR).

The VFI diagrams show additional properties that we chose not to include in DCLR. For example,

<sup>\*</sup>We used a smoothing function because the intensity of calculated colored spots varied over a large range. Although we wanted brighter rays to count more than dimmer rays, we did not want the large scale of these numbers to overwhelm other factors, such as the area. Thus, rather than use the intensity directly, we “smoothed” it with an “S-shaped” function. The center of the “S” set the intensity of colored streaks to be included, based on their brightness relative to the strongest rays, and the smoothed function avoided an abrupt transition between the included rays and slightly dimmer excluded rays.

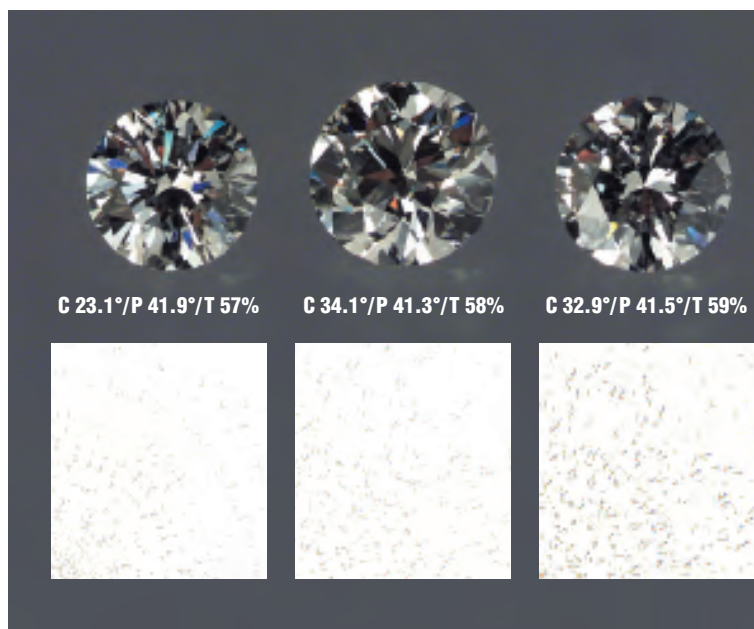


Figure 8. These three diamonds (0.50–0.64 ct) have rather different proportions (crown, pavilion, and table given here), and the VFI diagrams calculated for their proportions show different patterns. However, all three diamonds appear bright and display comparable fire. Photo by Elizabeth Schrader.

we included the angular distribution of the colored streaks in this metric, but not a radial term (which would have, e.g., differentiated flares coming from bezel facets from flares coming from star facets), because we believe that a human observer cares about fire from the diamond as a whole. Similarly, we did not use the color distribution within a given streak (that is, whether it contains a whole rainbow or only a few colors) or the orientation of a streak, choosing instead to focus on the overall impact of colored flashes. Last, we did not consider the color distribution of the spots (i.e., the relative number of red spots to green, yellow, or blue spots), because the various VFI diagrams we plotted showed balanced representations of all colors, a property we also observed in real diamonds.

Before starting the calculations, we needed to establish an appropriate brightness threshold for DCLR, to determine the range between the brightest and dimmest rays a person could be expected to see against a generally bright background (as in the light we typically use in our homes or offices, whether fluorescent or incandescent). The scientific literature dealing with human vision contains several works about the least amount of light that can be seen, or the brightest light in which objects can be discriminated, but almost nothing about the range of light levels perceived by humans in

## BOX B: COMPARISON OF MODELED RESULTS TO ACTUAL ROUND BRILLIANT PROPORTIONS

We analyzed interpolated DCLR values for the proportions of 67,943 round brilliant cut diamonds sent to the GIA Gem Trade Laboratory for grading to discover the range and distribution of DCLR shown by a group of typical commercial diamonds. (“Interpolated” means that we estimated the value for each proportion set from the values of their nearest neighbors in proportion space among the 26,000 points we had calculated.) This population of diamonds had crown angles ranging from 19.6° to 45°, pavilion angles from 36.1° to 44.8°, and table sizes from 54% to 68%. Star facet lengths were assumed to be 50% and lower-girdle facet lengths were assumed to be 75%, chosen to be at the reference values (see table 1 in the text) because we lacked these proportion measurements for this group of diamonds. These proportion combinations yielded DCLR values from 1.5 to 4.3, with a mean of 3.1.

The 680 sets of proportions (1% of the total) that yielded the highest DCLR values (3.5 or greater) had crown angles ranging from 25.8° to 42.8°, with most falling in the narrower range of 31° to 37°; pavilion

angles of 36.2° to 41.5°, with the majority falling between 39.0° and 41.0°; and table sizes of 54% to 68%, with most in the smaller range of 54% to 63%. In contrast, the 1% of proportion combinations that yielded the lowest DCLR values (2.2 or less) had crown angles from 26.9° to 40.9°, with most in the narrower range of 32.0° to 37.0°; steeper pavilion angles, from 41.8° to 44.8°, with most being greater than 42.0°; and tables that varied from 57% to 68%, with most 62% or larger.

Also relevant to the evaluation of modeled results for fire is the large population of proportion sets with DCLR values near the mean. We therefore examined the proportions of the middle 68% of the entire group; those proportions yielded DCLR values between 2.85 and 3.40. The range of each proportion for this group was the same as for the whole group of 67,943 diamonds. However, the majority of the crown angles for these diamonds fell in the narrower segment of 26.5° to 39.5°; only eight diamonds had crown angles of 43° or greater. Most pavilion angles were between 40.0° and 42.6°, and typical table sizes were 54% to 66%.

ordinary lighting situations (Dr. R. Brown, pers. comm., 2000). The only clear point of agreement we found is that this range is greater than the 256 tones (grayscale) used by a computer monitor (see, e.g., Begbie, 1969; Boynton, 1979).

Therefore, we empirically derived an estimate of the brightness of the least intense flare a person could be expected to perceive, using a combination of (1) the hemisphere described above for observing fire in actual diamonds, (2) four diamonds, and (3) four human observers. The observers compared the actual patterns of chromatic flares displayed by each diamond to six VFI diagrams calculated for that diamond’s proportions at different brightness thresholds. The observers agreed strongly in all four cases, which eliminated the need for more extensive testing. This comparison revealed that human observers see chromatic flares over a brightness range of about 3,000 against a background of ordinary room light: That is, the dimmest rays seen were 3,000 times less bright than the brightest rays. Consequently, we set the threshold at that level (3.5 orders of magnitude) for the calculations presented here.

The diamonds in figure 1 span DCLR values from 1.1 to 4.0, and show a range of appearances of fire. Under standardized lighting conditions (with sufficient directed light), we found that trained

observers may see differences in DCLR levels of 0.5, and readily see differences of 1.0. We interpolated DCLR values for the averaged proportions of 67,943 round brilliants received in the GIA Gem Trade Laboratory for diamond grading, to evaluate the numerical range and distribution of DCLR in a commercially relevant group of real diamonds (see box B). For the purposes of this article only, and for the convenience of the reader, we offer three categories for DCLR, based on the distribution of DCLR values for the diamonds in box B:

Above average > 3.5  
Average 2.8–3.5  
Below average < 2.8

These categories should not be taken as fire “grades.” They are offered as a convenience only, to compare the relative display of fire for virtual diamonds of various proportions.

### RESULTS

**VFI Plots.** We determined that there was a good match between the chromatic flares we saw from the 45 actual samples and the VFI diagrams calculated for their proportions. Figure 9 compares the photograph of the chromatic flares from a 0.61 ct round brilliant with high symmetry to a VFI dia-

gram for a virtual diamond with the averaged proportions of this actual diamond. The positions of the calculated colored streaks are an excellent match for the positions of chromatic flares recorded from the diamond. However, the display of colors in the chromatic flares is compressed (i.e., colors recombine into white light), both because the photographed hemisphere is much closer to the actual diamond than the modeled hemisphere is to the virtual diamond and because of the limitations of photography. All 45 calculated VFI diagrams showed similar matches to the corresponding chromatic flare photographs, despite the differences between the virtual and actual diamonds (e.g., asymmetries, inclusions, color, or fluorescence).

**Dependence of DCLR on Proportions.** As of July 2001, we had calculated DCLR values for more than 26,000 proportion combinations, varying seven of the eight model parameters independently and five of the eight model parameters simultaneously (again, see table 1). We found that DCLR depends on these parameters singly and in combination. In other words, DCLR, like WLR, can be maximized by proportion combinations in a number of different ways.

**Results for Individual Parameters.** Our investigation of the dependence of DCLR on proportions began with an examination of how DCLR varies with each parameter while the remaining seven parameters are held constant. Except where otherwise noted, we fixed the remaining parameters at the reference proportions given in table 1.

**Crown Angle.** In general, DCLR increases as crown angle increases; but, as figure 10A shows, DCLR hovers around a value of 3.5 for crown angles between 20° and 40°. There are two local maxima in this region, at about 25° and 34°, and DCLR rises steeply for crown angles greater than 41°. Note that moderately high crown angles of 36°–40° yield a slightly lower DCLR value than either of the local maxima.

**Pavilion Angle.** Diamond manufacturers often cite this parameter as the one that matters most for brilliance (e.g., G. Kaplan, pers. comm., 1998). In Hemphill et al. (1998), we reported that most “slices” of the WLR data that varied only pavilion angle showed a sharp maximum at one angle (see, e.g., figure 5 of that work), although which pavilion angle gave the highest WLR depended on the other parameters. We found a substantial, but uneven, decrease in DCLR for pavilion angles between 38° and 43°; this is the single parameter that caused the

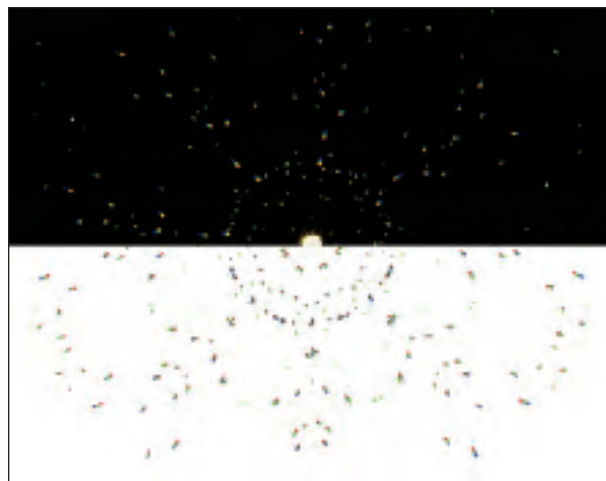


Figure 9. Comparison of the pattern of chromatic flares from a 0.61 ct round brilliant with very high symmetry (top, photographed on the hemisphere described in figure 4) to the VFI diagram calculated for a virtual diamond with the averaged proportions of the actual diamond (bottom) reveals that the calculated diagram matches the positions of real light output quite well. Photo (top) by Al Gilbertson.

most significant variation across the commercially common range. Figure 10B shows an overall decrease in DCLR with increasing pavilion angle, with an overall maximum at 38.5°, and a local maximum (“hump”) at 40°–41°.

**Table Size.** DCLR generally decreases as table size increases, with the values falling into three distinct regions: DCLR is higher for small tables (less than 58%), approximately constant for table sizes between 58% and 64%, and decreases further for larger tables, as shown in figure 10C.

**Star Facet Length.** We calculated the variation in DCLR with changes in the length of the star facet for three values of the crown angle: 25°, 34°, and 36° (figure 10D). (The angles of the star and upper-girdle facets relative to the girdle plane depend on both the star facet length and the crown angle. Thus, we expected DCLR results for different star lengths to vary at different crown angles.) Although the range of DCLR values is relatively small, each curve shows a clear maximum. At the reference crown angle of 34°, a star length of about 64%–65% yields the highest DCLR. This maximum shifts to about 56% for a crown angle of 36°. In our shallow (25°) crown example, the maximum DCLR value is found for 52%–54% star lengths.

**Lower-Girdle Facet Length.** One of the most dramatic results was the variation in DCLR with changes in lower-girdle length (figure 10E). DCLR values climbed from below average to above average

as the length of the lower-girdle facets increased from 45% to 85%, but then fell as this parameter further increased to 95%. As the lower-girdle facets get longer, they make a shallower angle with the girdle plane (closer to the pavilion angle) and very slightly shallower angles with each other and with the pavilion mains on either side. They also cause the pavilion mains to be narrower.

*Girdle Thickness and Culet Size.* DCLR showed very little change over the whole range of girdle thickness, with a slight minimum for a medium girdle (figure 10F). DCLR drops fairly smoothly as culet size increases from none to extremely large (figure 10G).

**Combined Effects.** Ideally, we would like to have shown the combined effects of crown angle, pavilion angle, table size, and star and lower-girdle facet length on DCLR in one graphic image. However, only two of these independent proportion variables can be displayed with the complete variation of a dependent value (such as DCLR) on a single graph. One way to illustrate the effects of two parameters is to draw contours showing ranges of DCLR values, similar to the WLR contours in Hemphill et al. (1998, figures 7–11). The “peaks” on such a contour plot represent proportion combinations that produce the highest calculated DCLR values. By grouping several contour plots together, we can show the results when two additional proportions are varied.

The nine contour plots in figure 11 show DCLR values with variations in both crown angle and pavilion angle, for a table size of 60%. They also demonstrate the effects of varying star and lower-girdle facet length, for three values of each. This figure contains a large amount of information about how these proportions work together to change DCLR.

The graph in the bottom center of figure 11 contains the point closest to our reference proportions (i.e., 34° crown angle and 40.5° pavilion angle), marked “R”, with a DCLR of 3.38. For this 60% table size, 50% star, and 75% lower-girdle facet length, the highest DCLR values are found at low pavilion angles of 36°–37° and a high crown angle of 46°. DCLR decreases sharply for most crown angles at high pavilion angles (greater than 42°). However, the DCLR at shallow crown angles depends strongly on the pavilion angle as well.

Within the proportion space shown on this bottom center plot, there are two “ridges” of higher DCLR. These ridges represent combinations of crown and pavilion angles that work together to produce higher DCLR. One ridge ends at about a

16° crown angle and a 43° pavilion angle; DCLR decreases from there for both shallower and steeper pavilion angles. The other ridge, to the right, is broader and less distinct in this specific plot.

As we compare the topography shown on this plot with that of each of the other eight plots in figure 11, we can see: (1) the strong effect of lower-girdle facet length on DCLR (compare plots left-to-right); and (2) the weaker, but still significant, effect of different star facet lengths (compare plots top-to-bottom). Shorter lower-girdle facets greatly decrease DCLR for most combinations of crown and pavilion angle, with a few exceptions (e.g., for crown angles greater than 40°, or for crown angles of 22°–46° with pavilion angles of less than 37°). Longer lower-girdle facets yield a large number of crown and pavilion angle combinations with average or above-average DCLR.

In a broad region (i.e., with crown angles from 16° to 46° and pavilion angles from 36° to about 43°), the combination of star and lower-girdle facet lengths changes the location of the two ridges of higher DCLR, and alters the depth of the valley between the ridges. Overall, the center plot (for 60% star and 75% lower-girdle facet length) shows the largest number of crown and pavilion angle combinations that yield average and above-average DCLR values, but the upper-right plot (for 70% star and 85% lower-girdle facet length) shows the most combinations that yield DCLR values of 4.0 or higher.

The fifth proportion we varied was table size. The three regions found for DCLR variations with table size alone (i.e., high for small tables, approximately constant for table sizes between 58% and 62%, and lower for larger tables in figure 10C) held true for the most part in the multi-dimensional exploration as well. Figure 12 shows three contour plots for 54% (small), 60% (medium), and 66% (large) table sizes, with 50% star and 75% lower-girdle facet lengths (the reference values). Many more combinations of crown and pavilion angles with small tables yielded average or greater DCLR values than those with large tables. Although there were many crown and pavilion angle combinations that yielded these DCLR values with a 60% table, on average DCLR values were lower than with a small table. For large tables, only a narrow range of pavilion angles (shallower than typical) produced these DCLR values.

The combined effects of table size and lower-girdle facet length are shown in figure 13 for several significant combinations of crown and pavilion angle. We found that longer lower-girdle facet lengths generally yield higher DCLR values than



## INDIVIDUAL PROPORTION VARIATIONS VERSUS DCLR

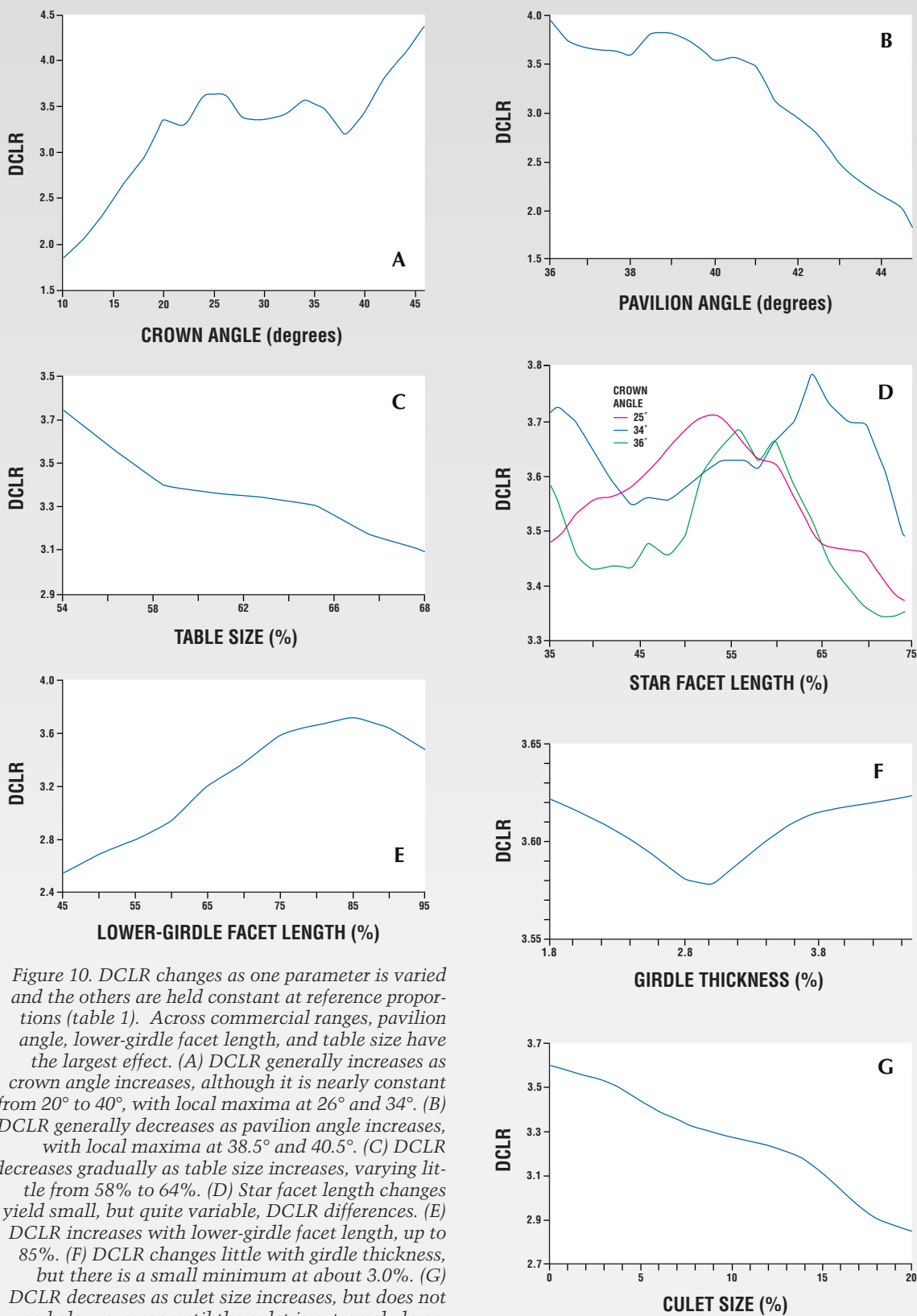


Figure 10. DCLR changes as one parameter is varied and the others are held constant at reference proportions (table 1). Across commercial ranges, pavilion angle, lower-girdle facet length, and table size have the largest effect. (A) DCLR generally increases as crown angle increases, although it is nearly constant from 20° to 40°, with local maxima at 26° and 34°. (B) DCLR generally decreases as pavilion angle increases, with local maxima at 38.5° and 40.5°. (C) DCLR decreases gradually as table size increases, varying little from 58% to 64%. (D) Star facet length changes yield small, but quite variable, DCLR differences. (E) DCLR increases with lower-girdle facet length, up to 85%. (F) DCLR changes little with girdle thickness, but there is a small minimum at about 3.0%. (G) DCLR decreases as culet size increases, but does not go below average until the culet is extremely large.

## DCLR – 60% TABLE

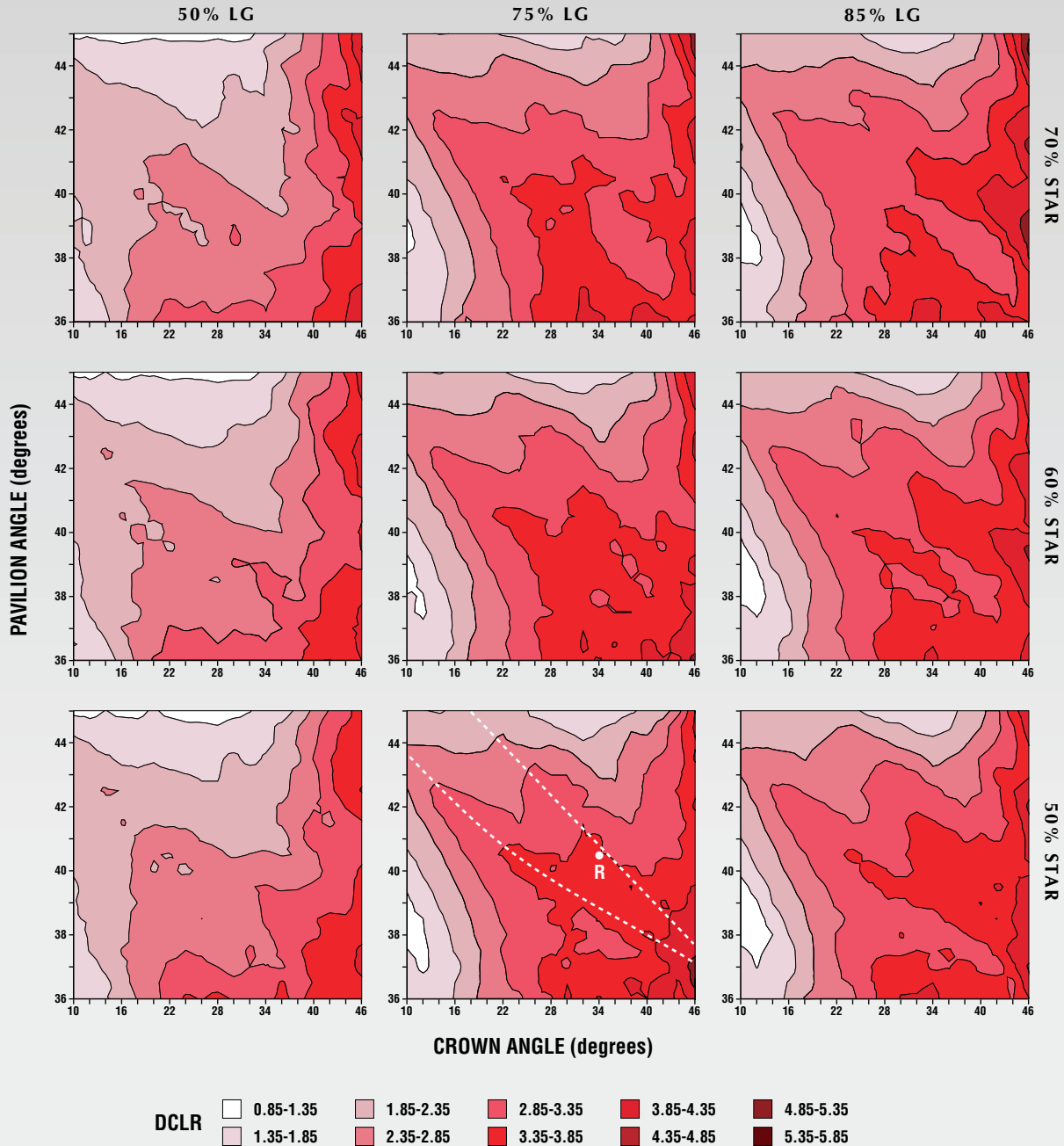


Figure 11. These nine contour plots show the variation in DCLR with changes in both crown and pavilion angles, for three values each of the star and lower-girdle (LG) facet lengths, at a table size of 60%. The DCLR surfaces are quite irregular, but they show that many proportion combinations yield above-average DCLR values, and others produce substantially lower values. The point marked “R” in the bottom center plot (75% lower-girdle length, 50% star length) is closest to our reference proportions (34° crown angle and 40.5° pavilion angle, although with a 60% table). The two dashed lines in this same plot indicate “ridges”—combinations of proportions that yield higher DCLR values than the proportions to either side. While each plot shows the detailed effects of varying crown and pavilion angles, comparison of the nine plots shows that star length and lower-girdle length also affect this metric.

## DCLR-50% STAR, 75% LOWER GIRDLE

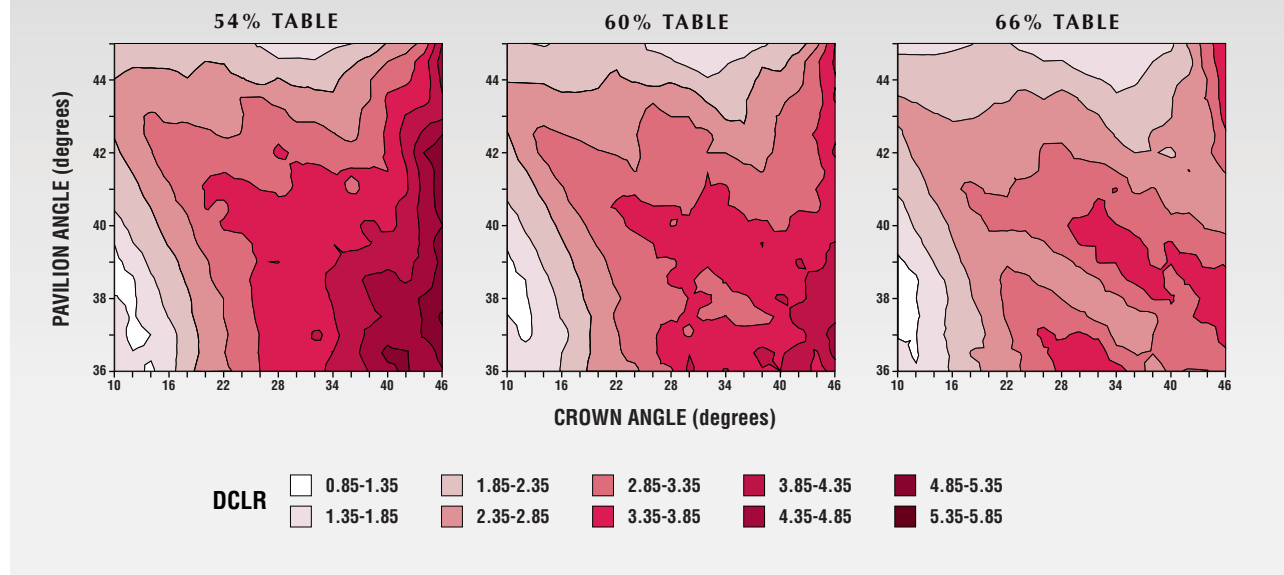


Figure 12. The possible combinations of crown angle and pavilion angle that yield above-average DCLR values greatly decrease as table size increases. In addition, the specific crown and pavilion angles that produce above-average DCLR values change toward higher crown angle and lower pavilion angle as table size becomes very large.

short or medium lengths for all these crown and pavilion angle combinations. Although steep pavilion angles are usually considered undesirable, the use of long lower girdle facets and small tables produces above-average DCLR values. Changing the star facet length for the same combinations of crown and pavilion angles had a less pronounced effect, as shown in figure 14.

**Back to Brilliance: The Effect on WLR of Varying Star and Lower-Girdle Lengths.** Recall that WLR values are much smaller than DCLR values; a change in WLR of 0.005 is discernable to trained observers (Hemphill et al., 1998). We analyzed data for sets of proportions (table size, crown angle, and pavilion angle) yielding high-average (0.280) and moderately low (0.265) WLR values when the star and lower-girdle facet lengths were at the reference proportions. Varying the length of the star or lower-girdle facets for these proportion combinations could increase WLR by 0.007, or decrease it by 0.015 (table 3). Many more proportion combinations led to decreases than to increases. Commercially common round brilliant proportions (see box B) showed smaller changes in the WLR value, whether increases or decreases, than more unusual proportions. The specific variations in star or lower-girdle facet length that produced the greatest increase in WLR depended strongly on the combination of crown angle, pavilion angle, and

table size. For a broad, commercial range of crown angles and pavilion angles, with smaller tables (53%–57%), longer star facet lengths produced increases in WLR (see, e.g., figure 15).

## DISCUSSION

**DCLR and Proportions.** Some proportion combinations that yield high DCLR values are not contiguous to one another, as shown in the contour plots (again, see figures 11–14). Thus, for some given values of two proportions, changes in the third proportion in a single direction may produce lower and then higher DCLR values. This variation in DCLR with different proportion combinations prevents the simple characterization of the “best” diamonds, in terms of fire, by evaluation of individual proportion parameters. Rather, it is the interaction between the proportions of the pavilion (pavilion angle and lower-girdle facet length) and those of the crown (table size, crown angle, and star facet length) that determines how light is dispersed by the round brilliant. Although certain generalizations may be made about the effects of a single proportion, in most cases there exist combinations of proportions that compensate to change DCLR. For example, large tables generally produce low DCLR, but with sufficiently high crown angles and shallower pavilion angles, a round brilliant with a table as large as

## DCLR WITH COMBINED PROPORTIONS

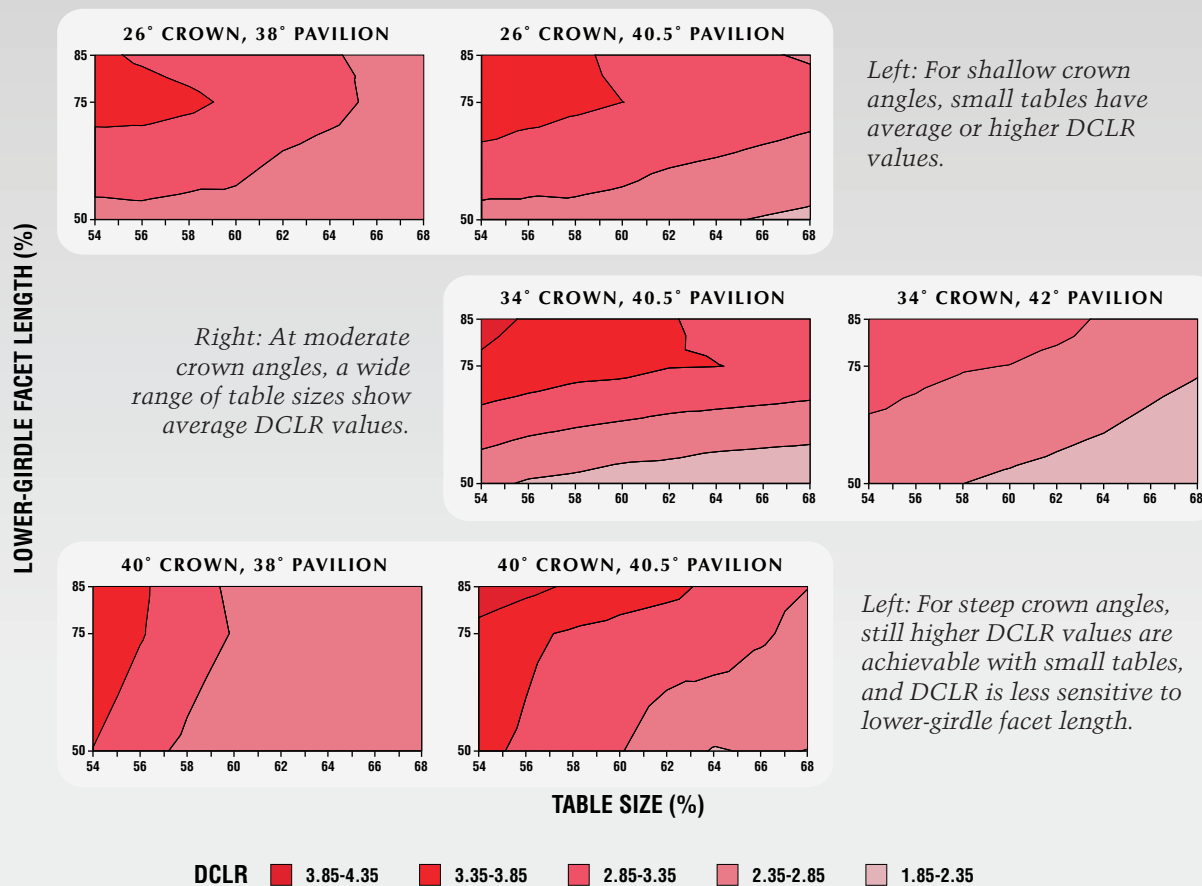


Figure 13. By grouping the contour plots, we can see how lower-girdle facet length, table size, and crown and pavilion angles work together to affect DCLR. Moderate to longer lower-girdle facet length generally increases DCLR. This effect is most pronounced at moderate pavilion angles.

66% can still yield an average or better DCLR value (see, e.g., diamond RD24 in table 2).

A short lower-girdle facet length of 50%, common early in the 20th century, greatly decreases DCLR and thus creates relatively poor fire (see, e.g., figure 11). Because Marcel Tolkowsky also chose this lower-girdle facet length, he made the reasonable—at that time—assumption that dispersion within the diamond could be neglected (see p. 56 of his 1919 treatise). Given the longer lower-girdle facets cut today, however, such an omission results in a poor approximation of how light moves within a round brilliant diamond.

Recall that fire is the visible extent of light dispersed into spectral colors. The type of lighting under which a round brilliant cut diamond is observed strongly affects the quantity and quality of colored light that emerges from it. With increasing distance, this colored light can spread out over a

wide area; however, the eye can see only a fairly small area from one viewpoint. Thus, observation of fire depends strongly on where the eye is relative to the diamond, particularly how far away the observer is. Capturing all of the fire from the crown of a diamond required a multitude of observer positions, as if the diamond was being rocked. To achieve this, we used the same hemisphere of observations, and the same position-dependent weights for observations, for fire (DCLR) as we did for brilliance with the WLR metric.

However, we used a very different lighting condition for modeling fire than we used for modeling brilliance. For actual diamonds, diffuse lighting brings out brilliance and suppresses fire, while spot lighting does the opposite (again, see figure 1). By examining brilliance with fully diffuse light, and fire with a point source of light, we have explored the maximum extent to which the proportions of a

## DCLR WITH COMBINED PROPORTIONS

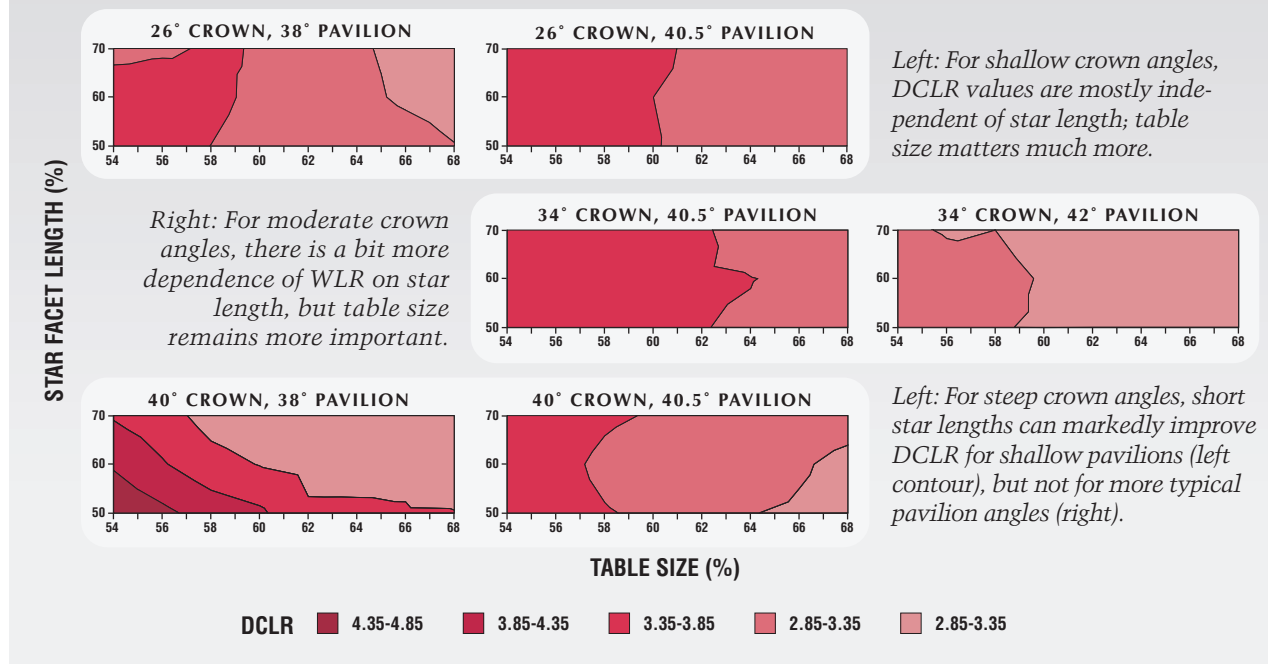


Figure 14. Changes in star facet length produced less change in DCLR values than was the case for lower-girdle facet length.

round brilliant can affect each of these appearance aspects. Every kind of lighting in the real world is some combination of diffuse light and directed (spot) light, and can be approximated in a computer model by combining fully diffuse and single-point sources.

Although three other teams of investigators (see Background on p. 175) modeled three-dimensional light movement in round brilliant cut diamonds, only two of these groups provided metrics for fire. Dodson (1978, 1979) offered three metrics (brilliance, fire, and “sparkliness”), and calculated their value for 120 proportion combinations of pavilion angle, crown angle (given as crown height), and table size. The MSU group (“Diamond cut study,” 2001) offers three metrics (brilliance, fire, and a combination of these called Q for “quality”), and they calculate these metrics across a broad range of crown and pavilion angles for two table sizes (53% and 60%).

These researchers and our group use similar verbal definitions for *brilliance*, *fire*, and *scintillation*, but the exact metrics differ, particularly the ones for fire. The DCLR surfaces that we calculated as a function of five proportion parameters are quite irregular, more so than the WLR surfaces (again, see Hemphill et al., 1998). These multiple “peaks” imply that there are many combinations of parameters that yield equally fiery round brilliant diamonds, which is in general agreement with the

results of Dodson and the MSU group, notwithstanding the differences in detail.

Dodson used “pseudo-diffuse illumination,” and recorded his output on a virtual plane at a finite distance above his modeled diamond, after the spot technique of Rösch (1927). He then rotated the colored streak pattern, and evaluated fire by measuring the largest distance between observed red and blue streaks (which are actually circles, because the pattern is rotated 360°). Like Tolokowsky, Dodson tried to determine the widest spread of dispersed light from the diamond, rather than include, for example, the total number of flares and their intensities. Since this approach is so different from ours, it is not surprising that Dodson’s numerical results show no particular correlation to our results. For instance, Dodson’s most fiery diamond example had a 26.5° crown angle, a 43° pavilion angle, and a 60% table, which our model predicts would produce average fire (DCLR value of 2.9).

The MSU group calculates their fire metrics by finding the colored areas visible at the surface of the virtual diamond, seen from all directions within a 60° cone around the vertical axis. For each patch of fire, they compute the color difference from white ( $\Delta E$  or  $\Delta H$ ; see again C.I.E., 1963), multiply it by the square root of the area the patch covers, and sum these values. Their fire metric MF 30 averages the calculated

**TABLE 3.** Largest WLR changes from variation of both star and lower-girdle facet lengths.<sup>a</sup>

Table size (%)	Crown angle (°)	Pavilion angle (°)	Highest WLR found	At star facet length (%)	And at lower girdle-facet length (%)	Lowest WLR found	At star facet length (%)	And at lower girdle-facet length (%)
<b>Sets of proportions that yield the high-average WLR value of 0.280<sup>b</sup></b>								
54	31	38.5	<i>0.284</i>	68	75	0.273	30	85
54	35	40.5	0.281	54	75	0.273	74	50
54	33	42.5	0.283	66	50	0.275	30	85
59	30	43.0	<i>0.287</i>	74	50	0.273	30	85
59	32	41.5	0.281	72	50	0.273	30	85
60	29	43.0	<i>0.287</i>	74	50	0.275	30	85
60	26	38.0	<i>0.283</i>	34	75	0.268	74	85
60	30	39.75	0.283	62	75	0.271	30	85
62	29	42.0	0.285	74	50	0.273	30	85
62	28	42.75	<i>0.287</i>	74	50	0.274	30	85
<b>Sets of proportions that yield the moderately low WLR value of 0.265<sup>b</sup></b>								
54	38	38.75	0.266	58	75	0.260	30	50
54	37	42.25	0.265	56	75	0.259	30	85
57	38	41.75	0.265	52	75	0.257	74	85
59	59	40.5	0.265	50	75	0.259	74	85
59	59	42.0	0.265	48	75	0.257	74	85
60	60	38.5	<i>0.266</i>	58	75	0.262	30	50
60	60	40.5	0.265	42	75	0.259	74	85
60	60	42.0	0.265	48	75	0.257	74	85
62	62	38.25	<i>0.268</i>	68	75	0.255	30	85
62	62	41.75	0.266	46	75	0.258	74	85

<sup>a</sup>Proportions that are not commonly seen in the trade are italicized here.

<sup>b</sup>Each example yielded the WLR value of 0.280 (or 0.265) with a star length of 50% and lower-girdle length of 75%.

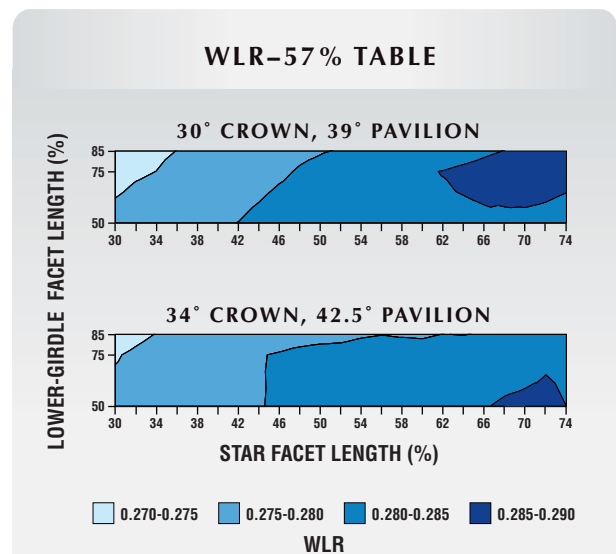
fire from a combination of diffuse and directed light.

Their results for 53% and 60% table sizes (again, see “Diamond cut study,” 2001) show the highest fire for diamonds with very shallow crown angles (less than 20°) and very steep pavilion angles (45°–50°). They found the least fire for diamonds with typical crown angles (30°–36°) and steep pavilion angles (greater than 43°) at both table sizes. In contrast, we found that diamonds with steeper crown angles (greater than 36°) show high fire across the range of pavilion angles we considered (36°–45°); the lowest fire predicted by our model is produced by diamonds with very shallow crown angles and either very shallow or very steep pavilion angles (again, see figure 11).

**Additional WLR Results.** We stated in 1998 that differences in WLR values as small as 0.005 could be discerned by trained observers in actual diamonds under controlled conditions. Varying the length of the star or lower-girdle facets (or both) can increase WLR by slightly more than this amount, or decrease it by three times this amount. Since these facets are polished at the end of the manufacturing process, judicious choices for their lengths can help improve the appearance of a round brilliant when the shape of the rough prompts choices of crown

angle, pavilion angle, and/or table size that typically produce only moderate values of WLR. Note that none of the major current grading systems includes

Figure 15. As seen in these plots for two different sets of crown and pavilion angles (with a constant table size of 57%), varying the lengths of the star and lower-girdle facets can have a significant impact on WLR.



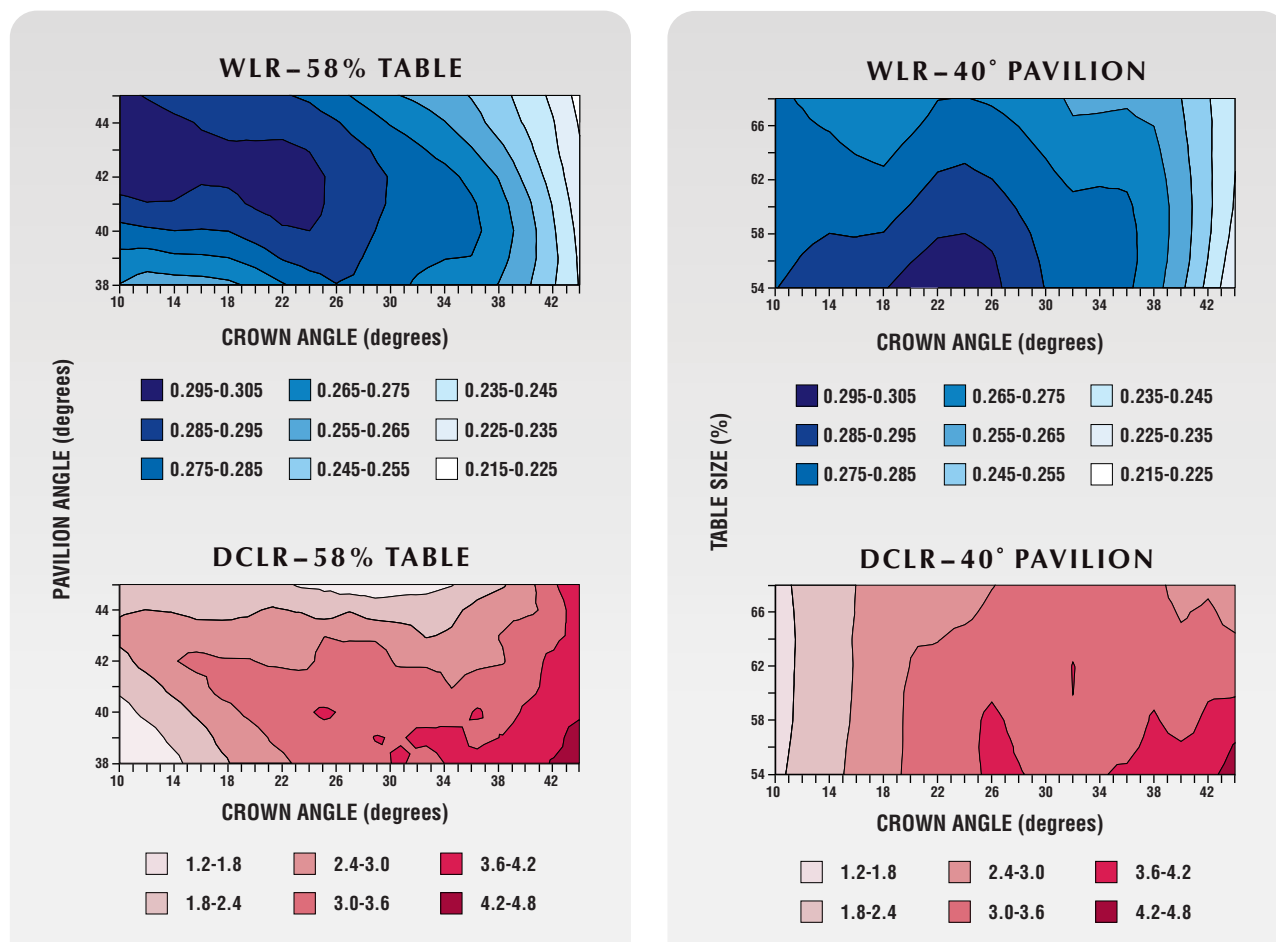


Figure 16. Left: These contour plots show WLR and DCLR across the same ranges of crown and pavilion angle for a 58% table, 50% star facet length, and 75% lower-girdle facet length. Although there is no overlap in the proportions that produce the highest values of each of these metrics, many proportion combinations produce average (0.270–0.280 WLR, 2.8–3.5 DCLR) or higher values of both metrics. Right: These contour plots show WLR and DCLR for a range of crown angles and table sizes for a pavilion angle of 40°. While the value of both metrics decreases as table size increases, many crown angles produce above-average values of both for table sizes up to 58%.

the length of star or lower-girdle facets in their analysis of cut.

**Interplay of Brilliance and Fire.** It is difficult to say at this time whether brilliance or fire has more of an impact on the overall appearance of a round brilliant diamond. Nevertheless, with the results modeled for both brilliance (WLR) and fire (DCLR), we are able to identify proportion combinations that produce above-average values of both appearance aspects. In figure 16, we show two cross-sections through proportion space with WLR contoured in shades of blue and DCLR contoured in shades of red. Each metric can be compared to the mean values for our population of more than 67,000 actual diamonds (see box B in this article and the corresponding box B in Hemphill et al., 1998).

Figure 16 (left) shows variations in WLR and

DCLR with variations in crown angle and pavilion angle for the commercially important table size of 58% and reference values for the other properties. The highest WLR values appear at shallow crown angles and moderate-to-steep pavilion angles. However, the WLR values are still above average for many crown and pavilion angle combinations. The highest DCLR values occur in a small area at the opposite corner of the plot (at a steep crown angle and a shallow pavilion angle), but the range of proportions that show above-average fire is quite large. Although there is no overlap in the areas that produce the *highest* values shown for each metric, there is considerable overlap in the proportion combinations that produce average or higher values of both at this table size. For example, crown angles from 24° to 32° combined with pavilion angles from 38° to 42° yield WLR above 0.270 and DCLR of 3.0 or

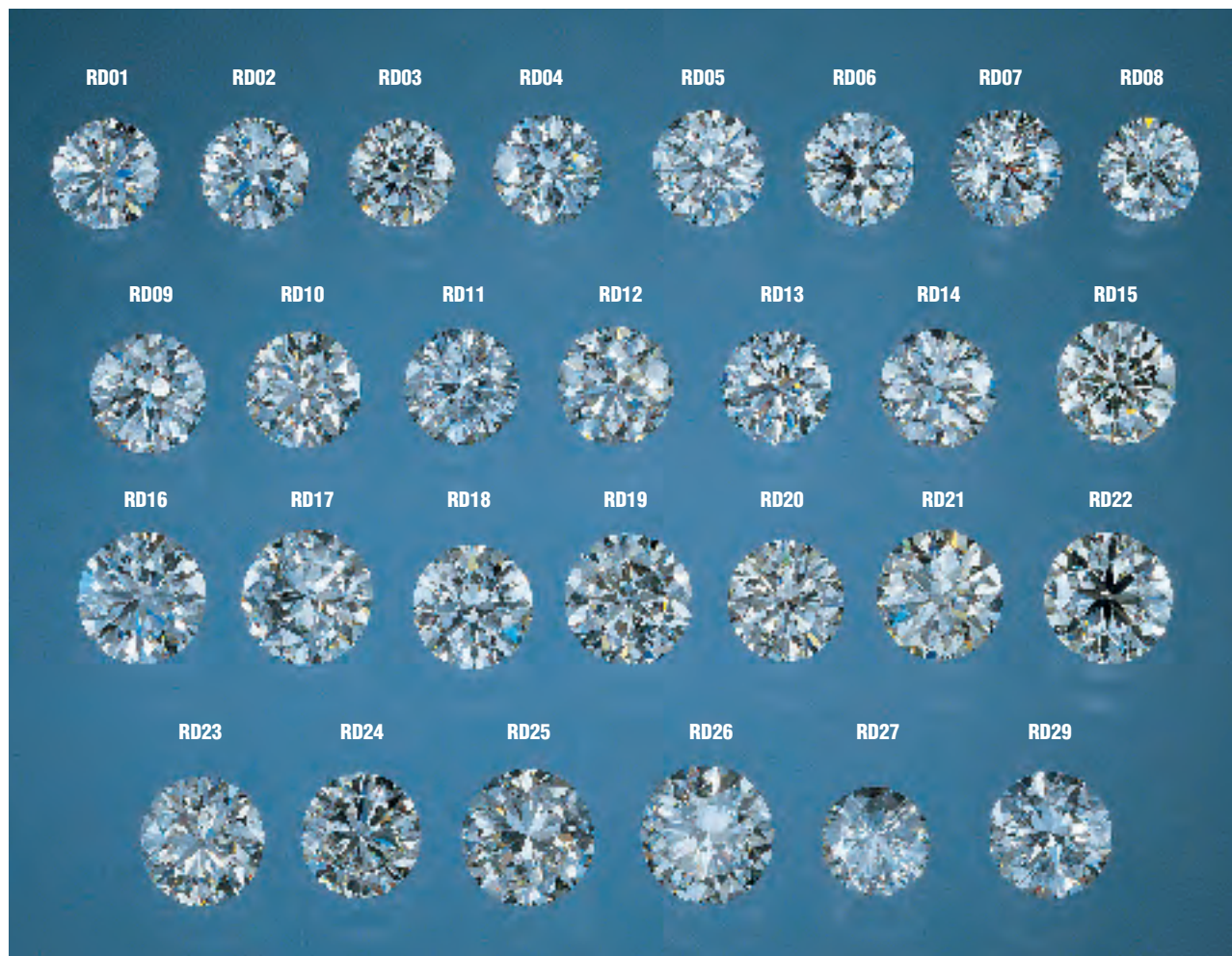


Figure 17. These 28 diamonds (0.44–0.89 ct) were used to examine the brilliance and fire associated with different sets of proportions. Some sets of proportions in this group are decidedly non-commercial (again, see table 2). Photo by Harold & Erica Van Pelt.

more; and crown angles from  $20^{\circ}$  to  $36^{\circ}$  accompanied by pavilion angles of  $40^{\circ}$  to  $41^{\circ}$  yield the same results.

Figure 16 (right) illustrates the dependence of WLR and DCLR on variations in crown angle and table size for a commercially relevant pavilion angle of  $40^{\circ}$  and reference values for the other parameters. There is one area of overlap where both WLR and DCLR are well above average, at crown angles of  $26^{\circ}$  to  $28^{\circ}$  and table sizes less than 58%. These smaller tables yield high values of DCLR at crown angles greater than  $35^{\circ}$ , but corresponding WLR values decrease steeply to below average as crown angle increases beyond  $36^{\circ}$ . However, there is a broad area (crown angles from  $26^{\circ}$  to  $36^{\circ}$  and table sizes up to 62%) that yields above-average values for both metrics.

The specific combinations of crown and pavilion angles that produce above-average values for each

metric vary with table size, star length, and lower-girdle length. For example, a lower-girdle facet length of 50% greatly reduces DCLR, but it can produce small increases in WLR; similarly, star facet lengths greater than 50% can increase WLR but will have a variable effect on DCLR, depending on the crown angle (again, see figures 14 and 15). Note also that there are far more combinations of crown angle and pavilion angle that work well with small tables (less than 55%) than with large tables (66% or more).

In some areas of proportion space, small changes in one or more proportions lead to fairly large changes in the WLR and DCLR values. If we use the analogy of land surfaces, these regions of proportion space are like steep mountainsides. Other areas are more like plateaus: regions where fairly large changes in proportions do not have a significant effect on WLR or DCLR values. The typical commercial range of proportions (again, see box B) lies



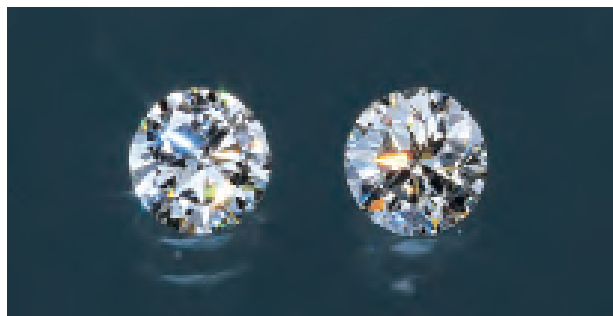


Figure 18. Although these two diamonds (RD19, left; RD21, right—see table 2) have different crown angles ( $29.2^\circ$  and  $35.8^\circ$ ), they display comparable amounts of fire with spot lighting. Photo by Harold © Erica Van Pelt.

within such a plateau. Thus, the cutter has a broad latitude for choices of proportions without risking a catastrophic effect on appearance.

**Comparing Model Results to Real Diamonds.** The ultimate verification of any model of diamond appearance is a comparison with actual diamonds cut to specific proportion combinations. We assembled the group of 28 round brilliant cut diamonds (0.44–0.89 ct) shown in figure 17; their proportions, color and clarity grades, and calculated WLR and DCLR values are given in table 2. As noted below, various round brilliants in this group (again, see figure 1) both confirm the fitness of our model and defy a few common beliefs in the trade about the relationship between proportions and appearance.

There are many combinations of crown angle, table size, and pavilion angle that produce average or higher DCLR values. This range of proportions is part of the “broad plateau” described above. For instance, diamond RD19 has a rather shallow crown angle, whereas RD21 has a fairly steep crown angle; yet both show considerable fire (figure 18). In both cases, the model indicates that this fire results from the combination of the diamond’s particular pavilion angle with the crown angle and table size (as well as additional proportions).

Diamond RD13, with a 52% table, gave the highest DCLR value (4.01). The next two highest DCLR values (3.97 and 3.92) were calculated for diamonds RD01 and RD23, which also have small tables (54%). However, one diamond with a large (66%) table, RD24, yielded a high average DCLR value of 3.23 (figure 19).

We also compared our model results for the combination of WLR and DCLR (again, see figure 1 and table 2) with the appearances of actual diamonds cut to these proportions. For steep pavilion

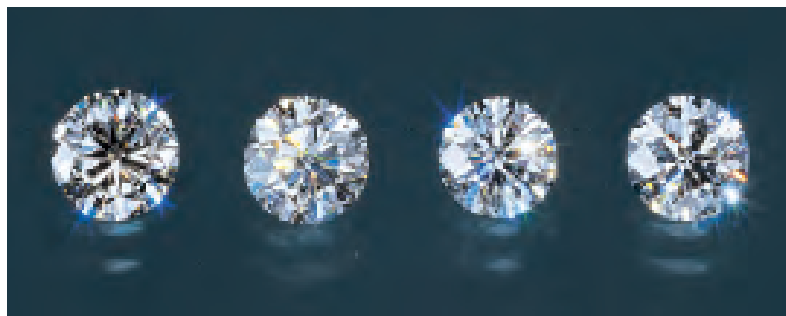


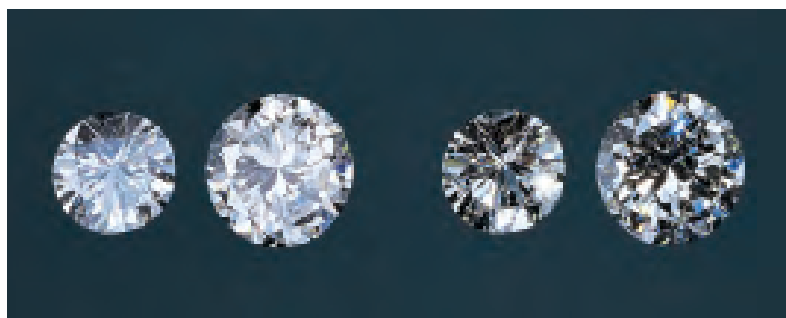
Figure 19. As reported in table 2, the diamond on the far left (RD24) has a large (66%), table while the other three (RD01, RD23, and RD13) have much smaller tables (52% to 54%). However, all have comparable DCLR values. Photo by Harold © Erica Van Pelt.

angles, there were no crown angles that yielded particularly high values of both WLR and DCLR; RD25 is both dark and lacking in fire despite its steep crown angle (figure 20). Also shown is RD27, with a much deeper pavilion angle and an extremely shallow crown; it shows little brilliance or fire (although MSU results would suggest it to be quite fiery).

## CONCLUSIONS

Our overall research goal is to understand why a round brilliant cut diamond looks the way it does. Its appearance is a complex mixture of the effects of various lighting and observing conditions, the specific characteristics of each diamond, and the interpretation by the human visual system of the overall pattern of light shown by the diamond. For our study thus far, we found that different lighting conditions are needed to bring out the maximum brilliance (totally diffused light) and fire (directed light). We made simplifying assumptions about the diamond

Figure 20. These two diamonds, with  $50.7^\circ$  (RD27, left image in each pair) and  $41.8^\circ$  (RD25, images at the right) pavilion angles, are neither bright (left pair, with diffuse lighting) nor fiery (right pair, with spot lighting). Composite of photos by Harold © Erica Van Pelt.



(e.g., colorless and perfectly symmetric, among other conditions) and the observing conditions (e.g., that a weighted average of viewing positions corresponds to the observation of a diamond being “rocked”).

Through this research, we have gained a much better understanding of some of the key factors that govern the appearance of a round brilliant cut diamond, particularly how the proportions of that diamond (expressed as eight independent proportion parameters) affect its brilliance and fire. In this article, we showed that VFI diagrams (our model’s graphic output of dispersed light from virtual diamonds) match the pattern of chromatic flares from actual diamonds. We presented our metric for fire, dispersed colored light return (DCLR), which we have computed for more than 26,000 combinations of the proportion parameters. We also showed that star and lower-girdle facet lengths could have a noticeable effect on WLR, our metric for brilliance.

*Every facet matters in a round brilliant diamond.* In general, DCLR is higher for smaller table sizes and larger crown angles, but at least three other parameters also are important: pavilion angle, star facet length, and lower-girdle facet length. Our modeling results indicated that a diamond with a shallow crown angle or a large table could still display higher-than-average fire if combined with the right pavilion angle, star facet length, and lower-girdle facet length. The relative appearances of our 28 actual diamonds with specific proportions confirmed these predictions.

When analyzing fire, both lighting and observing conditions strongly affect the analysis of fire. We used two distinct lighting conditions: fully diffused light to analyze brilliance (WLR), and a point-light source (i.e., a modeled spotlight) to analyze fire (DCLR). These different idealized lighting conditions are useful for determining the maximum

extent of these appearance aspects. By its nature, fire spreads out as it emerges from a diamond, so multiple views are needed to observe it. For this reason, we used the same weighted hemisphere of observation that we used for analyzing brilliance. Other researchers have investigated fire, but their metrics and their results are substantially different from ours.

We have not found a “bull’s-eye” of “best” proportions for either DCLR or WLR. Rather, both metrics show a complex dependence on proportion combinations, with many sets of proportions that yield similar values. Comparison of these two metrics shows that some proportion combinations yield the highest DCLR values, and others yield the highest WLR values, but in general these proportions do not overlap. Nevertheless, there are many choices of diamond proportions that give average or higher values for both parameters. Star and lower-girdle facet lengths can increase or decrease the calculated value of either metric, but the proportion variations that increase one metric may decrease the other.

Although our research is not yet complete, we believe that this understanding as to how cut proportions work together may bring a new degree of freedom to diamond manufacturers. By offering a wider range of cutting choices, this information may help manufacturers produce round brilliant diamonds with both above-average performance and potentially higher weight yields from the rough. Although this approach provides more options for cutting rough efficiently, it will also require more precision on the part of manufacturers. In addition, we feel the detailed information gathered to date on the levels of brilliance and fire provided by different proportion combinations can potentially serve as a basis for a more in-depth cut evaluation system.

#### ABOUT THE AUTHORS

Dr. Reinitz is manager of Research and Development at the GIA Gem Trade Laboratory (GIA GTL) in New York. Dr. Johnson is manager of Research and Development, Mr. Gilbertson is a research associate, Mr. Green is technical writer, and Dr. Shigley is director, at GIA Research in Carlsbad, California. Mr. Hemphill is a research associate in the GIA Gem Trade Laboratory and is located in Boston, Massachusetts. Mr. Geurts is Research and Development manager at GIA in Antwerp, Belgium.

*ACKNOWLEDGMENTS:* The authors thank the following companies for manufacturing diamonds of various proportions that

*made it possible to carry out this research: D. Swarovski & Co., Wattens, Austria; and the Smolensk State-Owned Unitary Enterprise (Kristall Production Company) in Smolensk, Russian Federation. Thanks to the GIA Gem Trade Laboratory for their help in this project, especially Lisa Moore, Kyaw Moe, Diana Moore, Takao Kaneko, Joe Truong, Jessica Kim, and Kimberly Boyce-Patton in Carlsbad, and Elizabeth Schrader in New York. We would also like to thank Dr. R. Brown of the Exploratorium, San Francisco, California, and George Kaplan of Lazare Kaplan International in New York City for their comments. Finally, the authors would like to thank their long-suffering families (and editors) for their equanimity throughout this project.*

## REFERENCES

- American Gem Society (1975) *Manual: Diamond Grading Standards*. American Gem Society, Los Angeles.
- Attrino T. (1999) True ideals: Making the AGS grade. *Rapaport Diamond Report*, Vol. 11, No. 42 (November 5), pp. 27–28.
- Bates R., Shor R. (1999) Still the Ideal? *Jewelers' Circular-Keystone*, Vol. 170, No. 2, pp. 96–99.
- Begbie H. (1969) *Seeing and the Eye: An Introduction to Vision*. Natural History Press, Garden City, NY, 227 pp.
- Born M., Wolf E. (1980) *Principles of Optics: Electromagnetic Theory of Propagation, Interference, and Diffraction*, 6th ed. Pergamon Press, New York, 808 pp.
- Boyajian W.E. (1996) Letter to the editor—GIA's Boyajian on cut grading. *Rapaport Diamond Report*, Vol. 19, No. 28 (August 2), p. 9.
- Boynton R.M. (1979) *Human Color Vision*. Holt Rinehart and Winston, New York, 438 pp.
- C.I.E.—Commission Internationale de L'Éclairage (1963) *Proceedings of the 15th Session of the C.I.E., Vienna, Austria*. C.I.E., Vienna, Austria, 207 pp.
- Dake H.C. (1953) Proportions for the brilliant cut. *The Gemmologist*, Vol. 22, No. 258, pp. 17–18.
- Demand for ideal proportions in diamonds (1939) *Gems & Gemology*, Vol. 3, No. 2, p. 24.
- Dengenhard W.E. (1974) The measurement of brilliance of diamonds. *Gems & Gemology*, Vol. 14, No. 9, pp. 259–270.
- Diamond cut study (2001) *Russian Gemological Server*, Gemological Center in Lomonosov Moscow State University (MSU), <http://www.gemology.ru/cut/index.htm> [date accessed: 09/07/01].
- Diamonds discussion forum (2001) *DiamondTalk.com*, <http://www.diamondtalk.com> [date accessed: 09/07/01].
- Ditchburn R.W. (1976) *Light*, 3rd ed. Academic Press, London, 775 pp.
- Dodson J.S. (1978) A statistical assessment of brilliance and fire for polished gem diamond on the basis of geometrical optics. Ph.D. thesis, Imperial College of Science and Technology, London, 253 pp.
- Dodson J.S. (1979) The statistical brilliance, sparkliness, and fire of the round brilliant-cut diamond. *Diamond Research*, pp. 13–17.
- Eulitz W.R. (1974) The optical quality of two different brilliant cut diamonds: A comparative investigation. *Gems & Gemology*, Vol. 14, No. 9, pp. 273–283.
- Federman D. (1997) Make believe. *Modern Jeweler*, Vol. 96, No. 9, pp. 23–39.
- GIA Diamond Dictionary*, 3rd ed. (1993) Gemological Institute of America, Santa Monica, CA, 275 pp.
- GIA on Diamond Cut* article archive (2001) *GIA on Diamond Cut*, Gemological Institute of America, <http://www.gia.edu/giaresearch/diamond-cut-archive.cfm> [date accessed: 09/07/01].
- Gilbertson A., Walters C. (1996) Cut grading: Do the numbers add up? *Rapaport Diamond Report*, Vol. 19, No. 45 (December 6), pp. 49–50.
- Gilbertson A. (1998) *Letting Light Speak for Itself*. Diamond Profile, Inc., Portland, OR, 31 pp.
- Green B., Gilbertson A., Reinitz I., Johnson M., Shigley J. (2001) What did Marcel Tolokowsky really say? *GIA on Diamond Cut*, <http://www.gia.edu/giaresearch/diamond-cut8.cfm> [date accessed: 09/25/01].
- Hearts on Fire debuts in U.S. (1997) *New York Diamonds*, Vol. 41, p. 10.
- Hemphill T.S., Reinitz I.M., Johnson M.L., Shigley J.E. (1998) Modeling the appearance of the round brilliant cut diamond: An analysis of brilliance. *Gems & Gemology*, Vol. 34, No. 3, pp. 158–183.
- Holloway G. (2000) Latest research supports new take on old ideal. *Rapaport Diamond Report*, Vol. 23, No. 24 (July 7), pp. 21, 23, 25.
- Kaplan G. (1996) Letter to the editor—Response to Boyajian on cut grading. *Rapaport Diamond Report*, Vol. 19, No. 34 (October 11), p. 9.
- Liddicoat R.T. (1957) Are present diamond rulings adequate? *Gems & Gemology*, Vol. 9, No. 2, pp. 38–42.
- Manson D.V. (1991) Proportion considerations in round brilliant diamonds. In A.S. Keller, Ed., *Proceedings of the International Gemological Symposium 1991*, Gemological Institute of America, Santa Monica, CA, p. 60.
- Nestlebaum K. (1999) Chasing the ideal. *Rapaport Diamond Report*, Vol. 22, No. 42 (November 5), p. 35.
- New AGS lab issues grading reports (1996) *Jewelers' Circular-Keystone*, Vol. 167, No. 5, pp. 60–62.
- Newton I. ([1730]1959) *Optiks*, 4th ed. reprinted. Dover Publications, New York, 406 pp.
- Perfectly cut Hearts on Fire (1997) *Bangkok Gems & Jewellery*, Vol. 10, No. 12, pp. 39–40.
- Phillips W.R. (1971) *Mineral Optics: Principles and Techniques*. W.H. Freeman and Co., San Francisco, 249 pp.
- Rösch S. (1927) Beitrag zum Brillanzproblem. *Zeitschrift für Kristallographie*, Vol. 65, pp. 46–48.
- Roskin G. (1999) Brilliance Scope makes debut. *New York Diamonds*, Vol. 54, pp. 16–17.
- Shannon P., Wilson S. (1999) The great cut debate rages on. *Rapaport Diamond Report*, Vol. 22, No. 5 (February 5), pp. 89–90, 95.
- Shor R. (1998) Computer engineers create proportion grade program. *New York Diamonds*, Vol. 44, pp. 26–28.
- Tolokowsky M. (1919) *Diamond Design: A Study of the Reflection and Refraction of Light in a Diamond*. E. & F.N. Spon, London, 104 pp.
- Ware J.W. (1936) New diamond cuts break more easily. *Gems & Gemology*, Vol. 2, No. 4, p. 68.
- Weldon R. (1998) Gourmet cuts: EightStar diamonds are a study of the internal light path. *Professional Jeweler*, Vol. 1, No. 11, pp. 24, 26.

# PYROPE FROM THE DORA MAIRA MASSIF, ITALY

By Alessandro Guastoni, Federico Pezzotta, Margherita Superchi, and Francesco Demartin

Large pyrope crystals containing gem-quality portions have been collected since the early 1990s from the Dora Maira Massif, Western Alps, Italy. These crystals have yielded pale purple to purplish pink gemstones typically up to 1 ct. The chemical composition and physical properties compare favorably to those reported for near-end-member pyrope. Absorption spectra suggest that the color is related to  $\text{Fe}^{2+}$  and  $\text{Mn}^{2+}$ . The pyrope formed in a mica schist-quartzite layer within Paleozoic basement rocks that underwent an Alpine high-pressure/low-temperature metamorphic event. The deposit appears extensive, but future production undoubtedly will be limited due to environmental restraints. Currently about 100 carats per year enter the marketplace.

For several years, large pyrope crystals have been known from the Varaita Valley in the Dora Maira Massif (a massive topographic and structural feature, particularly within a mountain range) in Italy's Western Alps (Schert et al., 1994). Since the early 1990s, local mineral collectors have recovered and cut crystals containing gem-quality portions. Although the gemstones have rarely exceeded 1 ct (the largest known to date are about 2 ct), a few hundred good-quality faceted Dora Maira pyropes have entered the Italian gem collector's market. The distinctive features of these gem pyropes are their pale purplish pink color (figure 1), near-end-member composition, and mineral inclusions. Of particular interest are inclusions of ellenbergerite, for which Dora Maira is the type locality.

## LOCATION AND ACCESS

The Dora Maira Massif is located in the Piedmont region, 50 km (31 miles) southwest of Turin (figure 2). Pyrope is found in the Varaita Valley, between the villages of Brossasco and Martiniana Po. Gem pyropes have been collected in several outcrops over an extended area (about 15 km long) from high-grade quartz-phengitic metamorphic rocks. Large-scale mining is forbidden by environmental policy, but local collectors do considerable hand digging.

## GEOLOGIC SETTING

The Dora Maira Massif consists of Paleozoic basement rocks with an overlying Mesozoic series of rocks that are characterized by an Alpine high-pressure/low-temperature metamorphic overprint. The pyrope crystals occur in a light-colored phengitic schist-quartzite layer, measuring a few meters thick, which was referred to as "micascisti splendenti" by Stella (1895) and Franchi (1900). The quartzite layer contains large flakes of phengite (a high-pressure mica; Mandarino, 1999) and pale purplish pink pyrope crystals that reach 25 cm in diameter. Vialon (1966) mapped the quartzite layer over a distance of about 15 km, and suggested that the protolith (original unmetamorphosed rock) was a leucocratic granitic vein that was strongly deformed by metamorphism. Other rocks in the area include fine-grained felsic paragneisses that are associated with lenses of marble and metabasite. In describing

---

See end of article for author information and acknowledgments.  
 GEMS & GEMOLOGY, Vol. 37, No. 3, pp. 198–204  
 © 2001 Gemological Institute of America

the mineralogy and petrogenesis of the quartzitic layer, Chopin (1984) pointed out the presence of coesite, a mineral indicative of extreme metamorphic conditions (pressures over 28 kilobars and temperatures up to 700°–750°C).

### DESCRIPTION OF THE CRYSTALS

The pyrope crystals have a rounded shape formed by rough trapezohedron faces (figure 3). The crystals are heavily fractured and always covered by a thin layer of white to pale green phengite. As noted above, some of the pyrope crystals contain clear portions that can be faceted into attractive gemstones.

### MATERIALS AND METHODS

We examined 11 faceted Dora Maira pyropes (0.24–0.85 ct; see, e.g., figure 4), which were obtained from the gem collection of the Natural History Museum of Milan and loaned by L. Merlo Pich. All of the samples are from the Brossasco and Martiniana Po areas, and they show a range of color



Figure 1. Pyrope from the Dora Maira Massif in Italy's Western Alps has been mined since the early 1990s by local mineral collectors. The 0.85 ct stone on the left was loaned by L. Merlo Pich, and the 0.76 ct gem on the right belongs to the Natural History Museum of Milan. Photo by R. Appiani.

and intensity that is representative of the material from this region. These samples also were selected on the basis of their distinctive inclusions. Mr. Pich

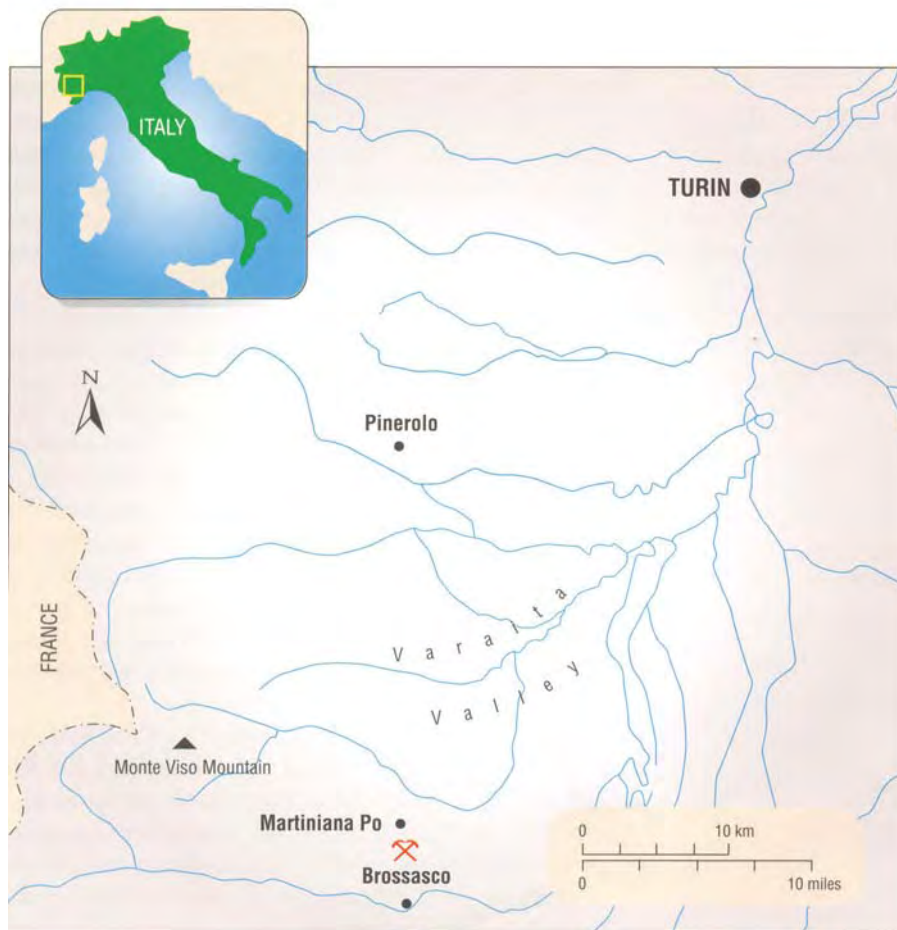


Figure 2. Pyrope is mined from several outcrops over an extended area (about 15 km long) near the villages of Brossasco and Martiniana Po.



Figure 3. The pyrope crystals (here, 4 cm across) are typically formed by rounded trapezohedron faces that are covered by a thin layer of white to pale green phengite. The crystals are heavily fractured (see inset; the larger specimen weighs 30 grams), although some contain clear portions that can be faceted into attractive gemstones. Specimens from the L. Merlo Pich collection; photos by R. Appiani.

provided fragments (from the same crystals used to facet some of the gems) for electron-microprobe and X-ray diffraction analyses.

The following tests were conducted on all 11 of the faceted gems. Refractive indices were measured on a Krüss refractometer with a monochromatic sodium-equivalent light source. Specific gravity was measured by the hydrostatic method, with a Sauter MC1 RC 210 D digital balance (three sets of measurements per sample). We observed internal features with a stereozoom microscope (up to 50×

Figure 4. Eight of the Dora Maira pyropes used in this study (0.24–0.50 ct) were photographed with Macbeth Spectralight (daylight equivalent, 6500K) illumination. Courtesy of the Natural History Museum of Milan; photo by A. Donini.



magnification), using several illumination techniques. We made color measurements using Munsell color charts and a Macbeth Spectralight (daylight equivalent, 6500 K). We tested for ultraviolet fluorescence with 8 watt short-wave (254 nm) and long-wave (365 nm) UV lamps.

Absorption spectra of all the faceted samples were obtained with a Lambda 9 Perkin-Elmer UV-Vis spectrophotometer. Infrared spectra of all samples were measured with a Nicolet 510 spectrometer at a resolution of  $2\text{ cm}^{-1}$ . To identify the mineral inclusions, we used a Renishaw 1000 laser Raman microspectrometer with an Ar163-C4210 Spectra Physics laser source. Quantitative chemical analyses were performed on 10 pyrope fragments with an ARL-SEMQ electron microprobe that was equipped with a wavelength-dispersive X-ray spectrometry unit. To identify some of the inclusions in the fragments, we performed single-crystal X-ray diffraction analysis using an Enraf-Nonius CAD4 diffractometer.

## RESULTS AND DISCUSSION

**Visual Appearance.** The faceted pyropes were purple to purplish pink in hue, with very low to moderate saturation. We obtained Munsell color values of 2.5RP 9/2, 5RP 8/4 to 7/4, 5RP 9/2 to 9/1, and 10RP 7.5/4 (table 1). In many of the gems, the color was not homogeneously distributed. All of our samples showed some color (in both fluorescent and incandescent light), although near-colorless gem pyrope is known from the Brossasco area.

**Physical Properties.** The refractive indices ranged from 1.717 to 1.730, with the lowest values measured on the palest samples (again, see table 1). The low values come close to the R.I. (1.714) reported by Deer et al. (1992) for a natural pyrope with a near-end-member composition, and approach the theoretical end-member value of 1.705 reported by Webster (1994). The range of R.I. values obtained in this study correlates to the iron content (manganese is close, and chromium is below, the detection limit of the electron microprobe for these elements, which is 0.02 wt.% oxide).

Specific gravity ranged from 3.58 to 3.67; in general, the lowest values were obtained for the palest stones. The lowest value is identical to that reported in the literature for a near-end-member pyrope (Deer et al., 1992), but is significantly higher than the 3.51 reported by Webster (1994) for the theoretical end member. The highest S.G. values

correspond to the greatest concentrations of iron. However, some gemstones with a moderately intense purplish pink color contained abundant heavy inclusions (rutile), which prevents a straightforward correlation between specific gravity and chemical composition.

All of the samples were inert to both short- and long-wave UV radiation.

**Internal Features.** Microscopic examination with cross-polarized light revealed undulatory extinction in some areas of the pyrope gemstones (figure 5), which is apparently due to strain caused by tectonic deformation subsequent to peak metamorphism (see, e.g., Hofmeister et al., 1998).

The pyrope samples contained several types of microcrystalline inclusions (see, e.g., figure 6), most of which we were able to identify by Raman analysis. Crystals of rutile were commonly disseminated throughout the gemstones. These minute crystals

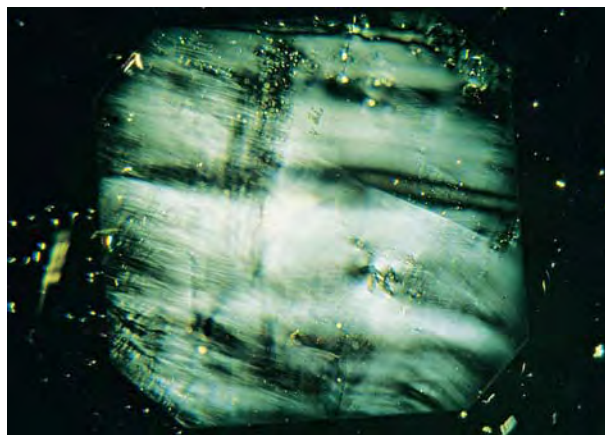


Figure 5. Undulatory extinction was seen in some areas of the Dora Maira pyropes with cross-polarized light. Photomicrograph by A. Donini, magnified 50 $\times$ .

were translucent dark orange (figure 7), or metallic black with dark red internal reflections (figure 8). Apatite occurred as colorless subhedral crystals with a rounded shape. Swarms of extremely thin laminar crystals, usually formed along small healed fractures, were identified as mica (probably phen-gite; see figure 9). Also present were colorless elongated subhedral zircon crystals (figure 10). Infrequently seen were thin, colorless, rectangular kyanite crystals.

Some extremely thin, needle-like, parallel inclusions could not be identified (figure 11). No fluid inclusions were observed in the cut samples.

Figure 6. A variety of mineral inclusions were present in the Dora Maira pyropes (here, 0.49 ct). Courtesy of the Natural History Museum of Milan; photo by R. Appiani.



**TABLE 1.** Properties of sample pyropes from the Dora Maira Massif, Italy.

Weight (ct)	Color (Munsell)	R.I.	Specific gravity	UV-Vis absorption bands (nm)
0.76	Pale purplish pink (2.5 RP 9/2)	1.717	3.61	Fe <sup>2+</sup> : 502, 522, 575 Mn <sup>2+</sup> : 365, 419, 460
0.27	Pale purplish pink (5RP 9/2)	1.718	3.58	Fe <sup>2+</sup> : 495, 525, 579 Mn <sup>2+</sup> : 363, 396, 421, 437, 458
0.32	Pale purple to purplish pink (5RP 9/2 to 9/1)	1.718	3.59	Fe <sup>2+</sup> : 501, 522, 575 Mn <sup>2+</sup> : 421
0.50	Pale purplish pink (5RP 9/2)	1.719	3.59	Fe <sup>2+</sup> : 503, 523, 577 Mn <sup>2+</sup> : 365, 377, 397, 422
0.26	Pale purplish pink (5RP 9/2)	1.719	3.62	Fe <sup>2+</sup> : 522, 577 Mn <sup>2+</sup> : 367, 419, 479
0.28	Pale purplish pink (5RP 8/4)	1.719	3.63	Fe <sup>2+</sup> : 502, 524, 575 Mn <sup>2+</sup> : 366, 419, 460
0.49	Pale purplish pink (5RP 9/2)	1.720	3.62	Fe <sup>2+</sup> : 502, 524, 576 Mn <sup>2+</sup> : 394, 421, 462
0.25	Pale purplish pink (5RP 8/4)	1.720	3.64	Fe <sup>2+</sup> : 503, 521, 575 Mn <sup>2+</sup> : 365, 398, 422, 458
0.24	Pale purplish pink to grayish purplish pink (5RP 8/4 to 7/4)	1.721	3.66	Fe <sup>2+</sup> : 503, 522, 576 Mn <sup>2+</sup> : 365, 398, 422, 458
0.85	Moderate purplish pink (10RP 7.5/4)	1.728	3.67	Fe <sup>2+</sup> : 503, 523, 575 Mn <sup>2+</sup> : 367, 420, 479
0.60	Moderate purplish pink (10RP 7.5/4)	1.730	3.67	Fe <sup>2+</sup> : 495, 525, 579 Mn <sup>2+</sup> : 366, 398, 421, 462

<sup>a</sup>For comparison, Stockton (1988) reports R.I. values of 1.714–1.742 and absorption bands at 410, 421, 430, 504, 520, and 573 nm for colorless to light orange and pink pyropes.

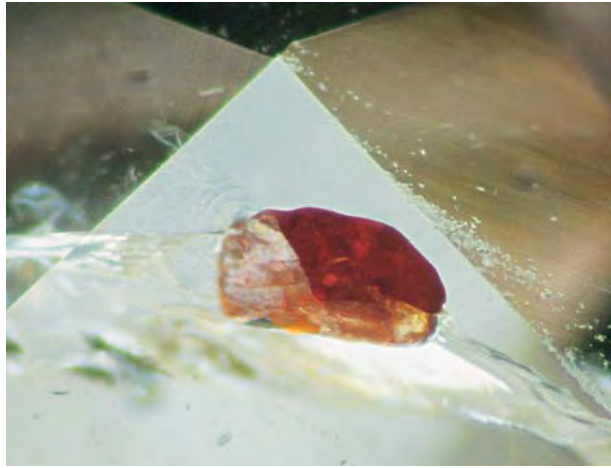


Figure 7. This translucent dark orange rutile inclusion in a Dora Maira pyrope measures 0.22 mm long. Photomicrograph by A. Donini.

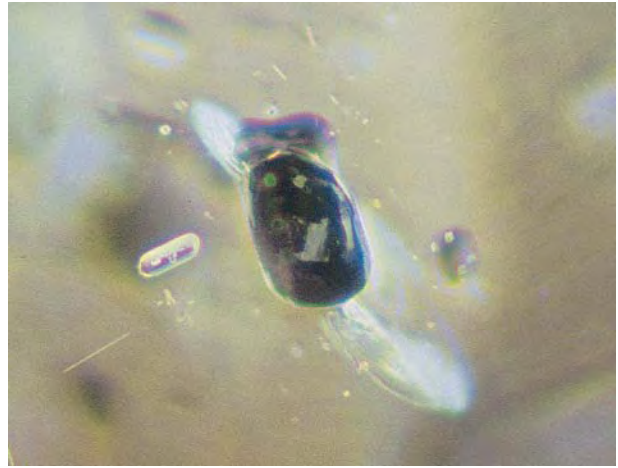
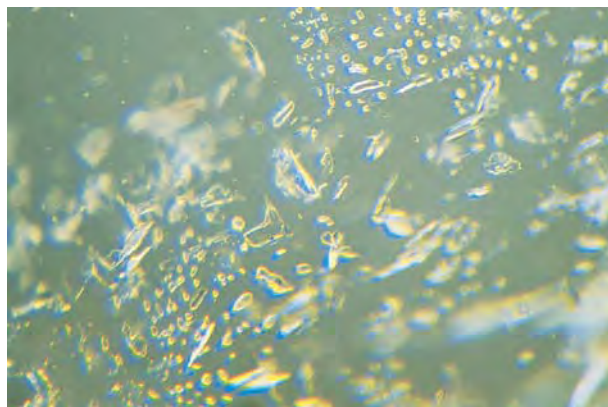


Figure 8. Rutile inclusions in the pyropes also appeared metallic black (here, 0.18 mm long), sometimes with dark red internal reflections. Photomicrograph by A. Donini.

Elongate (up to 0.15 mm) pinkish purple crystals were seen in one of the stones, but we could not identify them by Raman analyses because there was no matching spectrum in our Raman library. We selected inclusions with the same appearance from the rough pyrope fragments left after cutting this stone (figure 12), and identified them as ellenbergerite using X-ray diffraction analysis. This very rare silicate of magnesium, aluminum, titanium, and zirconium was described for the first time by Chopin et al. (1986) from rocks at Martiniana Po.

**Absorption Spectra and Chemistry.** Absorption bands measured with the UV-Vis spectrophotometer are reported in table 1 and shown in figure 13.

Figure 9. Formed along small healed fractures, these thin laminar inclusions were identified by Raman analysis as mica (probably phengite). The field of view is 1.2 mm wide; photomicrograph by A. Donini.



As indicated by Stockton (1988), bands around 501–503 and 521–524 nm can be correlated to  $\text{Fe}^{2+}$ , while those at 419–422 nm are related to  $\text{Mn}^{2+}$ . Other bands listed in table 1 are related to  $\text{Fe}^{2+}$  (i.e., 495 and 575–579 nm) or  $\text{Mn}^{2+}$  (i.e., 363–365, 398, and 458–462 nm). Rossman et al. (1989) studied the infrared spectra of Dora Maira pyrope, and found four sharp bands in the  $3660\text{--}3600\text{ cm}^{-1}$  region due to a hydrous component that has not been reported in pyrope from other localities. The same IR features were obtained on our samples (see, e.g., figure 14).

Electron microprobe analyses of four purplish pink (low to moderate saturation) gem-quality pyrope fragments are presented in table 2, together

Figure 10. This colorless elongated zircon inclusion measures 0.20 mm long. Photomicrograph by A. Donini.





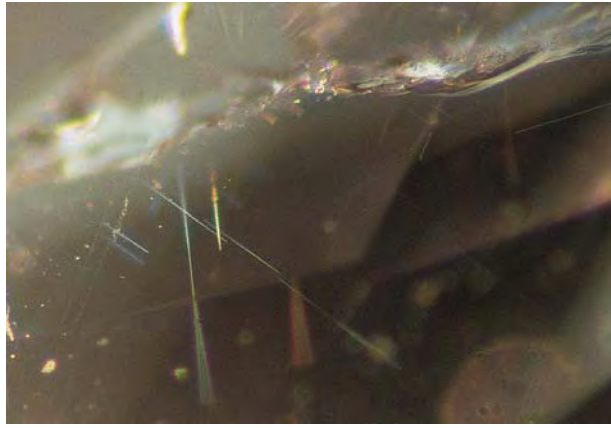


Figure 11. These extremely thin, needle-like inclusions could not be identified. The field of view is 0.07 mm wide; photomicrograph by A. Donini.

with analyses on two areas of a single Dora Maira crystal reported by Chopin (1984) for comparison. The pyrope shows the following range in composition: 87.8–97.5 mol.% pyrope, 1.8–10.2 mol.% almandine, and 0.2–2.6 mol.% grossular. Our results suggest that the color is strongly influenced by the iron content, with the darker gemstones having greater FeO (up to 5.18 wt.%).

#### IDENTIFICATION OF DORA MAIRA PYROPE

Pyrope gemstones with a near-end-member composition are very unusual, and the pale-colored

Figure 13. This representative UV-Vis absorption spectrum of purplish pink pyrope from the Dora Maira Massif shows bands that can be correlated to Fe<sup>2+</sup> (e.g., 501–503 and 521–524 nm) and Mn<sup>2+</sup> (e.g., 419–422 nm).

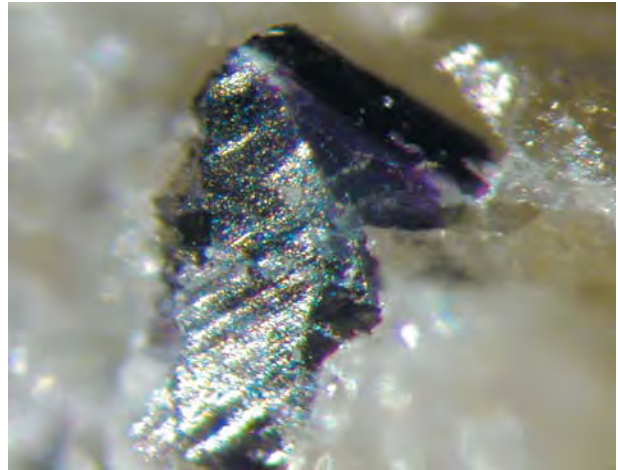
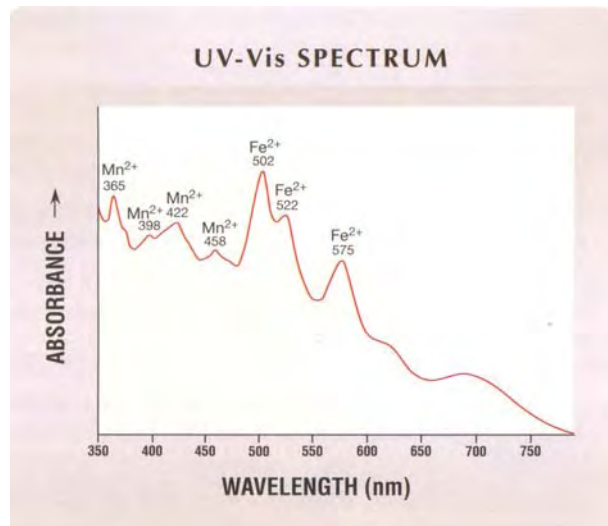
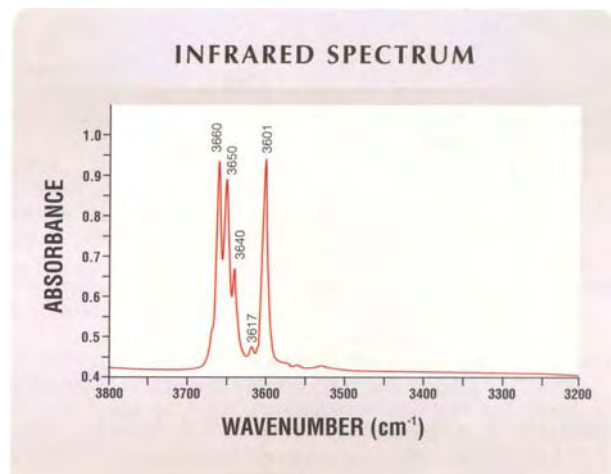


Figure 12. The rare mineral ellenbergerite (here, 0.2 mm long) was identified as inclusions in pyrope from the Dora Maira Massif. Photomicrograph by A. Guastoni.

stones from Dora Maira—which are unfamiliar to most gemologists—are commonly misidentified as grossular. However, these garnets can be separated correctly on the basis of their visible spectrum and refractive indices, as indicated by Stockton (1988). The refractive indices of the Dora Maira pyropes we examined here approach the lowest R.I. values reported for pyrope by Stockton (1988). Furthermore, the UV-Vis absorption spectrum and characteristic inclusions provide additional criteria for the identification of Dora Maira pyrope. The infrared spectra show four sharp bands in the

Figure 14. The four sharp bands in this infrared spectrum (3660–3600 cm<sup>-1</sup> range) are unique to pyrope from Dora Maira.



**TABLE 2.** Electron microprobe analyses of pyrope from the Dora Maira Massif, Italy.

Hue	Purplish pink <sup>a</sup>	Purplish pink <sup>b</sup>	Purplish pink <sup>c</sup>	Purplish pink <sup>d</sup>	Not reported <sup>e</sup>	Not reported <sup>f</sup>
Saturation	Low	Low	Low to moderate	Moderate		
Oxide (wt.%)						
SiO <sub>2</sub>	44.46	44.13	44.02	43.52	45.21	45.13
TiO <sub>2</sub>	0.02	0.01	0.04	0.03	0.00	0.02
Al <sub>2</sub> O <sub>3</sub>	26.07	25.81	25.72	25.61	25.55	25.39
FeO <sup>g</sup>	1.48	2.50	3.33	5.18	0.91	1.35
MnO	0.02	0.05	0.05	0.08	0.02	0.03
MgO	27.97	27.16	26.41	25.02	28.83	28.98
CaO	0.59	0.61	0.94	0.77	0.28	0.09
Total	100.61	100.27	100.51	100.21	100.80	100.99
Mol.% end-members						
Pyrope	95.7	92.6	91.2	87.8	97.5	97.2
Almandine	2.9	4.8	6.4	10.2	1.8	2.6
Grossular	1.5	2.6	2.4	2.0	0.7	0.2

<sup>a</sup> Average of 6 analyses of crystal fragments from the same material as the 0.27, 0.32, and 0.76 ct gemstones in table 1.

<sup>b</sup> Average of 10 analyses of crystal fragments from the same material as the 0.26, 0.49, and 0.50 ct gemstones in table 1.

<sup>c</sup> Average of 7 analyses of crystal fragments from the same material as the 0.24 and 0.25 ct gemstones in table 1.

<sup>d</sup> Average of 9 analyses of crystal fragments from the same material as the 0.60 and 0.85 ct gemstones in table 1.

<sup>e</sup> From Chopin (1984): rim of a 2 mm pyrope crystal.

<sup>f</sup> Core of the crystal mentioned in footnote e.

<sup>g</sup> Total iron as FeO.

3660–3600 cm<sup>-1</sup> region that are unique for this pyrope, and inclusions of ellenbergerite provide unequivocal evidence that a pyrope is from Dora Maira.

## REFERENCES

- Chopin C. (1984) Coesite and pure pyrope in high-grade blueschists of the Western Alps: A first record and some consequences. *Contributions to Mineralogy and Petrology*, Vol. 86, pp. 107–118.
- Chopin C., Klaska R., Medenbach O., Dron D. (1986) Ellenbergerite, a new high-pressure Mg-Al-(Ti,Zr)-silicate with a novel structure based on face sharing octahedra. *Contributions to Mineralogy and Petrology*, Vol. 92, pp. 316–321.
- Deer W.A., Howie R.A., Zussman J. (1992) *An Introduction to the Rock-Forming Minerals*, 2nd ed. Longman Scientific & Technical, Essex, England.
- Franchi S. (1900) Sopra alcuni giacimenti di rocce giadeitiche nelle Alpi occidentali e nell'Appennino ligure. *Bollettino. Regio Comitato Geologico Italiano*, Vol. 4, pp. 119–158.
- Hofmeister A.H., Schaal R.B., Campbell K.R., Berry S.L., Fagan T.J. (1998) Prevalence and origin of birefringence in 48 garnets from the pyrope-almandine-grossularite-spessartine quater-

## CONCLUSION

Pyrope from the Dora Maira Massif has been faceted into pale purple to purplish pink gemstones that rarely exceed 1 ct. Although production to date has been minor, these gem pyropes add to the gemological significance of the Alpine area, with their unusual color and attractiveness.

The deposit appears to be extensive, but future production will undoubtedly continue to be limited by environmental restrictions on mining. Currently, about 100 carats per year enter the marketplace, and no more than a few hundred carats have been cut. Much of the faceted pyrope is sold to private gem collectors, with only a few having been set in jewelry.

## ABOUT THE AUTHORS

Dr. Guastoni (guastoni@yahoo.com) is assistant curator of mineralogy, and Dr. Pezzotta is curator of mineralogy, at the Natural History Museum of Milan, Italy. Dr. Superchi is director of CISGEM, the Gemological Centre of the Milan Chamber of Commerce. Dr. Demartin is professor in the Department of Structural Chemistry and Inorganic Stereochemistry, University of Milan.

**ACKNOWLEDGMENTS:** The authors thank the staff members at the CISGEM laboratory (in particular, Eng. Antonello Donini) for Raman analyses, UV-Vis and FTIR spectroscopy, and photomicrography. The National Research Council (CNR) Center for the Study of Alpine and Quaternary Geodynamics (Milan, Italy) is thanked for allowing access to their electron microprobe.

Also thanked are mineral collector L. Merlo Pich, who provided information about the locality and loaned some of the rough and cut pyrope for study, and Roberto Appiani, who photographed the pyropes.

This manuscript benefited from constructive reviews by three referees.

- ary. *American Mineralogist*, Vol. 83, pp. 1293–1301.
- Mandarino J.A. (1999) *Fleischer's Glossary of Mineral Species*. Mineralogical Record, Tucson, Arizona, 225 pp.
- Rossmann G.R., Beran A., Langer K. (1989) The hydrous component of pyrope from the Dora Maira Massif, Western Alps. *European Journal of Mineralogy*, Vol. 1, pp. 151–154.
- Schert H.P., Medenbach O. (1994) Coesit-führender-Pyrop-Quarzit-ein spektakuläres Gestein aus dem Dora-Maira-Massiv in den Westalpen. *Mineralien Welt*, No. 1, pp. 14–16.
- Stella A. (1895) Sul rilevamento geologico eseguito nel 1894 in Valle Varaita (Alpi Cozie). *Bollettino Regio Comitato Geologico Italiano*, Vol. 26, pp. 283–313.
- Stockton C.M. (1988) Pastel pyropes. *Gems & Gemology*, Vol. 24, No. 2, pp. 104–106.
- Vialon P. (1966) *Etude Géologique du Massif Cristallin Dora Maira, Alpes Cottiniennes Internes, Italie*. M.S. thesis, University of Grenoble.
- Webster R. (1994) *Gems—Their Sources, Descriptions and Identification*, 5th ed. Revised by P.G. Read, Butterworth-Heinemann, London.

# JEREMEJEVITE: A GEMOLOGICAL UPDATE

By Kenneth Scarratt, Donna Beaton, and Garry DuToit

The submission of a large (4.54 ct) jeremejevite of an unusual—yellow—color to the AGTA Gemological Testing Center prompted a search of the available gemological literature and a detailed examination of five additional samples to learn more about this rare gemstone. It was found that the information in some English-language texts was either confusing or contributed little to our gemological knowledge. The authors confirm the available standard gemological properties and add pertinent data for the UV-visible, infrared, and Raman spectra, as well as for trace elements measured by EDXRF.

In November 2000, we encountered a light yellow stone that reportedly had been mined from Cape Cross, Swakopmund, Namibia (figure 1). Testing revealed all the gemological properties of jeremejevite ( $\text{Al}_6\text{B}_5\text{O}_{15}[\text{F},\text{OH}]_3$ ). The process of identifying this stone led to the current study of this relatively rare gem material, which typically is blue.

Jeremejevite was discovered in the late 19th century and named after Pavel V. Jeremejev, a Russian mineralogist and engineer (Arem, 1987). Most recorded faceted material is under 2 ct, but stones up to 5 ct are possible (Arem, 1987). Until relatively recently, the only two known localities for jeremejevite were at Mt. Sektuj, Transbaikal region, Russia (the type locality; Damour, 1883; Foord et al., 1981) and Cape Cross, Swakopmund, Namibia (Strunz and Wilk, 1974; Bank and Becker, 1977; Hertig and Strunz, 1978; Foord et al., 1981). Since the early 1980s, however, deposits have been reported from

four localities in the Eifel volcanic area of Germany, where small or micro-crystals are found (Beyer and Schnorrer-Koehler, 1981; Rondorf and Rondorf, 1988; Blass and Graf, 1999); from the southwestern Pamirs (Ananyev and Konovalenko, 1984); and from the Fantaziya and Priyatnaya pegmatite veins of the eastern Pamirs in eastern Tajikistan (Peretyazhko et al., 1999; Zolotarev et al., (2000); J. Hyrsl, pers. comm., 2001). Earlier this year, an exciting new deposit was discovered in Namibia, about 180 km east of Cape Cross in the Erongo Mountains near Usakos (Gebhard and Brunner, 2001).

The gemological literature contains very little



Figure 1. This 4.54 ct jeremejevite of unusual color is reportedly from Cape Cross, Namibia. The stone measures  $14.89 \times 7.01 \times 4.25$  mm. Photo by Sriurai Scarratt.

See end of article for author information and acknowledgments.  
GEMS & GEMOLOGY, Vol. 37, No. 3, pp. 206–211  
© 2001 Gemological Institute of America

Figure 2. These five jeremejevites were part of the study sample. Two of the predominantly blue stones (2.65 and 0.97 ct) are reportedly from Namibia (the locality of the third blue stone—1.56 ct—is unknown), and the two yellow jeremejevites (0.26 and 0.28 ct) are from eastern Tajikistan. Photo by Sriurai Scarratt.



information on jeremejevite, and most of the available publications list the color as being a blue similar to that of aquamarine (see Liddicoat, 1973, 1976; Webster, 1994). Arem (1987) recorded colorless, pale blue-green, and pale yellow-brown jeremejevite. Strunz and Wilk (1974) refer to the color of the material from Cape Cross as “cornflower” blue. Foord et al. (1981) also report “cornflower” blue as the color of jeremejevite from Cape Cross, and mention colorless material from the same locality.

Therefore, we decided to investigate this unusually colored jeremejevite from Namibia and compare it to other yellow jeremejevites from Tajikistan and some blue jeremejevites. We also took the opportunity to perform advanced testing, to characterize the material further.

#### MATERIALS AND METHODS

Six samples were examined for this report: The 4.54 ct light yellow jeremejevite reportedly from Cape Cross that came into the AGTA Gemological Testing Center in late 2000 (again, see figure 1); two blue jeremejevites from Namibia that weighed 2.65 and 0.97 ct (GIA collection nos. 5721 and 183); another blue jeremejevite of unknown origin, which weighed 1.56 ct (GIA collection no. 3958); and two yellow jeremejevites (0.26 and 0.28 ct) from the Fantaziya pegmatite in eastern Tajikistan that are in the collection of the senior author (figure 2). All six samples were tested by the standard and advanced methods described below.

Refractive indices were taken with a standard GAGTL (Gemmological Association of Great Britain Gem Trade Laboratory) refractometer illuminated with a monochromatic sodium-equivalent light source. Specific gravity determinations were

made hydrostatically (three sets of measurements per sample) with a Mettler CB203 electronic balance. Microscopic observations were made with a GIA GEM Instruments Gemolite microscope.

Ultraviolet-visible (UV-Vis) absorption spectra were recorded with a Unicam UV 500 spectrometer set to a 2.0 nm bandwidth, 120 nm/minute scan speed, and 1 nm data interval. All samples were analyzed over the range 190–900 nm, both parallel and perpendicular to the c-axis. Infrared spectra in the range of 7500–400  $\text{cm}^{-1}$  were recorded with a Nicolet Magna-IR 560 Fourier-transform infrared (FTIR) spectrometer set to 500 scans at a resolution of 4  $\text{cm}^{-1}$ , in transmittance mode. We recorded Raman spectra with a Renishaw Raman 1000 microscope system, using a 1  $\mu\text{m}$  analysis area with an argon-ion laser excitation wavelength of 514.5 nm. Chemistry was determined qualitatively with an EDAX DX95 energy-dispersive X-ray fluorescence (EDXRF) unit at 35 kV and 450  $\mu\text{A}$ , using a standard detector and a collection period of approximately 20 minutes.

#### RESULTS AND DISCUSSION

**Visual Appearance.** As illustrated in figures 1 and 2, each of the stones examined was step-cut. All were transparent. The three stones from the GIA collection had a similar banded, almost parti-colored, appearance that consisted of both wide and narrow light blue bands set against a colorless background for an overall blue appearance. The two stones from Tajikistan were an evenly distributed light yellow in color, and the 4.54 ct stone reportedly from Cape Cross also was light yellow but more saturated than the two from Tajikistan.

Dichroism in the blue jeremejevites was distinct:

**TABLE 1.** Optical properties and specific gravity for the six jeremejevites examined.

Property	0.28 ct yellow from Tajikistan	0.26 ct yellow from Tajikistan	4.54 ct light yellow from Namibia <sup>a</sup>	2.65 ct blue from Namibia (GIA 5721)	0.97 ct blue from Namibia (GIA 183)	1.56 ct blue locality unknown (GIA 3958)
Refractive index						
$n_{\epsilon}$	1.641	1.642	1.641	1.640	1.640	1.640
$n_{\omega}$	1.650	1.651	1.650	1.649	1.649	1.649
Birefringence	0.009	0.009	0.009	0.009	0.009	0.009
Specific gravity	3.31	3.31	3.27	3.31	3.30	3.28

<sup>a</sup>Locality as reported by the client.

blue and near-colorless. It was weak in the yellow samples: light yellow and near colorless.

**Refractive Indices and Specific Gravity.** The refractive index and specific gravity data for all the stones (table 1) were consistent with previously published ranges. For the refractive indices, the lower limit was 1.640 and the upper limit was 1.651. The birefringence was constant at 0.009. Specific gravity ranged from 3.27 to 3.31.

Webster (1994) in his identification tables (p. 898) lists jeremejevite as having a uniaxial optic character with a negative optic sign, and refractive indices of 1.639–1.648 (birefringence 0.009). However, in his text (p. 346) he states that jeremejevite belongs to the orthorhombic system (implying a biaxial optic character) and has a pseudo-hexagonal habit. Liddicoat (1973) also states that jeremejevite is uniaxial negative, but with indications of being biaxial with a very small 2V angle. These bewildering anomalous optical properties are explained by Foord et al. (1981) as being related to growth zoning in jeremejevite: The optic character of the rim of a crystal is different from that of the core. They state that the material from Mt. Sektuj consists of a biaxial core and a uniaxial rim; whereas the situation is reversed in jeremejevite from Cape Cross, which has a uniaxial core and a biaxial rim. Ananyev and Konovalenko (1984) expand on this further. However, for the stones reported here (possibly because fashioning removed the rim), there was no difficulty in obtaining clear and unambiguous R.I. measurements; all of the samples were uniaxial. Because the optical data are very similar to those of apatite, Foord et al. (1981) suggest that some confusion in identification might occur unless care is taken. However, the smaller birefringence of apatite, generally 0.002 to 0.004, should clearly separate it from jeremejevite.

**Features Seen with the Microscope.** All of the stones examined for this study contained healing “feathers.” Strunz and Wilk (1974) also reported healing feathers as well as (unidentified) included crystals in jeremejevite from Cape Cross. We were unable to locate any other gemological references to inclusions in jeremejevite.

A series of growth features that resembled “steps” similar to those sometimes seen in chrysoberyl (Webster, 1994) were observed in several stones. These features manifested themselves as a “lightning strike” growth phenomenon in one of the blue jeremejevites (figure 3), as well as in the 4.54 ct yellow stone.

Several stones had included crystals, all of which appeared to be the same mineral. The 1.56 ct blue jeremejevite contained a multitude of crystals that were aligned along a plane that ran across the width of the stone and from the table to the keel line.

Figure 3. A “lightning strike” growth phenomenon is seen here in one of the blue jeremejevites from Namibia. Such features are actually a manifestation of “step” growth features, which also were seen in the 4.54 ct yellow stone. Photomicrograph by Kenneth Scarratt; magnified 20 $\times$ .



Raman spectrometry identified these inclusions as feldspar (figure 4).

**Chemical Properties.** The chemical formula of jeremejevite is  $\text{Al}_6\text{B}_5\text{O}_{15}(\text{F},\text{OH})_3$ , and Si, Ga, Be, and Fe and several other elements are reportedly present in minor-to-trace amounts (Foord et al., 1981). The method (EDXRF) used by the authors to obtain chemical data on these jeremejevites cannot detect elements lighter in atomic weight than Na (i.e., B, O, and F) and it is not quantitative. However, such analyses may add useful identification information.

We recorded major Al and traces of Si, Mn, Fe, Cu, Zn, and Ga, although not all of the trace elements were detected in all samples. The most consistently present trace elements (detected in all the stones) were Fe and Ga.

**UV-Vis Spectroscopy.** The UV-Vis absorption spectra for the 4.54 ct light yellow jeremejevite recorded both parallel and perpendicular to the c-axis show a gradual but only slightly increasing absorbance from 400 to 900 nm (figure 5). Below 400 nm, the absorbance increases sharply to a point of total absorbance at about 280 nm (perpendicular to the optic axis). For both spectra, we noted one very weak band between 600 and 700



Figure 4. Feldspar crystals such as this were seen in most of the stones. Here, they occur along a plane in the 1.56 ct blue jeremejevite. Photomicrograph by Kenneth Scarratt; magnified 40 $\times$ .

nm, and another between 400 and 450 nm. Similar spectra were recorded for the other two yellow samples.

For the blue jeremejevites, in all three samples a broad, slight absorbance was noted between 510 and 680 nm and a lesser absorbance between 350 and 450 nm, especially perpendicular to the optic axis (figure 6). Total absorption perpendicular to the optic axis was reached at 284 nm.

If we compare the UV-Vis spectra of the light

Figure 5. The UV-Vis absorption spectra of the 4.54 ct light yellow jeremejevite are comparable to those recorded for the other yellow samples. The absorption edge perpendicular to the optic axis is at about 280 nm.

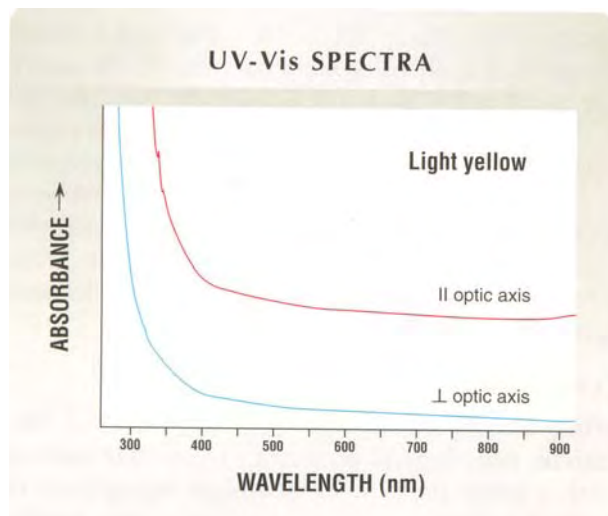
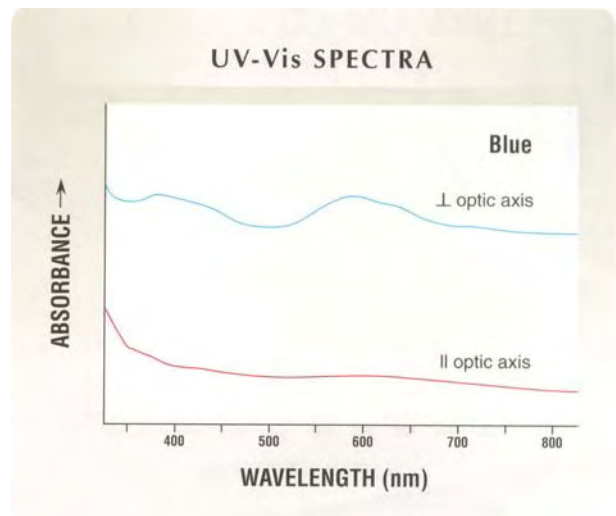


Figure 6. The UV-Vis absorption spectra recorded for the 1.56 ct blue jeremejevite are consistent with those recorded for the other two blue jeremejevites. The absorption edge perpendicular to the optic axis is at 284 nm (not shown).



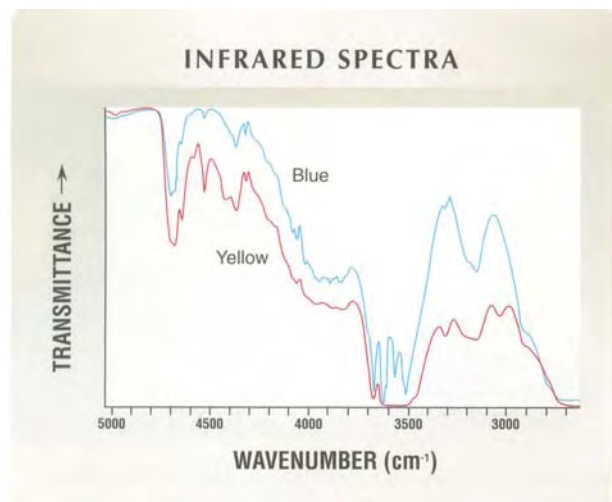
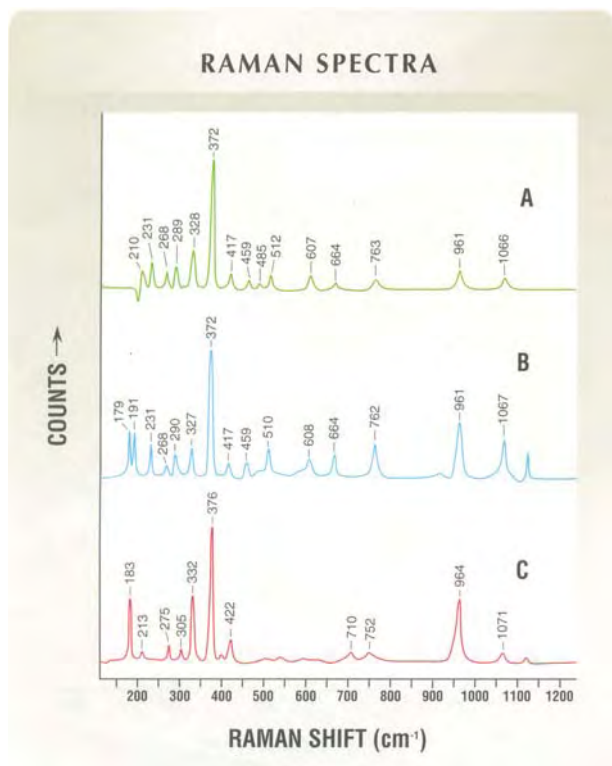


Figure 7. These infrared spectra are representative of those recorded perpendicular to the optic axis for the three yellow and three blue jeremejevites studied.

Figure 8. The Raman spectra for an unoriented blue jeremejevite (A) from the Mineral Spectroscopy Server (2001) is similar to the spectra obtained for the 4.54 ct light yellow stone in directions nearly parallel (B) and perpendicular (C) to the optic axis. Spectrum C shows the variations in peak intensity and position that are due to sample orientation effects.



yellow 4.54 ct (figure 5) and blue 1.56 ct jeremejevites (figure 6) taken perpendicular to the optic axis, it can be seen that the absorption between 510 and 680 nm of the blue jeremejevite is the strongest distinction.

Previously published UV-Vis spectra for jeremejevite have been for those with a blue color (Foord et al., 1981; Mineral Spectroscopy Server, 2001). The spectrum published by Foord et al. is in reflectance mode; it shows two minima at 280 and 600 nm and a maximum at 465 nm, which are responsible for the blue color. The spectrum on the Internet is in absorbance mode and shows a distinct band from approximately 500 to 700 nm and centered at approximately 600 nm.

**Infrared Spectroscopy.** Foord et al. (1981) published near- and mid-infrared spectra for both blue and colorless jeremejevite, and revealed that the relevant ranges were 800 to 2500 nm (4000 to 250  $\text{cm}^{-1}$ ). However, their spectra were obtained from crushed specimens embedded in KBr pellets, and in gemological laboratories normally only nondestructive FTIR analyses are carried out.

In our FTIR analyses of the six samples, we found the most useful data to be between 5000 and 2500  $\text{cm}^{-1}$  (figure 7). The features at 3700–3500  $\text{cm}^{-1}$  recorded in this study resemble those reported by Foord et al. (1981). Below 2500  $\text{cm}^{-1}$  the FTIR features were totally absorbed, so we did not record any of the fine detail that Foord et al. revealed in this region.

**Raman Analysis.** We explored the possibility of a distinctive Raman spectrum and found only one reference: a single spectrum on the Mineral Spectroscopy Server (2001). This spectrum is reproduced from a downloadable data file in figure 8A. Spectra B and C in figure 8 were recorded for the 4.54 ct light yellow jeremejevite in directions nearly parallel and perpendicular to the c-axis. Spectrum B is a near-perfect match with spectrum A, whereas spectrum C shows the variations in peak intensity and position that are due to sample orientation effects. All six stones showed the same Raman spectra for the two orientations.

## CONCLUSION

While faceted jeremejevite appears to have characteristic gemological properties (refractive indices with a lower limit of 1.640 and an upper limit of 1.651, birefringence constant at 0.009, and specific

gravity ranging from 3.27 to 3.31), some of the data reported in standard gemological textbooks might cause confusion.

When gemstones, rare or otherwise, are set in jewelry or other objects, the examination restrictions placed on the gemologist can be formidable. The data gained by more sophisticated yet still nondestructive means can be particularly useful in such situations. The chemical data established the elements that should be present (major Al, and traces of Si, Mn, Fe, Cu, Zn, and Ga in the case of jeremejevite), the FTIR spectra (figure 7)—generated by instrumentation that is now available in major gemological laboratories—revealed areas of absorption that are common to this material, and

the oriented Raman data (figure 8) readily identified this gem mineral as jeremejevite.

#### ABOUT THE AUTHORS

Mr. Scarratt is laboratory director, Mrs. Beaton is a laboratory gemologist, and Mr. DuToit is laboratory manager at the AGTA Gemological Testing Center, New York.

**ACKNOWLEDGMENTS:** The authors appreciate the permission given by Neal Litman, Neal Littman Co., to publish the data on the 4.54 ct yellow jeremejevite. We thank Jo-Ellen Cole of GIA in Carlsbad for loaning the three stones from the GIA collection. The advice and assistance of Tom Moses in the GIA Gem Trade Laboratory is also noted and appreciated. Alan Jobbins is thanked for locating various references and for his overall advice.

#### REFERENCES

- Ananyev S.A., Konovalenko S.I. (1984) Influence of internal stress upon the optical properties of jeremejevite. *Geologiya i Geofizika*, No. 9, pp. 97–103 [in Russian with English abstract].
- Arem J. (1987) *Color Encyclopedia of Gemstones*, 2nd ed. Van Nostrand Reinhold, New York, 118 pp.
- Bank H., Becker G. (1977) Blauer scheifwüdriger Jeremejewit aus SW-Afrika. *Zeitschrift der Deutschen Gemmologischen Gesellschaft*, Vol. 26, No. 3, pp. 161–165.
- Beyer H., Schnorrer-Koehler G. (1981) Jeremejewit-Neufund in der Eifel und die Beteiligung von Bor bei der Minerallbildung in Schlackenauswuerflingen Eifler Vulkane. *Der Aufschluss*, Vol. 32, No. 4, pp. 125–129.
- Blass G., Graf H.-W. (1999) Die Wannenköpfe bei Ochtendung in der Vulkaneifel und ihre Mineralien. *Mineralien Welt*, Vol. 10, No. 6, pp. 20–47.
- Damour M.A. (1883) Note sur un borate d'alumine cristallisé, de la Sibérie. Nouvelle espèce minérale. *Bulletin de la Société Minéralogique de France*, Vol. 6, pp. 20–23; or *Comptes Rendus de l'Académie des Sciences, Paris*, Vol. 96, pp. 675–677.
- Foord E.E., Erd R.C., Hunt G.R. (1981) New data for jeremejevite. *Canadian Mineralogist*, Vol. 19, pp. 303–310.
- Gebhard G., Brunner J. (2001) Mineral News: Jeremejevite from Ameib, Erongo, Namibia—A new and probably the best find ever made. [http://www.mineralnews.de/New\\_finds/Jeremejevite/jeremejevite.html](http://www.mineralnews.de/New_finds/Jeremejevite/jeremejevite.html) [date accessed: 8/16/01].
- Hertig S., Strunz H. (1978) Jeremejewit von Cape Cross in SW-Afrika. *Der Aufschluss*, Vol. 29, No. 2, pp. 45–53.
- Liddicoat R.T. (1973) Developments and highlights at GIA's lab in Los Angeles. *Gems & Gemology*, Vol. 14, No. 5, pp. 144–151.
- Liddicoat R.T. (1976) Developments and highlights at GIA's lab in Los Angeles. *Gems & Gemology*, Vol. 15, No. 5, pp. 138–142.
- Mineral Spectroscopy Server (2001) California Institute of Technology, Division of Geological and Planetary Sciences, Pasadena, California, <http://minerals.gps.caltech.edu> [date accessed: 08/29/01].
- Peretyazhko I.S., Zagorsky V.E., Prokof'ev V.Yu., Gantimurova T.P. (1999) Mirolitic pegmatites of the Kukurt Group of gemstone deposits, central Pamirs: The evolution of physical conditions in the Amazonitovaya vein. *Geochemistry International*, Vol. 37, No. 2, pp. 108–127.
- Rondorf A., Rondorf E. (1988) Jeremejewit von den Wannenköpfen bei Ochtending (Eifel). *Lapis*, Vol. 7, No. 8, pp. 70–82.
- Strunz H., Wilk H. (1974) Jeremejewit als Edelstein aus SW-Afrika. *Zeitschrift der Deutschen Gemmologischen Gesellschaft*, Vol. 23, No. 2, pp. 142–150.
- Webster R. (1994) *Gems—Their Sources, Descriptions and Identification*, 5th ed. Rev. by P.G. Read, Butterworth-Heinemann Ltd., Oxford, England, 1026 pp.
- Zolotarev A.A., Dzhuraev Z.T., Pekov I.V., Mikhailova K.V. (2000) Jeremejevite from pegmatite veins in the Eastern Pamirs. *Proceedings of the Russian Mineralogical Society*, No. 2, pp. 64–70 [in Russian with English abstract].

# GEMS & GEMOLOGY

For regular updates from the world of GEMS & GEMOLOGY, visit our website at:

[www.gia.edu/gandg/](http://www.gia.edu/gandg/)



# Gem Trade LAB NOTES



## Editors

Thomas M. Moses, Ilene Reinitz,  
Shane F. McClure, and Mary L. Johnson  
GIA Gem Trade Laboratory

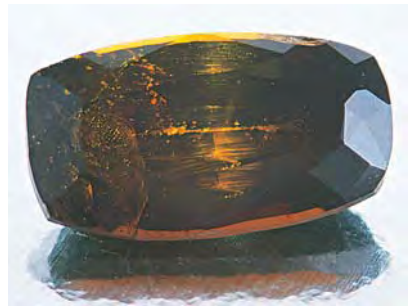
## Contributing Editors

G. Robert Crowningshield  
GIA Gem Trade Laboratory, East Coast  
Karin N. Hurwit, John I. Koivula, and  
Cheryl Y. Wentzell  
GIA Gem Trade Laboratory, West Coast

## BADDELEYITE as a Gemstone

Occasionally, the identification and full documentation of gemological properties for an unusual gem material provides a welcome challenge, and change of pace, for the laboratory gemologist. The requirements of this form of lab work allow gemologists to practice a wide range of laboratory skills that are not always needed to deal with natural-versus-synthetic separations or treatment determinations in commercial gems such as rubies and emeralds. Working with an unusual unknown is in many respects an extreme form of basic gem identification. This is particularly true when the material turns out to be a mineral that has never before been encountered as a gemstone. Such was the case when a partially

Figure 1. At 0.54 ct ( $5.37 \times 3.16 \times 2.27$  mm), this is the first faceted baddeleyite encountered in the Gem Trade Laboratory.



polished piece of very dark greenish brown transparent rough with a sub-metallic luster was sent to the West Coast laboratory. The rough weighed 14.54 ct and measured  $13.21 \times 12.05 \times 7.20$  mm.

With the microscope, we observed both unhealed and partially healed cleavages and fractures. Fiber-optic illumination revealed the presence of fine clouds and tiny pinpoint-size crystals in the form of short stringers. Although the material was over the limits of the refractometer, double refraction was visible with the microscope.

The sample revealed pleochroism in strong dark greenish brown and very dark reddish brown. It was inert to long-wave UV radiation, but showed a weak yellowish green reaction to short-wave UV. There was no chalkiness to the luminescence, and no phosphorescence was observed. Using the hydrostatic method, we determined the specific gravity to be 5.88. Also, using a visible-light spectroscope, we observed total absorption through the blue up to 500 nm.

Laser Raman microspectrometry provided a very close match for baddeleyite, a monoclinic form of zirconium oxide ( $ZrO_2$ ), which is better known to gemologists in its stabilized isometric form as the diamond substitute synthetic cubic zirconia. Energy-dispersive X-ray fluorescence (EDXRF) spectroscopy showed that the unknown sample contained zirco-

nium as a major element, with traces of titanium and hafnium. This fits well with the expected chemistry for baddeleyite.

Shortly after we examined the above-described rough, we received a 0.54 ct rectangular cushion-shaped mixed cut for examination from C. D. (Dee) Parsons, of Santa Paula, California. The very dark greenish to yellowish brown stone (figure 1) was represented to Mr. Parsons as baddeleyite from Sri Lanka. We subjected this stone to the same sequence of tests that we performed on the larger piece of rough. This testing confirmed that the mixed cut was baddeleyite. The only significant differences we observed between the two were a slight variation in color and a hydrostatic specific gravity for the cut stone of 6.07, as compared to 5.88 for the rough sample. This is the first time we have encountered the mineral baddeleyite as a faceted gemstone.

*JIK, Maha Tannous,  
and Sam Muhlmeister*

*Editor's note: The initials at the end of each item identify the editor(s) or contributing editor(s) who provided that item. Full names are given for other GIA Gem Trade Laboratory contributors.*

Gems & Gemology, Vol. 37, No. 3, pp. 212–219  
© 2001 Gemological Institute of America

## CONCH “PEARL,”

### Highly Unusual Necklace Layout

Although conch and other non-nacreous “pearls” are not submitted to the Gem Trade Laboratory as frequently as their nacreous counterparts, we are fortunate to see them intermittently. Recently, we received a layout (i.e., individual undrilled beads selected for use as a strand) that consisted of 75 round conch “pearls” that were graduated from approximately 13.56 mm in the center to 2.57 mm at the ends (figure 2).

Both the number of samples and the range of colors make this layout particularly interesting. The various colors are believed to be caused by organic compounds from the carotenoid group (see E. Fritsch and E. Misiorowski, “The history and gemology of queen conch ‘pearls,’” Winter 1987 *Gems & Gemology*, pp. 208–221). Their shape is another important feature. Fritsch and Misiorowski noted that conch “pearls” are only “very rarely” spherical. Our client revealed that this group took over 15 years to collect, with the most important criterion being the round shape. Since he did not always have access to a measuring device to check the roundness, he made sure each would roll in a straight line before adding it to the collection. An additional difficulty for the client was achieving a size range that would provide a smooth graduation in the strand.

Even though this layout made an ideal graduated necklace, it is very rare to see non-nacreous “pearls” drilled, because the drilling process tends to cause them to develop cracks or actually break into pieces. Nevertheless, our client later informed us that all of these conch “pearls” were drilled successfully, and none was damaged in the process. *TM*

### DATOLITE, 13 ct Yellowish Green

The West Coast lab recently identified another rare gemstone: a 13 ct datolite. This particular stone was remark-



Figure 2. This layout consists of 75 variously colored undrilled conch “pearls” that are graduated from 13.56 mm to 2.57 mm.

able because of its large size, very pleasing color, and unusual cutting style. Colored stones typically are faceted as step or brilliant cuts, or as a combination of these two styles called a mixed cut. This stone, however, was fashioned almost cabochon-like without a table or girdle, just a crown and pavilion (figure 3). The domed crown was covered by a multitude of almost square facets. The pavilion showed two rows of triangular-shaped facets, with the elongated bottom facets coming to a point at the culet. We described it as a faceted buff-top cut.

Datolite is typically colorless or pale yellow or green. In the face-up position, this datolite showed a pleasing yellowish green color overall. On closer visual examination from all angles, however, we noticed that the

Figure 3. This 13 ct datolite was faceted in an unusual cabochon-like style, with squarish facets on the domed crown and triangular facets on the pavilion, to maximize the impact of the color in the culet.



stone was essentially colorless except for a small yellowish green area near the culet. Undoubtedly, this particular cutting style was chosen to maximize the color appearance in the cut stone.

Standard gemological testing revealed the following properties: R.I. of 1.622–1.669, biaxial, no absorption spectrum in the visible range, and inert to UV radiation. We determined the S.G. to be 3.00 using hydrostatic weighing. When we examined the stone with magnification, we noticed just a few scattered fluid inclusions. These properties indicated that the material was datolite. To verify our conclusion, we performed an X-ray diffraction analysis. The pattern we obtained matched that for datolite, thus confirming our identification. Since the library of standard Raman spectra is still incomplete, we took the opportunity to record the Raman spectrum of this datolite for future reference. *KNH*

## DIAMOND Carved "Hamsa" Diamond

The 11.4 ct diamond shown in figure 4 was submitted by Zvi Gluck to the East Coast GIA Gem Trade Laboratory for an identification report. The piece, which was identified as natural diamond by standard testing, was fashioned into the shape of a "Hamsa" (which means *five* in Arabic and Hebrew, referring to the digits of the hand). This is an ancient Mediterranean symbol that represents the protective hand of the creator. A Hamsa often has a single eye, usually made of turquoise and embedded in the middle of the palm, that symbolizes the watchful eye of God. It is also believed to deflect evil. The Hamsa has been used as a good luck symbol for centuries. Typically, it is fashioned to be worn as an amulet or, less commonly, to be used as a wall plaque.

This Hamsa (20.60 × 16.08 × 5.75 mm) has a hollow spot in the palm area where the eye is usually placed, presumably for the addition of another



Figure 4. This 11.4 ct diamond was fashioned in the form of a Hamsa to symbolize the protective hand of the creator and ward off evil.

gem. To create this unusual piece, the cutter first fashioned the rough mechanically with the same bruting tools and wheels that are used to shape fancies and place the groove in heart shapes. Then the two-thumbbed, bilaterally symmetrical form was shaped by a laser. According to Mr. Gluck, the original piece of rough weighed 14.22 ct. Although we did not see the crystal prior to cutting, the high percentage of weight recovery

Figure 5. This 1.58 ct round brilliant is typical of a natural-color black diamond.



indicates that its shape was favorable for fashioning into this distinctive object. With the introduction of laser shaping to diamond manufacturing, we have encountered many fanciful cutting styles over the last 25 years, but this is the first time we have seen a crystal fashioned into a Hamsa.

*TM and Maha Tannous*

## Heat-Treated Black Diamond: Before and After

In the Spring 1971 issue of *Gems & Gemology* (pp. 287–288), Robert Crowningshield discussed and illustrated a 10 ct black diamond. He described the intensely flawed and fractured appearance that for decades we have associated with natural-color black diamonds (see, e.g., figure 5). More recently, R. Kammerling et al. ("An investigation of a suite of black diamond jewelry," Winter 1990 *Gems & Gemology*, pp. 282–287) provided a more thorough description of black diamonds. This account included both treated (through laboratory irradiation) and natural black diamonds, in addition to black diamond simulants. Historically, the principal method of color treatment in black diamonds has been irradiation, and the separation of the treated-color stones from their natural-color counterparts has been relatively straightforward. As a direct

Figure 6. Transmitted light reveals randomly dispersed graphitization, which gives the natural-color black diamond in figure 5 a "salt and pepper" appearance. Magnified 15×.



result of the body color produced by irradiation (actually a very dark green rather than a true black), the irradiated diamonds virtually always show green glints either in the body color or reflecting from a fracture

Over the last several months, however, we have encountered a number of black diamonds (ranging from melee size to several carats) in which the origin of color has been difficult to determine. When these diamonds were examined with a gemological microscope, they did not exhibit either the mottled “salt and pepper” appearance seen in natural-color black diamonds (figure 6) or the hints of green that are characteristic of laboratory-irradiated diamonds. However, these “new” black diamonds consistently revealed low clarity with extensive fracturing. They also showed a black “lining” in most of the surface-reaching fractures (figure 7). Raman analysis revealed that this black lining matched the pattern for graphite.

Although it is not uncommon for graphite to form in fractures and around mineral inclusions in untreated diamonds (again, see Kammerling et al., 1990), we suspected that the blackening of the fractures in these recent stones might not be natural. J. W. Harris and E. R. Vance (“Induced graphitisation around crystalline inclusions in diamond,” *Contributions to Mineralogy and Petrology*, Vol. 35,

*Figure 7. This isolated feather in the pavilion of a heat-treated black diamond displays graphite nucleation predominantly along the fracture plane. Magnified 30×*

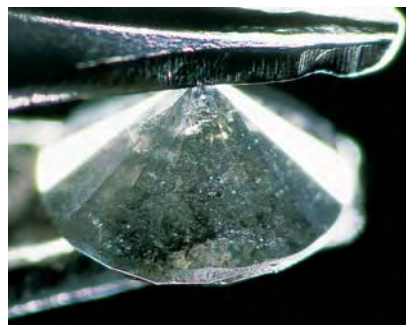


*Figure 8. This 0.085 ct highly fractured “milky white” diamond (left) was submitted to high-temperature treatment in a vacuum. After treatment (right) the diamond appeared black because of the graphitization of surface-reaching fractures.*

1972, pp. 227–234) described how this graphitization might occur naturally in diamonds, and further explained the experimental conditions they used to create similar graphitization in the laboratory.

To help determine whether or not the graphitization within these diamonds was laboratory induced, we conducted experiments to see if we could reproduce the effect. The 0.085 ct milky white diamond on the left in figure 8 is representative of the “before” starting material we used. After a review of the literature, combined with our own empirical knowledge, we chose controlled heating in a vacuum using an electric furnace in the temperature range 900°–1,650°C, for periods ranging from a few minutes to several hours. This was the temperature range discussed by Harris and Vance (1972). We suspect that one could graphitize a diamond more efficiently using high pressure/high temperature (HPHT) conditions, but this would be more complicated and costly, and the tolerance range of treatment conditions outside of the diamond stable region would be quite narrow.

As illustrated in figure 8 (right), the high-temperature treatment produced a predominantly black appearance in the originally white stone. Magnification revealed that the color is caused by the presence of graphite lining the fractures; the adjacent near-colorless

“milky” areas remain unchanged. Unlike natural-color black diamonds, in which the graphitization is randomly dispersed throughout the stone, graphitization in this heat-treated diamond (and others we have examined) is predominantly relegated to areas near the surface of surface-reaching fractures and cleavages. Furthermore, on the basis of the stones we have examined to date, we believe that the initial chemical composition of the diamond (the diamond type) is not a critical factor in the resultant color, unlike the more common HPHT treatments (such as the de-colorization of brown type IIa diamonds).

We are conducting an ongoing research effort to establish additional identification criteria by studying more known natural-color black diamonds and other heat-treated black diamonds that appear on the market, as well as by conducting further “before and after” experiments.

*Matt Hall and TM*

### **Update on Blue and Pink HPHT-Annealed Diamonds**

Recently, Bellataire Diamonds submitted one blue and two pink high pressure/high temperature (HPHT) processed diamonds to the East Coast laboratory (figure 9). This report provides a brief follow-up to the Lab



Figure 9. These fancy-color (one blue and two pink) HPHT-processed diamonds recently submitted to the lab by Bellataire weigh 0.73 ct (left), 4.57 ct (center), and 7.54 ct (right).

Note on 11 pink and four blue HPHT-processed diamonds that was published in the Fall 2000 issue (pp. 254–255). The 7.54 ct pear shape and the 4.57 ct emerald cut appeared to have colors equivalent to GIA color grades Fancy purplish pink and Fancy Deep brownish pink, respectively. The color of the 0.73 ct marquise cut was equivalent to Fancy Intense blue.

The gemological properties (color zoning, reaction to UV radiation, etc.) of these diamonds overlapped those of their natural-color counterparts. Both pink diamonds are type IIa (i.e., they contain a nominal amount of nitrogen), and the blue diamond is type IIb (i.e., it exhibits boron-related absorption peaks in the infrared, and is electrically conductive). However, close

Figure 10. Magnification at 30× reveals etching on one of the pavilion facets of the 7.54 ct diamond. This feature suggests that the diamond was subjected to the extremely high temperatures used in HPHT processing.



examination of the 7.54 ct pear shape revealed an etched and pitted surface on a facet of the pavilion. Although at first this etching appeared similar to the natural surface of a diamond crystal, higher magnification (figure 10) indicated that it was probably the result of the high temperature to which the diamond was exposed to enhance its color. We have noted this feature in other HPHT-processed diamonds. When it is present, careful examination with a microscope provides a clear indication of the process responsible for color enhancement.

Using a Raman microspectrometer equipped with a 514 nm laser, we obtained low-temperature photoluminescence (PL) spectra from each of these diamonds. On the basis of our own criteria, in addition to the criteria published by D. Fisher and R. A. Spits ("Spectroscopic evidence of GE POL HPHT-treated natural type IIa diamonds," Spring 2000 *Gems & Gemology*, pp. 42–49) and C. P. Smith et al. ("GE POL diamonds: Before and after," Fall 2000 *Gems & Gemology*, pp. 192–215), we were able to differentiate the spectra of these diamonds from those in our collection of more than 800 low-temperature PL spectra of natural-color pink and blue diamonds. These results further confirmed the usefulness of low-temperature photoluminescence in the identification of color-enhanced diamonds.

Matt Hall and TM

### Fracture-Filled "Bloodshot" IOLITE

The West Coast lab recently had the opportunity to examine a very unusual example of iolite (the gem variety of the mineral cordierite), which was sent to us by K & K International of Falls Church, Virginia. Iolite itself is not unusual, but this stone displayed strong chatoyancy. Cat's-eye iolite is considered quite rare, and only a few have come through the laboratory (see Lab Notes, Fall 1982, p. 171; and Gem News, Spring 1990, p. 101 and Fall 1990, p. 232). This stone, however, was unusual even for this rare gem mineral.

At 25.98 ct, the oval double cabochon was extremely large for this material, and the eye was sharp, straight, and well oriented. Physical and optical properties matched those previously reported for iolite. The stone was heavily included, with tiny oriented platelets and needles of what is possibly hematite that gave the cabochon a somewhat orange appearance face up. Such material is known as "bloodshot" iolite. The inclusions caused the chatoyancy in this stone, so the eye appeared orange (figure 11).

This combination of factors also probably caused the final unusual feature we observed. The cabochon contained several large fractures, some of which extended almost entirely through the stone from top to bottom; these fractures were quite wide at the



Figure 11. The inclusions (possibly hematite) that cause the chatoyancy in this 25.98 ct “blood-shot” iolite are also responsible for the orange color of the eye.



Figure 12. In reflected light, the filled fractures in this cat’s-eye iolite showed a distinctly lower relief than the rest of the stone. Magnified 24×.



Figure 13. With 40× magnification, the crackled texture of the filler in this large fracture is easily visible among the multitude of reddish platelets and needles that cause the chatoyancy in the host iolite.

surface and were filled with a hardened material. The fractures were probably filled before the stone was cut, so that a larger finished piece could be obtained. In reflected light, the filled areas appeared to have distinctly lower relief (figure 12) than the rest of the stone, and a network of stress fractures was visible throughout most of them. These stress fractures gave the filler a crackled appearance (figure 13), similar to that seen in some fracture-filled diamonds (see, e.g., Kammerling et al., “An update on filled diamonds: Identification and durability,” Fall 1994 *Gems & Gemology*, pp. 142–177).

We have seen filled fractures in many different gem materials, but this was probably the most unusual example to come to our attention.

SFM

### MAW-SIT-SIT Beads

A decorative necklace that featured variously colored round beads alternating with opaque bright green cylindrical carved beads was sent to our West Coast lab for identification of the carved material. These beads averaged approximately 19 mm long × 12 mm in diameter and were intricately carved with different flora and fauna motifs (figure 14). When examined with the unaided eye, each bead appeared to have been carved out of a single homogeneous piece of rough. When we examined the beads with a

gemological microscope at standard magnification, however, it became evident that the material itself was not homogeneous. Using strong overhead illumination, we noticed at least two different types of minerals: (1) a dark green main body mass that was partially fibrous; and (2) areas of a transparent, near-colorless, fine-grained material. The presence of at least two different constituents indicated to us that the bead was carved from a rock.

Because the bead showed a fairly good polish, we were able to obtain a refractive index reading of approximately 1.52 for a near-colorless area and another vague reading in the middle 1.7s for the green portion. There was no absorption spectrum and no reaction to UV radiation. Since initial gemological testing did not provide enough useful information about the material, we turned to advanced testing to identify the constituents. We were able to obtain useful Raman spectra for each component: The spectrum for the green portion matched that listed as ureyite (a bright green chromian pyroxene, for which the accepted name is now kosmochlor), whereas the spectrum for the near-colorless portion matched that of albite feldspar. The refractive indices we had obtained were within the limits for both materials. This type of rock, which contains primarily kosmochlor, albite, and possibly

other minerals, is known among gemologists as maw-sit-sit, after its locality in Myanmar. Dr. Edward Gübelin first described this rock in the Winter 1964–65 issue of *Gems & Gemology* (pp. 227–238, 255). Quite recently, F. Colombo et al. published another detailed study on the mineralogical composition of this attractive rock (*Journal of Gemmology*, Vol. 27, No. 2, 2000, pp. 87–92).

KNH

Figure 14. This 19 × 12 mm carved bead was identified as the rock maw-sit-sit.



## Two Unusual OPALS

Opal is known for its bright, multi-hued play-of-color patterns, which have been given various descriptive names such as “pinfire” and “harlequin.” It is these color patterns that give opal its lasting appeal and value as a gemstone.

Recently, however, the West Coast lab received two opals with an unusual structure to their play-of-color that made them particularly interesting for a gemologist. While the identification of these two opals as natural was routine, the patterning they showed is worthy of further description.

The first opal was a bezel-set freeform cabochon that measured  $37.51 \times 15.68 \times 3.42$  mm (figure 15). It

was submitted by Blaine Buckman of Jonesboro, Arkansas, who believed that it came from the 14-Mile area of Coober Pedy, Australia. This opal showed an unusual, spotted, “leopard” play-of-color pattern that consisted of more-or-less green circular spots against a predominantly orangy red background (again, see figure 15). The pattern may have resulted from opalization of some type of fossil plant. When examined with  $10\times$  magnification and surface incident light, the individual green spots were seen to be lighter green in their centers and darker at the rims (figure 16, left). In transmitted light (figure 16, right), they appeared light brownish orange, again with centers or cores. This is the first time we have encountered this type of

play-of-color pattern in an opal.

Structurally, the second opal was an obvious cell-by-cell wood-to-opal replacement that preserved the macroscopic banded structure of the original wood (figure 17). This 15.10 ct cabochon was cut by Tucson-based lapidary Kevin Lane Smith, from material he obtained at the Rainbow Ridge mine, in Virgin Valley, Nevada. While the play-of-color in this gem was predominantly green, all of the other spectral colors were visible, particularly with magnification. The original cell grain of this opalized wood was also clearly seen when examined with the microscope, and it varied considerably in appearance with viewing direction. Looking perpendicular to the length of the grain, we saw the play-of-color as distinct streaks or compact parallel bands (figure 18). Looking parallel to the length of the grain (as in a cross-sectional view), we observed that the individual opalized cells were lined up in orderly rows (figure 19). It is in this micro-view that the delicate cell-by-cell opalization can be most appreciated.

*JIK and Maha Tannous*

*Figure 15. This bezel-set opal shows an unusual spotted play-of-color that suggests the opal may be a fossil replacement.*

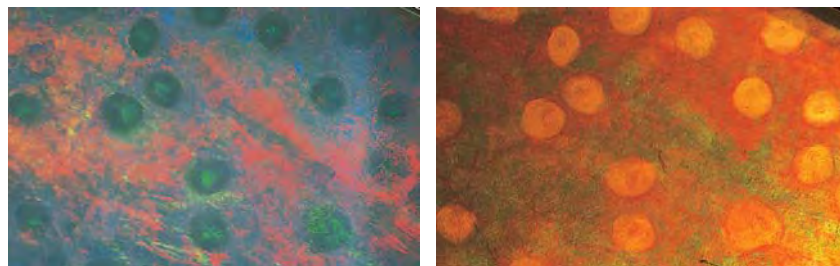


*Figure 16. At  $10\times$  magnification with surface incident illumination (left), the green spots in the opal shown in figure 15 appear darker at their borders and lighter in their centers. In transmitted light (right), the spots appear light brownish orange and have obvious centers or cores, which further suggests that this might be a fossil replacement.*

## Star SAPPHIRE with Two Stars of Two Different Colors

Black asteriated sapphires from Thailand that show distinct “silvery” white six-rayed stars are relatively well known in the gem trade, and they are also relatively common as compared to other colors of star sapphires. Occasionally, however, we see less typical asterism in this material. For example, some stars show 12 rays instead of six, or the star may appear “golden.”

Very recently, gem dealer Elaine Rohrbach of Pittstown, New Jersey, sent an unusual oval black star sapphire to the West Coast lab for examination. Not only did this 1.51 ct double cabochon ( $7.30 \times 6.04 \times 3.05$  mm) show a six-rayed star on each of its opposite sides, but the two stars also had distinctly different colors. The star on one side was the fairly common “silvery” white to very light

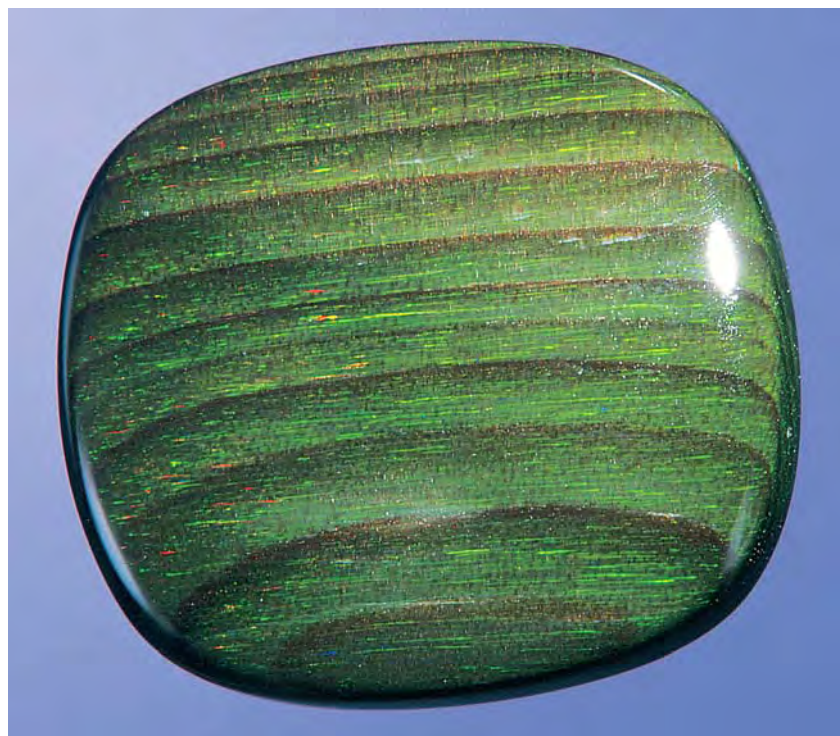


Figure 17. This 15.10 ct cabochon of opalized wood still shows the banded structure of the original wood.

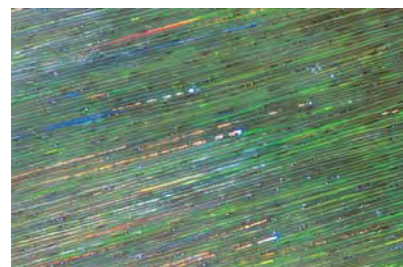


Figure 18. In a view perpendicular to the length of the grain in the 15.10 ct cabochon of opalized wood, the play-of-color is seen as distinct streaks or compact parallel bands. Magnified 35 $\times$ .

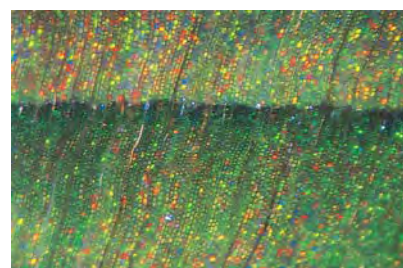


Figure 19. In a cross-sectional view, the individual cells in the opalized wood are clearly lined up in orderly rows. Magnified 35 $\times$ .

brown (figure 20, left), whereas the star on the opposite side was a strong yellow-brown “golden” color (figure 20, right).

Magnification at 10 $\times$  showed that two factors—the depth of the star and the body color of the stone—were responsible for the obvious difference

in color of these two stars. On the side with the “silvery” star, the inclusions causing the asterism were right at the surface, which greatly reduced or eliminated any potential color in the star that might be supplied by the body color of the host. On the side that showed the “golden” star, the

inclusions responsible for the asterism were a considerable distance from the surface, so that perhaps 2 mm of deep yellow-brown transparent sapphire covered the star-causing inclusions. Consequently, the star reflected through this yellow-brown zone took on the body color of the host sapphire. While the potential probably exists for other black star sapphires to be fashioned creatively in this manner, this is the first double-star cabochon of this kind that we have seen.

*JIK and Maha Tannous*

Figure 20. One side of this 1.51 ct (7.30  $\times$  6.04  $\times$  3.05 mm) black star sapphire shows the familiar “silvery” white six-rayed star (left). On the reverse side, the strong yellow-brown body color of the stone imparts its color to the star (right).

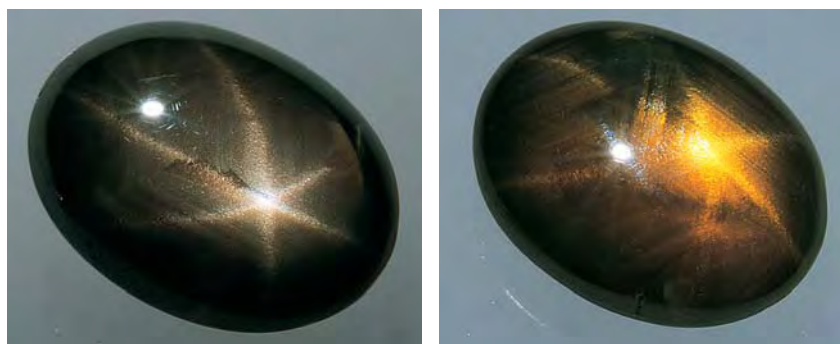


#### PHOTO CREDITS

Maha Tannous—figures 1, 3, 4, 11, 14, 15, 17, and 20; Elizabeth Schrader—figures 2, 5, 8, and 9; Vincent Cracco—figures 6, 7, and 10; Shane F. McClure—figures 12 and 13; John I. Koivula—figures 16, 18, and 19.



# GEMS & GEMOLOGY

## Challenge

### Winners 2001



This year, 285 dedicated readers participated in the 2001 *Gems & Gemology* Challenge. Entries arrived from all corners of the world, as readers tested their knowledge on the questions listed in the Spring 2001 issue. Those who earned a score of 75% or better received a GIA Continuing Education Certificate recognizing their achievement. The participants who scored a perfect 100% are listed below. Congratulations!

AUSTRALIA *Coogee, Western Australia*: Helen Haddy. *Nedlands, Western Australia*: Eleanor Sanders. *Slacks Creek, Queensland*: Ken Hunter  
 ◆ BELGIUM *Diegem*: Guy Lalous. *Diksmuide*: Honoré Loeters. *Hemiksem*: Daniel De Maeght. *Overijse*: Margrethe Gram-Jensen. *Ruiselede*: Lucette Nols ◆ BRAZIL *Rio de Janeiro*: Luiz Angelo ◆ CANADA *Cowansville, Québec*: Alain Deschamps. *Kingston, Ontario*: Brian Smith.  
*Oakville, Ontario*: Alethea Simone Inns ◆ CROATIA *Zagreb*: Sandra Crkvenac ◆ CYPRUS *Nicosia*: George S. Stephanides  
 ◆ CZECH REPUBLIC *Praha*: Karel Mar ik ◆ ENGLAND *Tenteroen, Kent*: Linda Bateley ◆ FRANCE *Paris*: Stephen Perera  
 ◆ GERMANY *Amberg*: Herbig Klaus. *Idar-Oberstein*: Josef Bogacz ◆ HONG KONG *Causeway Bay*: Cristina O. Piercey  
 ◆ INDONESIA *Ciputat, Jakarta*: Warli Latumena ◆ ITALY *Ferrara*: Sonia Franzolin. *Porto Azzurro, Livorno*: Diego Giuseppe Trainini.  
*Valenza*: Rossella Conti. *Vicenza*: Francesca Zen ◆ LITHUANIA *Vilnius*: Saulius Fokas ◆ NETHERLANDS *Rotterdam*: E. van Velzen.  
*Wassenaar*: Jane M. Orsak ◆ POLAND *Lublin*: Marek A. Prus ◆ SCOTLAND *Edinburgh*: James W.M. Heatlie ◆ SPAIN *Burjassot, Valencia*: Luis E. Ochando. *Madrid*: Shahrazad Krewi de Urquijo. *Oviedo, Asturias*: Consuelo Laspra. *Playa P. Farnals, Valencia*: Monika Bergel-Becker. *Port de Sóller, Baleares*: J. Maurici Revilla Bonnin ◆ SRI LANKA *Gampaha*: Nadee Abeykoon ◆ THAILAND *Conburi*: Watcharaporu Keankeo ◆ UNITED STATES *Alabama Mobile*: Lori Bryant. *Arizona Tucson*: David Arens. *California Burlingame*: Sandra MacKenzie-Graham. *Carlsbad*: Marla Belbel, Carl Chilstrom, Michael T. Evans, Diane Flora, William J. Herberts, Mark S. Johnson, Cathy Jonathan, Jan Lombardi, Lynn L. Myers, Diane H. Saito, Abba R. Steinfeld, Richard Taylor, Philip G. York. *Los Angeles*: Veronica Clark-Hudson. *Marina Del Rey*: Veronika Riedel. *Pacifica*: Diana L. Gamez. *Penn Valley*: Nancy Marie Spencer. *Redwood City*: Starla Turner. *Santa Clarita*: Beverly Nardoni-Kurz. *Watsonville*: Janet S. Mayou. *Colorado Colorado Springs*: Barbara Maffei.  
 Connecticut *Simsbury*: Jeffrey A. Adams. **Florida** *Clearwater*: Timothy D. Schuler. *Deland*: Sue Angevine Guess. *Vero Beach*: Lisa N. Perino.  
 Georgia *Buford*: Lisa Hazan. *Decatur*: Ella Golden. **Hawaii** *Makawao*: Alison Fahland. **Illinois** *Danvers*: Anne Blumer, William Duff. *Mokena*: Marianne Vander Zanden. *Northbrook*: Frank Pintz. *Peoria*: John Fitzgerald. **Indiana** *Fishers*: Laura D. Haas. *Indianapolis*: Mark Ferreira.  
 Iowa *West Des Moines*: Frank Herman. **Kansas** *Topeka*: Ann Solcolofsky. **Maine** *South Freeport*: Arthur E. Spellissy, Jr. **Maryland** *Darnestown*: Ron Suddendorf. **Massachusetts** *Braintree*: Alan R. Howarth. *Brookline*: Martin Haske. *Lynnfield*: John A. Caruso. **Michigan** *Saginaw*: Veronica Haldane. **Mississippi** *Hattiesburg*: A. Thomas Light. **Missouri** *Perry*: Bruce L. Elmer. **Nevada** *Las Vegas*: Deborah Helbling. *Reno*: Terence E. Terras. **New Jersey** *Fort Lee*: Lioudmila Tretianova. **New Mexico** *Santa Fe*: Leon Weiner. **New York** *City Island*: Marjorie Kos. *New York*: John Kearney, Wendi M. Mayerson. *Rye*: Gregory J. Cunningham. **North Carolina** *Creedmoor*: Jennifer Jeffreys-Chen. *Manteo*: Eileen Alexanian. *Matthews*: Terry A. Edwards. **Ohio** *Athens*: Colette M. Harrington. *Cuyahoga Falls*: Catherine S. Lee.  
**Oregon** *Salem*: Donald Lee Toney. **Pennsylvania** *Schuylkill Haven*: Janet L. Steinmetz. *Yardley*: Peter R. Stadelmeier.  
**Rhode Island** *Providence*: Sarah A. Horst. **Texas** *Austin*: Judith Darnell, Anne Hawken. *Corpus Christi*: Warren A. Rees.  
**Virginia** *Newport News*: Sonia Brannan. *Sterling*: Donna B. Rios. **Washington** *Poulsbo*: Ruth Jorgensen. *Seattle*: Thomas C. Estervog.  
**Wisconsin** *Beaver Dam*: Thomas G. Wendt. *Milwaukee*: William Bailey



Answers (See pp. 79–80 of the Spring 2001 issue for the questions):

(1) c, (2) b, (3) a, (4) c, (5) b, (6) a, (7) a, (8) d, (9) b, (10) c, (11) c, (12) a, (13) a, (14) c, (15) withdrawn, (16) d, (17) b, (18) d, (19) a, (20) d, (21) b, (22) a, (23) a, (24) c, (25) c



## EDITOR

Brendan M. Laurs (blaurs@gia.edu)

## CONTRIBUTING EDITORS

Emmanuel Fritsch, *IMN, University of Nantes, France* (fritsch@cnrs-immn.fr)

Henry A. Hänni, *SSEF, Basel, Switzerland* (gemlab@ssef.ch)

Kenneth V. G. Scarratt, *AGTA Gemological Testing Center, New York* (kscarratt@email.msn.com)

Karl Schmetzer, *Petershausen, Germany*

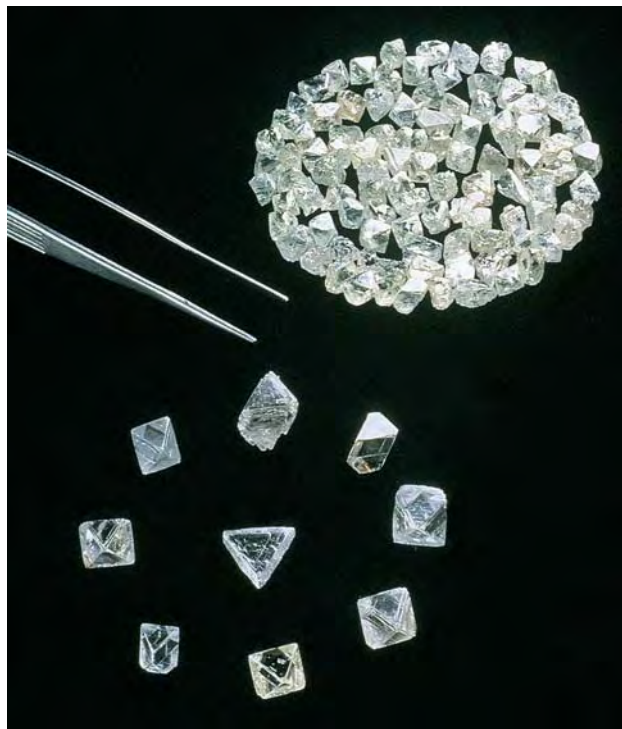
James E. Shigley, *GIA Research, Carlsbad, California* (jshigley@gia.edu)

Christopher P. Smith, *Gübelin Gem Lab, Lucerne, Switzerland* (cpsgg12@hotmail.com)

## DIAMONDS

**Report from the 2nd World Diamond Conference, Vancouver.** On August 22 and 23, 2001, approximately 400 participants from 29 countries converged in Vancouver, British Columbia, Canada for the 2nd World Diamond

*Figure 1. These rough diamonds were recovered during bulk sampling and evaluation of the A-154S pipe at the Diavik mine. Tiffany & Co. has already arranged to purchase some of the diamond production from this mine. Photo courtesy of Diavik Diamond Mines Inc.*



Conference. GNI editor Brendan Laurs attended the conference and provided this report. The well-rounded program consisted of approximately 40 presentations from mining and exploration company executives, mining engineers, government officials and diamond valuers, financial analysts, and international financiers. **Chaim Even-Zohar** (editor-in-chief and publisher, *Mazal U'Bracha Diamonds* and *Diamond Intelligence Briefs*) was the moderator of the conference, which focused mainly on Canadian diamond production, now and in the future.

In his introductory presentation, Mr. Even-Zohar stressed that the industry is in transition due to major changes in the diamond "pipeline" caused by the evolving roles of the traditional major producers and the emergence of new industry leaders (e.g., BHP-Billiton and Rio Tinto) in both mining and merchandising. He introduced the phrase *committed rough* for diamonds (mined or unmined) with a predetermined manufacturing destination—such as, for example, the arrangement by Tiffany & Co. to receive diamonds from the forthcoming Diavik mine in Canada (figure 1). The recent restructuring of De Beers is having a profound influence on the pipeline, as reduction of their diamond stockpile in 2000 contributed to the current overstocking in both the cutting centers and the retail sector. Mr. Even-Zohar also explained the legal challenges facing De Beers's "supplier of choice" initiative to create demand at the consumer level.

**Martin Rapaport** (*Rapaport Diamond Report*) echoed Mr. Even-Zohar's contention that the industry is undergoing fundamental, and irreversible, structural changes as the result of a convergence of factors—in particular, a weak global economy, changes in De Beers, the branding movement, and "conflict" diamonds. He stressed that the future will hold greater market uncertainty in distribution and pricing, with rough prices determined by the prices of polished goods (a reversal of the situation in the past); consequently, rough-diamond producers must add value through marketing. Diamond branding was a recurrent



Figure 2. Construction of the Diavik mine is underway in anticipation of diamond production in early 2003. Three kimberlite pipes (A154N, A154S, and A418) are located beneath Lac de Gras in the foreground, and a fourth pipe (A21) is located under the lake on the far left of the photo. The prominent arcuate structure in the foreground is a rock dike (to be completed in fall 2001) that will be used to hold back the lake surrounding the A154N and A154S pipes to allow for open-pit mining. Silt from dike construction is carefully contained to minimize the environmental impact on the lake. The processing plant (also under construction) and camp are located in the background on the left. The disturbance in the center is a quarry that supplies rock for construction of the dike, and an airstrip is visible on the right. Photo by Jiri Hermann; courtesy of Diavik Diamond Mines Inc.

theme during the conference, and at least one ambitious strategy, still in the formative stage, was outlined in a stimulating presentation by **Lindsey Hughson** of Auris Diamonds (a subsidiary of BHP-Billiton). He proposed a cooperative arrangement involving multiple suppliers to create consumer desire for diamonds through a carefully executed luxury branding campaign.

Conflict diamonds took center stage during a speech by Ohio Congressman **Tony Hall**, who emphasized that "This affects *you*." He reminded the audience that although the Clean Diamonds Bill enjoys widespread support in the U.S. Congress, it has yet to become law (as of October 12, 2001). He stated that the Kimberley Process—an international certification system for controlling the flow of rough—will be crucial to the bill's effectiveness. **Cecilia Gardner** (Jewelers Vigilance Committee) reviewed the "system of controls" that must be followed by countries exporting their rough under this bill. The full text of the pending legislation can be viewed on the Internet at <http://www.worlddiamondcouncil.org>.

Much of the conference was devoted to presentations by diamond explorers and producers, with an emphasis on activities in the world's most important emerging diamond frontier—Canada—which is projected to account for 12%–15% (by value) of world production by 2005. **Dr. Art Ettlinger** of Yorkton Securities estimated that between Can\$800 million and \$1 billion has been spent on diamond exploration in Canada in the last decade. Presentations by executives from several "junior" exploration companies were delivered with enthusiasm, despite uncertainties over the future of the rough diamond market and recent difficul-

ties in raising much-needed venture capital.

**Kowie Strauss** (BHP-Billiton) reviewed developments at the Ekati diamond mine, Northwest Territories (NWT), which has produced 7 million carats (Mct) of rough with an average value of US\$160/ct since it opened in late 1998. He also described continued exploration by his company for new diamond deposits in the NWT and other regions using "Falcon," a sophisticated airplane-based geophysical technique that can measure gravity, magnetics, radiometry, and digital elevation in the same survey. **Buddy Doyle** (Kennecott Canada Exploration, 100% owned by Rio Tinto) provided an overview on diamond exploration methodology and confirmed that the Diavik mine (a joint venture with Aber Diamond Corp.), also in the NWT, should become Canada's second diamond source by early 2003 (figure 2).

**Tom Beardmore-Gray** (De Beers Canada) stated that one-half of De Beers's diamond exploration budget has been allocated to Canada, with most attention focused on two projects, Snap Lake (a kimberlite dike) in the NWT and

*Editor's note: Bylines are provided for contributing editors and outside contributors; items without bylines were prepared by the section editor or other G&G staff. All contributions should be sent to Brendan Laurs at [blaurs@gja.edu](mailto:blaurs@gja.edu) (e-mail), 760-603-4595 (fax), or GIA, 5345 Armada Drive, Carlsbad, CA 92008.*

GEMS & GEMOLOGY, Vol. 37, No. 3, pp. 222–245  
© 2001 Gemological Institute of America

Victor (a kimberlite pipe) in the James Bay Lowlands area of Ontario. Snap Lake is expected to become Canada's third diamond mine, but during the conference De Beers's corporate headquarters announced a one-year delay in its development. When questioned by Mr. Even-Zohar, **Richard Molyneux** (De Beers Canada) cited two reasons for the delay: (1) the government permitting process will not be complete in time for De Beers to arrange for the transportation of heavy construction equipment and materials to the site along the winter 2003 ice road, and (2) unexpected variations in the morphology of the diamondiferous dike require more trial underground mining. Full production is now estimated to occur in 2006. The status of exploration at Gahcho Kué (also known as Kennady Lake) in the NWT, a joint project between De Beers and Mountain Province, was presented by **Jan Vandersende** (Mountain Province). Here, three kimberlite pipes are being evaluated, but it appears that a 15% increase in diamond prices would be needed to advance this project to the feasibility stage. In the territory of Nunavut, the Jericho project is undergoing a feasibility study, and **Joseph Gutnick** (Tahera Corp.) stated that it could supply 3 Mct/year of rough diamonds for eight years.

In addition to the NWT and Nunavut, diamond exploration and evaluation is occurring in other areas of Canada, particularly within the provinces of Alberta, Saskatchewan, Ontario, and Quebec. For example, kimberlites in Saskatchewan were reviewed by **William Zimmerman** (Kensington Resources Ltd.); Kensington and its partner De Beers are evaluating numerous kimberlites in the Fort à la Corne region. Although the inferred diamond grades are relatively low, the large size of the Saskatchewan kimberlites and good infrastructure in the area make them attractive for further evaluation. **Robert Boyd** and **Brook Clements** (Ashton Mining of Canada) provided an overview of their company's properties and aggressive exploration programs in the Buffalo Hills of northern Alberta, Otish Mountains in Quebec, and at Kikerk Lake and Ric in Nunavut. Of these, the K-252 pipe in the Buffalo Hills is most promising, with an estimated diamond content of 55 carats per 100 tonnes based on a 22.8 tonne sample collected in March 2001. **Jacques Letendre** (Majescor Resources) reviewed diamond-bearing rocks in Quebec, including the Otish Mountains and at Fortage, Tornat, and Wemindji. Several other companies (i.e., SouthernEra Resources, Navigator, Shear Minerals, and Shore Gold) presented the results of their current exploration projects, as well as plans for the future, in various parts of Canada.

A number of speakers described activities in other parts of the world. **Sergey Oulin** (Alrosa) predicted that in the next four years there would be significant expansion in prospecting, rough production, and vertical integration of the diamond industry in Russia, with a greater emphasis on manufacturing and retailing but less on the export of rough diamonds. **Howard Bird** (SouthernEra) described properties in Africa (Gabon, Angola, and South Africa) and western Australia (Yilgarn). Exploration activities at the Tsumkwe project in northeast Namibia were reviewed by

**Nigel Forrester** (Mount Burgess Mining).

Diamond valuation and government relations with diamond explorers were covered in several presentations, with emphasis on Canada and Africa. In South Africa, according to **Claude Nobels** (DVIC Valuations Ltd.), independent valuers help the government maintain its custodial role, so that the industry can operate with confidence and in an organized fashion. **Richard Wake-Walker**, whose company WWW International Diamond Consultants Ltd. holds a diamond-valuation contract with the Canadian government, explained how run-of-mine diamond rough from the Ekati mine is evaluated according to the market price set by other suppliers to ensure that correct royalties are paid. **Martin Irving** (Government of the Northwest Territories) described ambitious activities to support diamond manufacturing in that jurisdiction and to monitor the government's certification program for diamonds that are both mined and cut in the NWT.

The diamond industry in South Africa was described by **Abbey Chikane** (South African Diamond Board) and **Abe Mngomezulu** (South African Department of Minerals and Energy). A new Minerals Development Bill has been drafted to encourage mining and diamond trading in South Africa, especially on a small scale. Ministers responsible for the mineral industries in Namibia (**Jesaya Nyamu**), Angola (**Paulo Mvika**), and Tanzania (**Edgar Maokola-Majoga**) provided overviews of diamond production and outlined recent changes in royalty and/or mining regulations that should facilitate activities in their respective countries. **Luciano de Freitas Borges** (Ministry of Mines and Energy, Brazil) mentioned proposed changes to mining legislation in Brazil that are designed to help reduce bureaucracy and increase the attractiveness of this country's mining properties to foreign investors. He also described ongoing geologic mapping and geophysical surveys of prospective terrain for diamonds by the Brazilian Geological Survey, with computerized results available in GIS format.

In other presentations, **Colin Kinley** (Layne Christensen Canada) described developments in cost-effective bulk-sampling methods for diamonds using new hydraulic drilling technologies that reduce diamond breakage and allow rock samples up to 24 inches (61 cm) in diameter to be collected at depth underground. He predicted that, in the near future, new drilling technology will enable the subsurface recovery of bulk samples up to 60 inches (152 cm) in diameter from kimberlites covered with glacial till or other types of overburden. **Graham Popplewell** (Signet Engineering) described state-of-the-art computer-drafting and networking capabilities for the design of diamond ore-processing plants using remote workstations and password-protected Internet sites. **Frank Holmes** (U.S. Global Investors Inc.) and **Robert Bishop** (*Gold Mining Stock Report*) reviewed factors that affect the market price of diamond mining stocks for investors, including commodity price trends, political risk, mine "life cycle," and exploration funding.

The mood at the close of the conference was one of



Figure 3. A number of exploration trenches, similar to this one, have been dug for diamonds at Staggy Creek, Australia. Photo by Shane F. McClure.

anticipation, as participants absorbed the excitement of Canada's emergence as a major diamond player and the revolutionary changes that are taking place in the industry overall.

**Diamonds from Copeton, Australia.** Diamonds reportedly were first discovered in Copes Creek, Copeton, in 1872, and the major workings in nearby Staggy Creek began in the late 1880s. The Copeton area remained Australia's main producer of diamonds until the development of the Argyle mine in the early 1980s. Although production historically has been rather small, the Copeton diamonds are interesting because of their unresolved geologic origin and reports that they are harder than other diamonds (see, e.g., L. M. Barron et al., "Subduction model for the origin of some diamonds in the Phanerozoic of eastern New South Wales," *Australian Journal of Earth Sciences*, Vol. 43, No. 3, 1996, pp. 257–267). The deposits also are interesting because virtually all of the recovered diamonds are "gem quality," and apparently no micro-sized diamonds have been found there; the rough Copeton diamonds typically weigh 0.20–0.25 ct. Geologists continue to debate the geologic origin of these diamonds (see, e.g., the previous reference, as well as H. O. A. Meyer et al., "Unusual diamonds and unique inclusions from New South Wales, Australia," *Russian Geology and Geophysics*, Vol. 38, No. 2, 1997, pp. 305–331). Some researchers maintain that the deposits are alluvial in nature, as suggested by the abundance of round-

ed pebbles in the host tuffisite. Conversely, Peter Kennewell (managing director of Cluff Resources Pacific) thinks the deposit is primary.

As part of a trip arranged by Dr. Lin Sutherland of the Australian Museum in Sydney, these contributors visited some of the new diamond diggings in the Copeton area in May 2001 after attending the ICA (International Colored Gemstone Association) Congress in Sydney. At the time of our visit, Cluff Resources Pacific had excavated two tunnels. We visited the Streak of Luck tunnel (located on the southern side of Mount Ross), which has produced up to 8 carats of diamonds per 100 tonnes excavated. The tunnel has crossed a number of old shafts from earlier diggings, and then intercepted what appears to be a volcanic intrusion that thus far has not yielded any diamonds. We were unable to visit the Star tunnel (which reportedly produced the highest quality stones recovered by Cluff at Copeton), because it has been flooded since 1999 due to above-normal rainfall. Significant restoration will be necessary before this shaft and tunnel can be worked again.

Cluff also is investigating another site in the Copeton area known as Staggy Creek. Several exploratory trenches (figure 3) have yielded relatively low returns so far. A lamprophyre/dolerite dike runs through the center of this deposit, but it is barren of diamonds. The highest concentrations of diamonds are recovered from the adjacent tuffisite. According to Cluff's 1998 annual report, more than 3,000 diamonds (totaling over 400 carats) were recovered from the pits and trenches at Staggy Creek.

Cluff is also mining another, similar diamond deposit in Bingara, approximately 60 km west of Copeton. According to their 2000 annual report, the Monte Christo diamond mine produced almost 9,000 diamonds from September 1999 to December 2000, or an average of 9.94 carats per 100 tonnes of material mined.

CPS and  
Shane F. McClure  
GIA Gem Trade Laboratory, Carlsbad  
smcclure@gia.edu

## COLORED STONES AND ORGANIC MATERIALS

**Maxixe-type green-blue beryls with eye-visible pleochroism.** In May 2001, the AGTA Gemological Testing Center in New York examined two large (30.67 and 23.64 ct) faceted oval beryls with a face-up color that resembled aquamarine (figure 4). Standard and advanced gemological testing revealed that both green-blue stones had properties consistent with Maxixe-type beryl. The color, which is caused by natural or laboratory irradiation, is due to an unstable color center that fades on exposure to heat or light.

Both of the samples examined had similar gemological properties with refractive indices of 1.572–1.580, a specific gravity of 2.71 (measured hydrostatically), and a uniaxial optic figure; all of these aided in the identification of the stones as beryl, possibly aquamarine. The stones appeared



Figure 4. Both of these beryls (30.67 ct and 23.64 ct) show a strong green-blue color when viewed face-up parallel to the optic axis (left). Strong pleochroism is evident when viewed from the side, where a greenish yellow color is seen perpendicular to the optic axis (right).

yellow when viewed with a Chelsea filter, and were inert to long- and short-wave UV radiation. Microscopic examination revealed long needles and growth tubes that reached from crown to pavilion, as well as internal growth zoning. These proved the stones' natural origin, which was confirmed by FTIR spectroscopy.

The most striking aspect in the visual examination of the two stones was the difference between the strong green-blue face-up color and the greenish yellow color seen from the side (again, see figure 4). Such strong dichroism in a natural-color or heat-treated aquamarine is suspect. In addition, the darker pleochroic color was visible looking down the optic axis (along the ordinary ray), and the lighter pleochroic color was observed perpendicular to the optic axis (along the extraordinary ray). This is consistent with Maxixe-type beryl, and is opposite the behavior shown by natural-color or heat-treated aquamarine (see Winter 1998 Lab Notes, pp. 284–285).

Using a desk-model spectroscope, we found that the 437 nm "iron" line that is typically observed in strongly colored aquamarine was absent. Instead, there was a series of lines throughout the green to red regions of the spectrum. These findings also aided in the identification of the two stones as Maxixe-type beryl (see, e.g., K. Nassau et al., "The deep blue Maxixe-type color center in beryl," *American Mineralogist*, Vol. 61, 1976, pp. 100–107). Visible spectra measured by a Zeiss MCS 501 UV-Vis-NIR spectrophotometer showed a series of absorption bands and peaks not seen in natural-color or heat-treated aquamarine (figure 5).

Another feature of natural or treated Maxixe-type beryl is the presence of cesium (Cs), which rarely is detectable in aquamarine (figure 6; see also W. A. Deer et al., *Rock Forming Minerals—Disilicates and Ring Silicates*, Vol. 1B, 2nd ed., The Geological Society, London, 1997, pp. 372–409). According to Webster (*Gems*, 5th ed., Butterworth-Heinemann, Oxford, 1994, p. 127), the original Maxixe beryls mined in Brazil contained small amounts of cesium and lesser amounts of boron. Using EDXRF spectroscopy, we found Cs in both of the green-blue beryls along with small

quantities of iron (Fe) and traces of manganese (Mn). This is consistent with other Maxixe-type beryls we have examined at the laboratory. By comparison, most aquamarine has much more Fe and less or no Cs (again, see figure 6).

In June 2001, we received a dark violetish blue beryl set in a pendant at our mobile laboratory at the JCK Las Vegas Show. Since Maxixe-type beryl does not come through the laboratory very often, we were surprised when this stone, too, proved to be Maxixe-type. To date, we have examined five Maxixe-type beryls over an eight month period, none of which exhibited any residual radioactivity. We indicated on their lab reports that the color is produced by irradiation and has been known to fade in light and heat. The trade should take note that these stones are currently on the market, and are sometimes misrepresented.

Susan Paralusz

AGTA Gemological Testing Center, New York  
sparalus@msn.com

**Coloration of morganite from Pala, California.** Renewed gem mining in the historic Pala pegmatite district has recently produced some attractive gem tourmaline, as well as small amounts of kunzite and morganite (see "Recent gem discoveries..." below). Most of the facetable morganite from the district was recovered from the White Queen mine on Hiriart Mountain by the Dawson family in the 1960s and 1980s. Although the White Queen is not currently active, Bob Dawson of Temecula, California, recently brought two exceptional White Queen morganites to our attention that well illustrate the effect of sunlight exposure on the coloration of this beryl (figure 7). When mined, the typical color of morganite from this pegmatite is brownish pink. According to Mr. Dawson, after exposure to sunlight for about one week, the brown color disappears, resulting in an attractive pink to purplish pink that is stable under normal conditions of wear and care.

This simple process, capable of causing such a distinct color change in morganite, is not widely known. A similar color alteration due to sunlight is illustrated for Brazilian morganite in the Spring 1989 issue of *G&G* (see A. R. Kampf and C. A. Francis, "Beryl gem nodules from the Bananal mine, Minas Gerais, Brazil," pp. 25–29). According to Dr. George Rossman (as cited in the above-mentioned article), the brownish pink or orange color of the as-mined material is due to prolonged exposure to low levels of natural radiation in the pegmatite host rock. Exposure to sunlight (or mild heating) is generally sufficient to return electrons that were displaced by this radiation to their original sites in the morganite crystal structure, restoring the pink color.

**Vanadium-colored beryl from China.** An interesting green beryl crystal from a new locality, reportedly in the Guangxi Province of China, was recently sent to GIA by Jack Lowell of the Colorado Gem and Mineral Co. in Tempe, Arizona.

## UV-Vis SPECTRA

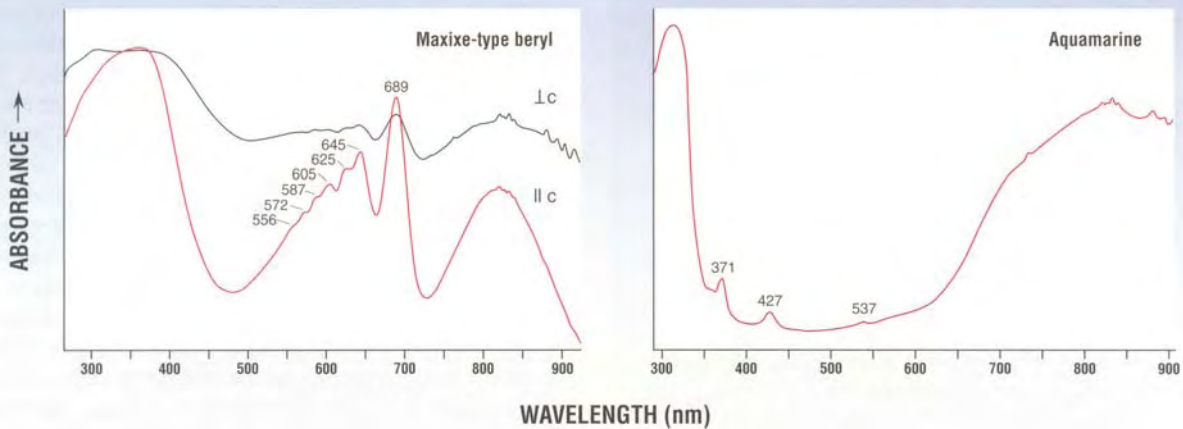


Figure 5. The polarized absorption spectra on the left depict the series of absorption peaks between 556 and 689 nm that were recorded in the green-blue Maxixe-type beryls. These peaks also are readily visible with a handheld spectroscope. In contrast, a typical absorption spectrum for natural-color aquamarine (right) shows strong “iron” lines at approximately 371 and 427 nm, and a small peak at 537 nm (which usually disappears after heat treatment).

The crystal, which was broken on both ends, measured 12.32 mm long and weighed 4.16 ct. The faces of the hexagonal prism were relatively flat and sharp edged, which indicates that the crystal was not recovered from an alluvial deposit. As shown in figure 8, the body color of the translucent crystal is a medium yellowish green, mottled with areas of white that are caused by dense clusters of light-scattering micro-fractures.

One of the flat prism faces yielded refractive indices of 1.575–1.581, with a birefringence of 0.006. A specific gravity of 2.69 was obtained hydrostatically. Microscopic examination revealed inclusions of tourmaline in the form of elongated individual rods, tight “nests,” and small clusters of needles. These inclusions show strong, very dark brown to light brown dichroism when examined with a single polarizing filter.

Figure 6. The EDXRF spectrum of one of the green-blue Maxixe-type beryls (left) shows small amounts of Cs, Fe, and Mn. The spectrum of a natural-color aquamarine (right) shows much more Fe and no Cs, although a minute amount of Mn may also be present. Heat-treated aquamarine generally shows an EDXRF spectrum similar to that of the natural-color aquamarine shown here. In both spectra, the peak at about 8.7 keV is an instrumental artifact.

## EDXRF SPECTRA

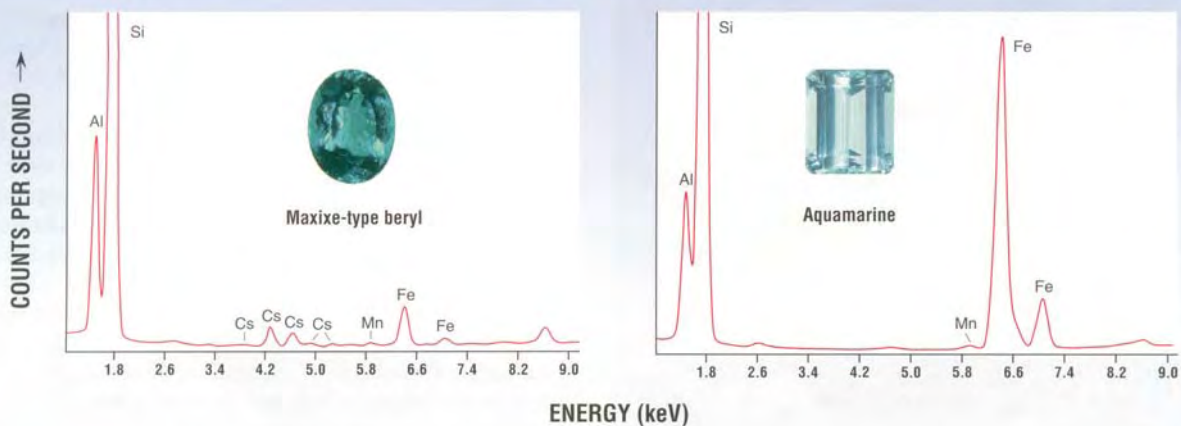




Figure 7. The 191.59 ct stone on the left shows the brownish pink color that is typical of morganite as it is mined from the White Queen mine in Pala, California. After exposure to sunlight for about one week, the brown color disappears, as shown in the 202.41 ct purplish pink White Queen morganite on the right. Courtesy of Bob Dawson; photo © Harold & Erica Van Pelt.

Figure 8. This 4.16 ct vanadium-colored beryl crystal reportedly was recovered from China's Guangxi Province. Photo by Maha Tannous.



The crystal was inert to both long- and short-wave UV radiation and showed no useful spectral features other than a moderate general absorption of the blue region when examined with a desk-model spectroscope. When the crystal was examined in transmitted light with a Chelsea filter, it took on the color of the filter itself, and no red transmission was observed.

EDXRF analysis revealed only the presence of vanadium and iron. No chromium was detected. The yellowish green body color of this crystal suggests that vanadium, and not iron, is the primary coloring agent, although the possible influence of iron cannot be ruled out. It is interesting to note that another relatively new locality for vanadium-bearing green beryl (which also contains some chromium) has been reported in China, in Yunnan Province (see F. Hongbin and L. Yongxian, "Mineralogical characteristics and exploitation perspective of emeralds in Yunnan Province," *Mineral Resources and Geology*, Vol. 12, No. 3, 1998, pp. 188–192).

Thus far most of the material recovered has been sold as "emerald" mineral specimens. According to Mr. Lowell, a few gems have been fashioned from these crystals, but they have been marketed only in China.

*John I. Koivula, Maha Tannous,  
and Sam Muhlmeister  
GIA Gem Trade Laboratory, Carlsbad  
jkoivula@gia.edu*

**Mini-faults in chalcedony.** Disquieting earthquakes and spectacular volcanoes generally serve to remind us of the powerful and potentially destructive forces of nature. Even though these mega-forces may play a role in certain gem-forming processes, we rarely see any obvious evidence of their effect in the miniature world of gems. With this in mind, it was interesting to examine two polished slabs of patterned jasper (a variety of chalcedony) that showed sharp displacements in their layering (see, e.g., figure 9).

The two colorful samples were purchased at the 2001 Tucson show from West Coast Mining, College Place, Washington. The jasper samples were said to originate from Mexico (more specific locality unknown). We had them recut for photography by Leon Agee, of Deer Park, Washington, to 56.41 ct (31.98 × 30.59 × 5.24 mm) and 3.98 ct (12.00 × 11.39 × 2.24 mm).

Once the specimens were recut, the bedding planes and their displacement across miniature faults were even more apparent (figures 9 and 10). Standard gemological testing and observation confirmed their identification as jasper.

*John I. Koivula and Maha Tannous*

**Recent gem discoveries in Pala, California.** Granitic pegmatites in the Pala district are once again yielding significant finds of tourmaline, kunzite, and other gems. In the early 1900s, mines in Pala and the nearby Mesa Grande district (particularly the Himalaya mine, located 30 km south-east of the town of Pala) made Southern California a world-



renowned source of fine gemstones and mineral specimens. After decades of little or no production, recent finds have occurred at three historic mines: the Tourmaline Queen on Queen Mountain, and the Pala Chief and Elizabeth R on Chief Mountain. GNI Editor Brendan Laurs visited these mines in July–August 2001 for this update.

Renewed work at the Tourmaline Queen by mine owner Edward Swoboda of Beverly Hills, California, began in August 1996. This mine was the major producer of gem tourmaline in the Pala district in the early 1900s. After it was closed in about 1914, there was no organized mining until Mr. Swoboda purchased the property in 1970, more than 50 years later. The Tourmaline Queen was leased to Pala Properties International (a partnership between Mr. Swoboda and Bill Larson of Fallbrook, California) and mined during the period 1971–1978. That activity resulted in the discovery of some superb mineral specimens and pieces of gem rough, particularly in January 1972 when the miners found a large pocket that contained well-formed crystals of pink tourmaline with blue terminations (or “blue caps”; see B. Larson, “The ‘Queen’ reigns again,” *Lapidary Journal*, Vol. 26, No. 7, 1972, p. 1002 et passim). Specimens from this find can be seen in several major museums, such as the Smithsonian Institution in Washington, D.C. Since 1978, the property was leased for brief periods by various individuals, but for the most part remained inactive.

When Mr. Swoboda resumed mining at the Tourmaline Queen in 1996, he extended the underground workings to the west and south of the historic zone that yielded abundant tourmaline-rich pockets in the early 1900s. A few blue tourmalines were recovered from this area, but no significant pockets were found after excavating more than 100 m (328 feet) of tunnel over a period of two years. In 1997–1998, a portion of the underground workings was scanned with ground penetrating radar by Jeffrey Patterson and Dr. Fredrick Cook (both from the University of Calgary, Alberta, Canada) as part of their research to detect gem-bearing cavities within pegmatite. Although the instrument detected several anomalies, none turned out to be a gem pocket when excavated.

In October 2000, Mr. Swoboda signed an agreement with Scott Ritchie and Erik Cordova of Southern California Gem Industries, Torrance, California, for additional exploration and mining activities at the Tourmaline Queen. The team improved the rough four-wheel-drive roads that access the mine, and in July 2001 began open-cut excavations of the pegmatite with a large trackhoe. They exposed several hundred feet of the pegmatite where it crops out to the east and north, and made a large cut in the area where much of the historic production occurred (figure 11). Here, excavation exposed two old tunnels, and further mining in late July revealed several gem pockets.

The first pocket contained a blue tourmaline crystal that yielded two attractive cat’s-eye cabochons of 13.57 and 31.50 ct. Two pink cat’s-eye cabochons (7.30 and 7.95 ct) were cut from a crystal found in another pocket (figure

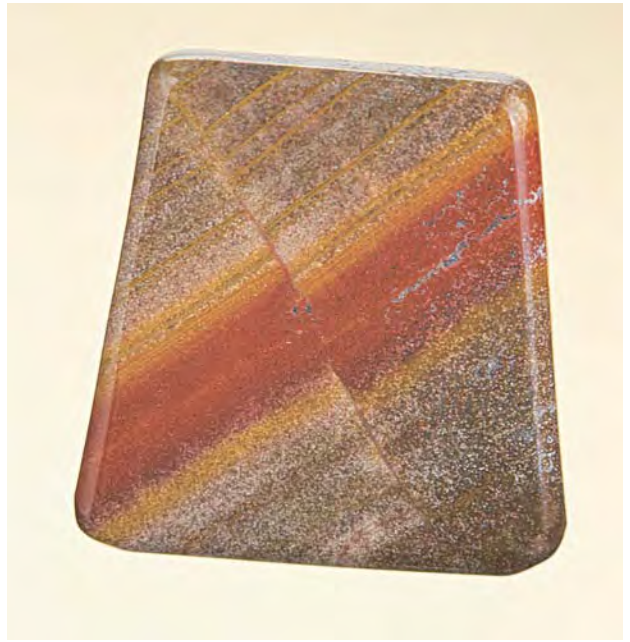


Figure 9. This 56.41 ct polished jasper shows an obvious displacement of the colorful bedding planes. Photo by Maha Tannous.

12). Chatoyant tourmaline from San Diego County is typically green—as found mainly at the Himalaya mine in Mesa Grande—so the blue and pink cat’s-eyes cut from material found in these new pockets are very unusual. Other cavities produced bright pink and bicolored pink-and-blue tourmaline rough, two of which have been preformed into stones that exceed 100 ct. Mr. Swoboda estimates that the recent finds have yielded several hundred carats of gem-quality tourmaline as well as several specimen-quality crystals (some with morganite). The open cut has now been mined out and filled in; future plans call for underground mining of several enriched sections of the pegmatite.

The historic Pala Chief mine is known mostly for its pink or “lilac” kunzite, in addition to fine tourmaline and

Figure 10. The high contrast of red and white layers in this 3.98 ct polished jasper makes the mini-faulting readily apparent. Photomicrograph by John I. Koivula; magnified 3 $\times$ .





Figure 11. In July 2001, Edward Swoboda and partners used a large excavator to open-cut part of the Tourmaline Queen mine in Pala, California. Several pockets containing gem- and specimen-quality tourmaline were found after the cut was extended several meters into the pegmatite. Photo by Brendan M. Laurs.

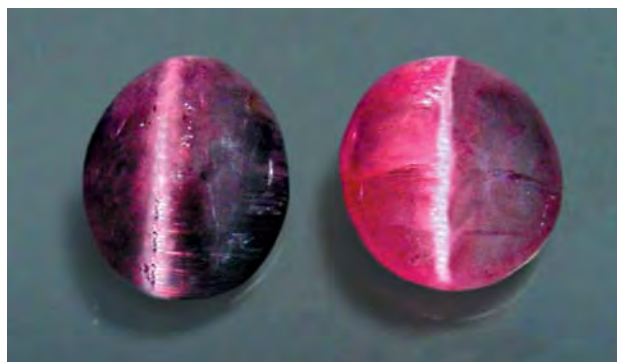


Figure 12. One of the gem pockets recently found at the Tourmaline Queen mine yielded a chatoyant tourmaline crystal that was cut into these two cat's-eyes (7.30 and 7.95 ct). Chatoyant tourmaline from San Diego County is typically green. Photo by Edward Swoboda.

morganite. The current owner, Bob Dawson of Temecula, California, purchased the property in the early 1990s. Mr. Dawson improved the roads and security in preparation for mining, and began extending one of the short tunnels in

October 2000. After drilling and blasting through about 3 m of pegmatite, he found a gem pocket approximately 1 m long  $\times$  0.5 m wide  $\times$  0.3 m thick in early November 2000 (figure 13). From this pocket, he recovered five well-formed crystals of pink tourmaline with flat pale blue-gray terminations (see, e.g., figure 14), as well as several pieces

Figure 13. At the Pala Chief mine, mine owner Bob Dawson found a gem pocket containing tourmaline and kunzite in November 2000. The pocket, which measured approximately 1 m long, was located in the pegmatite core zone next to the area with purple lepidolite to the left of Mr. Dawson; photo by Brendan M. Laurs. The inset shows the pocket as it was being excavated; the dark crystal on the lower right is tourmaline (6.3 cm across) on a matrix of quartz and cleavelandite feldspar that is attached to the top of the pocket. Photo by Bob Dawson.

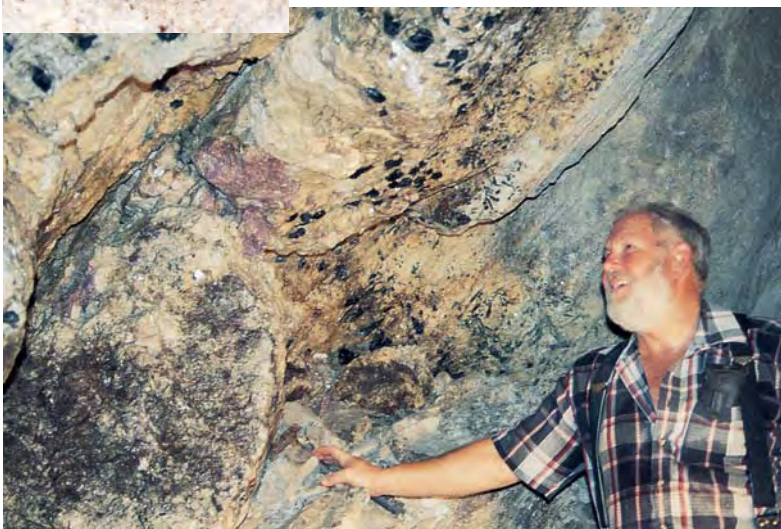


Figure 14. This well-formed crystal of tourmaline (8.4  $\times$  6.2 cm) was recovered at the Pala Chief mine in November 2000. Courtesy of Bob Dawson; photo by Maha Tannous.



of pink kunzite. The tourmalines formed stout prisms ranging from  $6.1 \times 2.3$  cm to  $8.4 \times 6.2$  cm, and the kunzites occurred as deeply etched, lustrous crystals up to  $10.7 \times 2.7$  cm. Further mining has uncovered a few additional small pockets or “vugs” that contained crystals of pink or blue-gray tourmaline.

The Elizabeth R mine is not as well known as the other two, but it has been operated intermittently for nearly three decades by Roland Reed of El Cajon, California. The property was originally purchased by Mr. Reed as the Hazel W claim in 1974, and he renamed it Elizabeth R in 1980. In 1973, he purchased the adjacent Ocean View claim, from which he obtained large quantities of quartz and morganite in well-formed crystals (some of the latter bicolored with aquamarine) in 1974–1975 and 1982. In September 2000, Mr. Reed sold the Ocean View mine to a group headed by Jeff Swanger and Stephen Koonce Jr. of Escondido, California.

In July 2000, Mr. Reed started a new tunnel on the Elizabeth R property, and in November 2000 the tunnel penetrated the down-dip extension of the Ocean View pegmatite. He was surprised when he immediately encountered a mineralized quartz-spodumene core zone, in which he found several small clay-filled vugs that contained pink, blue, and bicolored pink–bluish green tourmaline and lavender kunzite (figure 15). As of August 2001, the new tunnel at Elizabeth R had produced several hundred carats of gem rough, and some had been faceted or cut into cabochons (see, e.g., figure 16). The tourmaline- and kunzite-bearing zone that Mr. Reed has uncovered is completely unlike the beryl-bearing areas previously known on the property; it more closely resembles the mineralization at the Pala Chief and Tourmaline Queen. As work continues at all three mines, more gems and mineral specimens will likely become available in the marketplace.

**A statuette containing a large natural blister pearl.** This past summer, the AGTA Gemological Testing Center

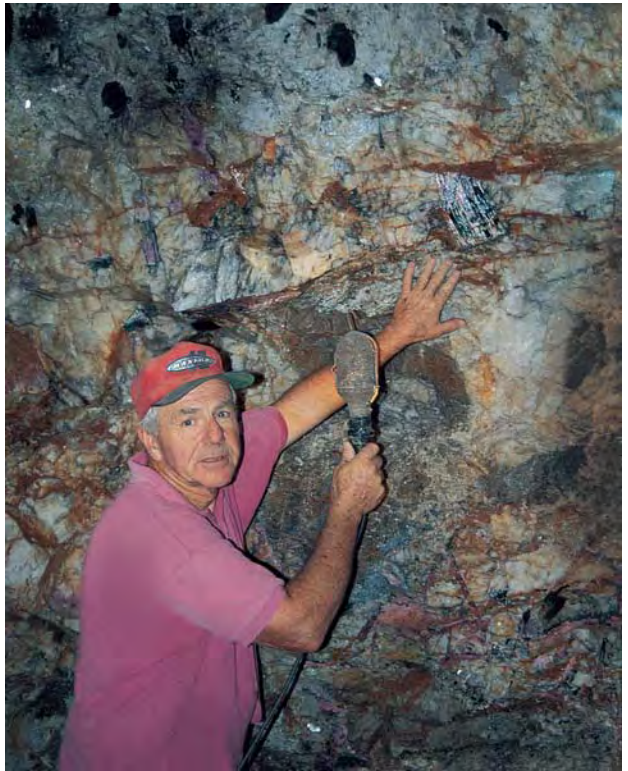


Figure 15. Beginning in November 2000, a new tunnel at the Elizabeth R mine in Pala penetrated a previously unknown pegmatite core zone that yielded several small clay-filled vugs with gem-quality tourmaline and kunzite. Mine owner Roland Reed is pointing to a large black-and-pink crystal of tourmaline that is “frozen” in the pegmatite. Photo by Brendan M. Laurs.

examined a large “pearl” set within a statuette of a centaur (figure 17). A centaur is a mythological creature with the head, arms, and chest of a man but the legs and lower half of a horse. Figurines that make use of oddly shaped pearls were particularly popular with artists during the Renaissance, when mythological themes were adopted for interesting ornaments, such as the circa 1560 Canning Jewel (in which a large natural pearl has been set as the

Figure 16. Several hundred carats of rough gem tourmaline and kunzite were recently recovered from the Elizabeth R mine. The faceted stones on the left (0.47–2.02 ct) show the range of color of the pink tourmaline. The middle photo depicts some unusual cat’s-eye tourmaline in blue, greenish blue, and bicolored pink-green colors (13.44–16.30 ct). The faceted kunzite on the right weighs 14.39 ct. Courtesy of Roland Reed; photos by Maha Tannous.

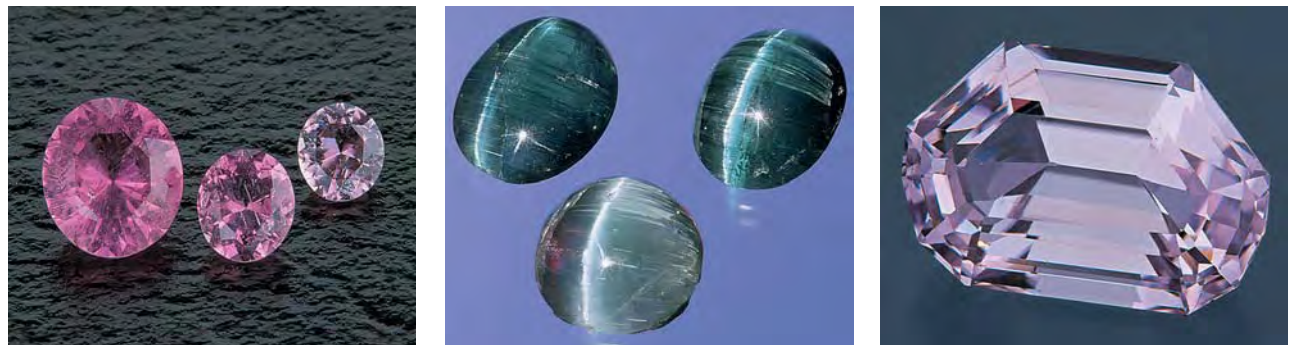




Figure 17. The torso of the centaur in this statuette is actually a natural blister pearl that weighs 856.58 ct. Photo by Kenneth Scarratt.

torso of a triton; see, e.g., figure 6 in D. M. Dirlam et al., "Pearl fashion through the ages," Summer 1985 *Gems & Gemology*, pp. 63–78). Although we had no information on the possible age of the statuette we examined in our lab, the practice of using oddly shaped pearls—both natu-

Figure 18. After being removed from the statuette, the 856.58 ct natural blister pearl could be examined from all directions. The back of the blister pearl (see inset) shows the banded structure of the shell from which it grew. Photos by Kenneth Scarratt.



ral and now cultured—in this manner has carried through to the present.

The centaur measures approximately 17 cm in height (excluding the base) and is about 15.5 cm long from tail to outstretched front hoof. The head and arms of the man and the entire horse portion are made of a yellow metal embellished with white, red, green, and black enamel work. Set at various points are old-cut diamonds with well-worn facet edges and foil-backed "red" corundum. The "saddle" is removable and facilitates the setting and unsetting of the "pearl." A yellow metal band wraps around the midriff and is similarly decorated with old-cut diamonds and foil-backed corundum.

The "pearl" is nacreous, and when removed from the setting it weighs 856.58 ct and measures  $69.13 \times 48.97 \times 34.68$  mm. The color is purplish brownish gray on the convex front and dark gray to black on the concave back (figure 18). The back has the banded structure of the shell from which it grew, indicating that it is not a true, fully formed pearl, but rather is a blister pearl. X-radiography showed that the structure of the blister pearl is banded throughout and not concentric (figure 19). The lack of a bead nucleus or any other indication of cultured pearl growth confirmed that it is natural.

Most nacreous pearls of extraordinary size are, in fact, found attached to the inner wall of the host mollusk's shell. Hence, they are termed *blister pearls*. The Hope pearl, thought to be one of the largest of all nacreous pearls, with an estimated weight of 450 ct, is a natural blister pearl (see, e.g., S. Kennedy et al., "The Hope pearl," *Journal of Gemmology*, Vol. 24, No. 4, 1994, pp. 235–239). The Summer 2001 issue of *Gems & Gemology* (Gem News International, p. 158) described a natural pearl recently discovered in waters off the coast of Myanmar that, at a reported weight of 845 ct and measuring  $62 \times 53 \times 30$  mm, was thought to be the world's largest (nacreous) natural pearl (U. T. Hlaing, "World's largest pearl," *Australian Gemmologist*, Vol. 21, No. 3,

Figure 19. This X-radiograph of the blister pearl shown in figure 18 reveals a layered growth structure, which confirms its identity as natural.



2001, p. 135). Although the reports thus far emerging from Myanmar do not confirm whether or not this is a blister pearl, the published images suggest that this may be the case. By comparison, the natural blister pearl set in the centaur statuette is about the same size and weighs slightly more than the Myanmar pearl. Certainly, both of these weigh more than the reported or assumed weights for such large, historically famous nacreous pearls as the 450 ct Hope pearl, the 605 ct Pearl of Asia, and the 575 ct Arco Valley pearl (G. F. Kunz and C. H. Stevenson, *Book of the Pearl*, Century Co., New York, 1908; J. Taburiaux, *Pearls—Their Origin, Treatment and Identification*, NAG Press, London, 1985, pp. 89-99).

In describing large individual natural or cultured pearls, and certainly when making claims regarding their relative sizes, it is important to note whether they are nacreous or non-nacreous (and, if possible, to state the type of mollusk from which they were recovered), as well as whether they have characteristics of blister growth. This allows for a clearer comparison to be made. *KVGS*

**Exceptional carpet shell pearl.** The “carpet shell” (or palourde) is a bivalve mollusk, very common off the coast of France, where it is much appreciated by shellfish enthusiasts for its flavorful yet subtle taste. Very rarely, it also produces small pearls (typically about 2 mm), which are generally very irregular and unattractive. Mrs. Gilberte Landré, janitorial manager at this contributor’s institute, nevertheless fished an exceptional specimen on October 17, 2000, from the Gois passage—the expanse of sand inshore of the French island of Noirmoutier that is covered by the sea only at high tide—south of Nantes (figure 20).

The pearl is almost perfectly round, with a diameter of 5.7–5.9 mm, and weighs 1.43 ct. It is nacreous and very lustrous, but without much orient. The pearl shows an even purple color; this hue is also present in a portion of the shell it came from, which is otherwise white and brown inside (again, see figure 20). There are several small, grayish blemishes on the surface. When exposed to long-wave UV radiation, the pearl luminesced a chalky whitish yellow, similar overall to the reaction of the inside of the shell (although the purple part of the shell is only weakly luminescent). The reaction was weaker to short-wave UV.

The sample was also examined with a JEOL 5800 scanning electron microscope (SEM) in the low-vacuum mode (no conductive coating necessary); a qualitative chemical analysis was obtained using a Princeton Gamma Tech detector with a high-resolution (115 eV) germanium crystal and an ultra-thin polymer window. This equipment ideally can measure elements as light as boron. The surface appeared granular at 1,500× magnification, with pits less than 1 mm in diameter evenly distributed over the area examined. As expected, the chemical analysis revealed mostly calcium, oxygen, and carbon (i.e., a calcium carbonate), with trace amounts of aluminum and sodium. *EF*



Figure 20. The “carpet shell” mollusk shown here was fished near the island of Noirmoutier off the coast of western France. It yielded this exceptional 5.8 mm purple pearl. Photo by Alain Cossard.

**Tahitian “keshi” cultured pearls.** Two “black” cultured pearls (figure 21), one near-round and the other oval (potato shaped), were recently submitted to the SSEF laboratory for identification. Both samples showed an uncommon surface feature: a small groove (or indentation) on the flatter side of the slightly button shape, which may correspond to internal growth inhomogeneities (see below). On closer examination, we saw that the samples were actually dark brown. Chemical analysis by EDXRF revealed a very low manganese content, which is typical of saltwater origin. We confirmed that the color was natural by measuring the reflectance spectra with a standard (Hitachi 4001) spectrophotometer. X-radiography showed multiple growth inhomogeneities that formed a typical pattern, but no evidence of a nucleus (figure 22). The shape of the cultured pearls as well as their typical irregular growth structures led us

Figure 21. These two samples (11 and 15 mm across) were found to be Tahitian non-nucleated cultured pearls (“keshi”). Photo by H. A. Hänni.



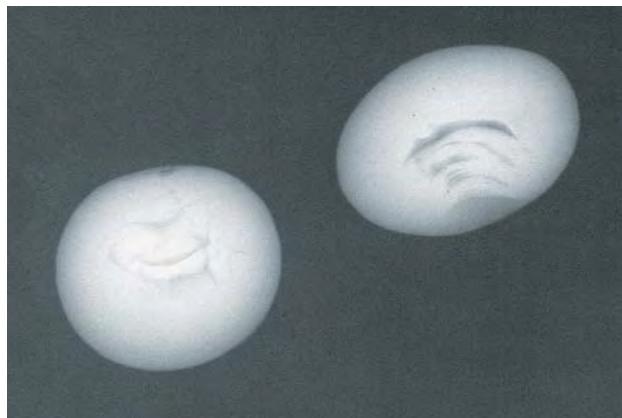


Figure 22. This X-radiograph reveals typical growth inhomogeneities within the two Tahitian “keshis” shown in figure 21.

to the conclusion that they are Tahitian non-nucleated cultured pearls (sometimes called “keshi”).

When a bead-nucleated cultured pearl is removed from a pearl sac, the cultivator can insert a second bead of the same diameter as the cultured pearl just harvested, or leave the pearl sac empty and wait for the possible formation of a “keshi.” However, this contributor suggests that these samples formed after rejection of the second bead, which would also result in a beadless cultured pearl when the pearl sac is filled with calcium carbonate from the mantle epithelium. “Keshi” cultured pearls are well known from Australia, but

Figure 23. At Bruce Brown’s pearl farm at Cygnet Bay in northwest Australia, nucleated oysters are placed in wire cages such as this. They are cleaned every two weeks to remove the fast-growing weed that collects on them. The cages are suspended from 350 “lines” (see inset), and each line holds 400 nucleated oysters. Photos by Shane F. McClure.



Tahitian “keshi” cultured pearls are more of a novelty (see, e.g., Spring 2000 Gem News, pp. 70–71). According to cultured pearl experts Andy Muller and Robert Wan (pers. comm., 2001), a small quantity of black “keshis” were released into the pearl market last year. HAH

**Pearl culturing in northwest Australia.** In May 2001, these contributors visited Cygnet Bay Pearls, a cultured pearl farm at Cygnet Bay that is owned and operated by Bruce Brown. Located approximately 200 km north of Broome (about a one hour flight by small plane), Mr. Brown’s farm was founded 40 years ago by his father and older brother. The farm now harvests 140,000 oysters in two-year cycles (typically every 20 to 24 months). In the main part of the bay, Mr. Brown has 350 “lines,” each of which contains 400 nucleated oysters. To maximize cultured pearl growth, he has the oyster shells cleaned every two weeks to remove a fast-growing weed that collects on them (figure 23). This ensures that the oysters get the full benefit of the nutrients necessary to promote nacre growth. Typically the pearls achieve 2–4 mm of nacre growth per year (with the greatest amount when the mollusks are younger and progressively less as they get older). The farm uses beads made from Mississippi freshwater mussel shells, typically with a diameter of 6 mm to yield cultured pearls from 11 to 12 mm.

Most of the mollusk shells open slightly when taken out of the water for harvesting. A wooden peg is inserted to keep the shell open until just prior to the extraction procedure, when the peg is replaced by a clamp that further separates the shell and holds it open just wide enough to remove the cultured pearl without traumatizing the mollusk. Those few oysters that do not open their shells are returned to the water until the next harvesting cycle. As noted above in the entry by Dr. Hänni (and illustrated in the Summer 2001 S. Akamatsu et al. article on Chinese freshwater cultured pearls, p. 105), farmers will insert another bead (similar in size to the cultured pearl just harvested) into the vacant pearl sac, which typically will produce a 14–15 mm cultured pearl by the next harvest. If the bead is smaller than the cultured pearl that was extracted, the pearl sac collapses and produces button- or off-shape cultured pearls with irregular nacre thickness. After harvesting the oysters and re-seeding them, the cultivators wash the shells with fresh water to kill the bacteria that cause disease in the animals.

A few of the cultured pearls from Mr. Brown’s farm are gray in color. He stated that when parasites drill through the shell, the oyster coats them with a black film to kill them. Sometimes the oyster also does this to the bead once it has been inserted. Subsequently, the coated bead is covered with nacre and the pearl develops as usual; however, the black film imparts a gray appearance to the resulting cultured pearl.

As a consequence of the culturing process, some non-nucleated (“keshi”) cultured pearls also are produced. When these are detected during a routine X-ray of the shells to determine if nacre is forming on the beads, the mollusks are placed in a separate area of the farm for

further development without intervention. Although small amounts of “keshis” are harvested, they are not being sold at this time. The largest “keshi” they have produced to date is a baroque shape that weighs 4.75 momme (89 ct).

Mr. Brown’s farm is represented by the marketing arm of the Autore Group of Companies, which was founded in 1991 by Rosario Autore. The Autore Group acts on behalf of 11 pearl producers (from Western Australia, Indonesia, and most recently, Papua New Guinea) that specialize in fine-quality South Sea pearls. According to Mr. Autore (pers. comm., 2001), the Autore Group of Companies sells 30% of the Australian production of South Sea cultured pearls, second only to Paspaley Pearls (which has a market share of approximately 50%). The Autore Group separated from the South Sea Pearl Consortium approximately two years ago, to develop its own classification system, marketing strategy, and brand. One of these contributors (CPS) was shown a magnificent cultured pearl necklace consisting of 18–21 mm round cultured pearls of very good surface luster and few or no surface blemishes (figure 24).

*CPS and Shane F. McClure*

**Green powellite from Chile.** Powellite,  $\text{CaMoO}_4$ , is one of the rarest gem materials. Transparent crystals suitable for faceting are known from India’s Maharashtra State, but only from one area, near Nasik, where they occur in basalt cavities with abundant zeolites. Indian powellite is colorless to yellow, and cut stones over 2 ct are very rare, although at least one attractive faceted stone over 50 ct exists (D. Blauwet, pers. comm., 2001).

Powellite from Chile has a completely different appearance. The locality is the Inca de Oro copper mine in the Atacama Desert, where powellite is found with a rela-

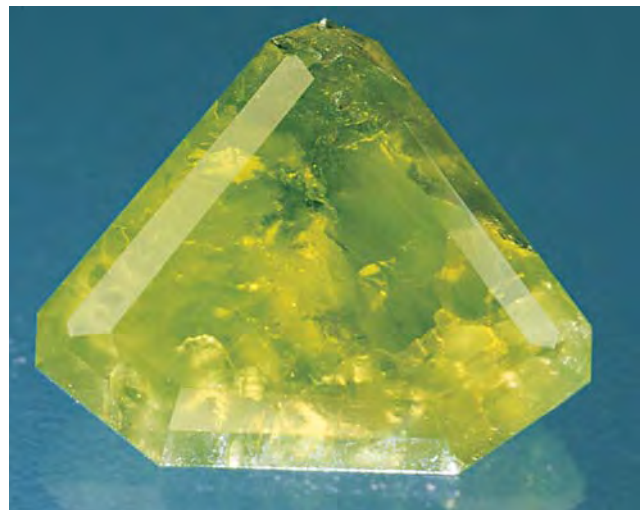
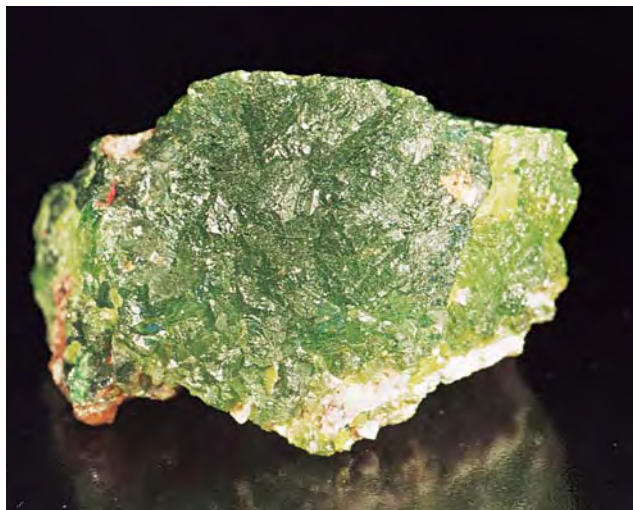


*Figure 24. Bruce Brown’s pearl farm is a member of the Autore Group of Companies, which specializes in fine-quality South Sea cultured pearls from farms in Western Australia, Indonesia, and Papua New Guinea. The top-quality cultured pearls in this necklace range from 18 to 21 mm. Courtesy of the Autore Group of Companies.*

tively new mineral, szenicsite, as described by C. A. Francis et al. (see “Szenicsite, a new copper molybdate from Inca de Oro, Atacama, Chile,” *Mineralogical Record*, Vol. 28, No. 5, 1997, pp. 387–394). This Chilean powellite occurs as yellow pseudomorphs after molybdenite, as small crystals and as very rare translucent green druses (figure 25); the drusy material has yielded a few interesting faceted stones. The most transparent gemstones range from 0.5 ct to 1 ct, but translucent stones can weigh more than 15 ct (again, see figure 25). However, powellite’s low hardness (3.5–4 on the Mohs scale) makes it unsuitable for jewelry, despite this interesting color.

This contributor studied 18 faceted powellites from Inca de Oro to document their gemological properties. These samples weighed 0.25–16.07 ct and were translucent to transparent. They ranged from yellow-green to green with weak pleochroism—in green and yellow-green.

*Figure 25. The 4 × 3 cm sample of translucent drusy powellite on the left is from the Inca de Oro copper mine in the Atacama Desert, Chile. The faceted Chilean powellite on the right weighs 16.07 ct. Photos by J. Hyrsl.*



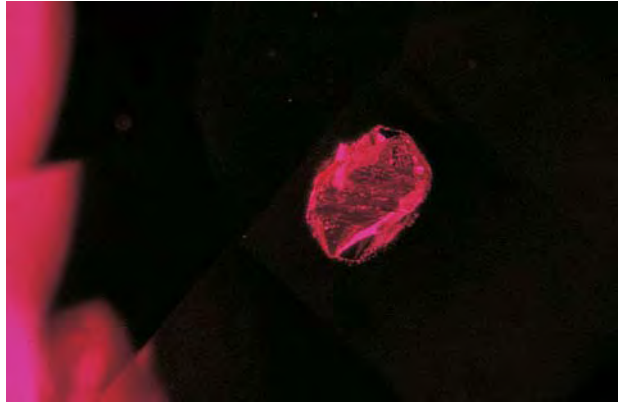


Figure 26. This colorless, roughly tabular inclusion in an unheated ruby from Myanmar was identified as anhydrite, which has not been identified previously as an inclusion in gem corundum. Photomicrograph by Christopher P. Smith; magnified 50×

The refractive indices were over-the-limits of a standard refractometer, and the specific gravity values were rather high at 4.17–4.22. When examined with a polariscope, powellite behaves as an anisotropic aggregate; only the smallest cut stones show normal extinction. Very characteristic is a bright yellow fluorescence to short-wave UV radiation, but the material is inert to long-wave UV. The spectrum seen with a handheld spectroscope exhibited complete absorption of the blue and purple regions, starting from about 460 nm. When viewed with a microscope, the samples showed a swirled structure, although one stone exhibited a layered agate-like structure.

Because of its unusual color, the Chilean material is sometimes described as “chrome-powellite.” However, the color is probably due to trace amounts of copper. In addition to calcium and molybdenum, Francis et al. (1997) reported 0.02–0.30 wt.% CuO in yellow, green, and brown powellite, with the greatest amounts measured in a dark green sample.

Jaroslav Hyrsl  
Kolin, Czech Republic  
hyrsl@kuryr.cz

**Anhydrite inclusion in a ruby from Myanmar.** As more advanced analytical techniques become commonplace in gemological laboratories, properties and features not reported previously will occasionally be encountered. Such was the case in the Gübelin Gem Lab (GGL) recently, when a 3.79 ct ruby was submitted for identification. The combination of inclusion features, internal growth structures, and chemical composition indicated that the ruby was unheated and originated from the Mogok stone tract of Myanmar. A crystalline inclusion situated just below the surface of the gemstone, however, had an unfamiliar appearance (figure 26). This colorless crystal had a roughly tabular habit with an irregular surface, and did not resemble any of the more common crystalline inclusions encountered in Burmese rubies, such as calcite, apatite, and sphe-

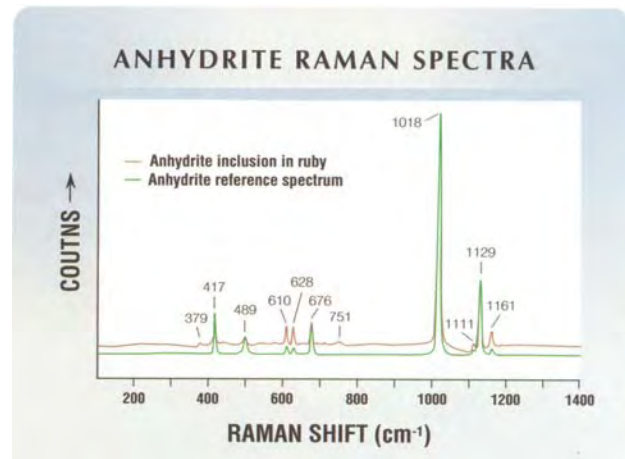
Analysis of the inclusion with a Renishaw 2000 Raman microspectrometer proved that the mineral was anhydrite,  $\text{CaSO}_4$  (figure 27). To our knowledge at GGL, this is the first time that anhydrite has been identified as an inclusion in gem corundum from any source. Anhydrite, a relatively common rock-forming mineral, is a nonhydrated form of gypsum. It is often associated with gypsum, which is commonly derived from anhydrite by the process of hydration. Occurrences of anhydrite have been identified underlying thick layers of gypsum in northern Shan State (see, e.g., F. Bender, *Geology of Burma*, Gebrüder Borntraeger, Berlin, 1983), east of the Mogok stone tract.

CPS and Christian Dunaigre  
Gübelin Gem Lab  
Lucerne, Switzerland

**Ruby and sapphire mining at Barrington Tops, Australia.** In addition to diamond mining in the Copeton and Bingara fields (see the “Diamonds from Copeton...” entry above), Cluff Resources Pacific operates the ruby and sapphire deposits in Gloucester, in the Barrington Tops area of New South Wales (see also Winter 1995 Gem News, pp. 281–282). Additionally, they operate a joint-venture sapphire mine in central Queensland. As part of the trip arranged by Dr. Lin Sutherland, these contributors visited the Barrington Tops ruby and sapphire deposit in May 2001.

Apparently discovered by a prospector in the 1970s, the deposits occur along several river tributaries (principally from the Manning river) and are classified into three types (i.e., recent alluvials, middle terraces, and upper terraces). Corundum has been found throughout the flatland

Figure 27. The Raman spectrum of the crystalline inclusion shown in figure 26 clearly identified it as anhydrite, with the two primary peaks positioned at 1018 and 1129  $\text{cm}^{-1}$ , respectively. Here, the Raman spectrum of the anhydrite inclusion is compared to that of an anhydrite reference spectrum in the Renishaw database. No peaks were recorded in the region 1400–1800  $\text{cm}^{-1}$ .





region between the various tributaries. Managing Director Peter Kennewell believes that the entire region of terraces was formerly a swamp where gem-bearing basaltic eruptions deposited an extensive ash layer ranging from 1 to 2 m thick. Heavy minerals (including gems) in these deposits have been reworked into recent alluvial systems. The rubies and sapphires are apparently recovered mostly from these alluvial sediments (figure 28), together with gem-quality zircon and black spinel.

Cluff negotiated with the landowner to begin a bulk sampling program in 2000. To date, several trenches have been dug that are approximately 3–4 m wide, 4 m deep and up to 200 m long. The largest gem-quality ruby recovered weighed 5.8 ct. The company has established a laboratory and processing facility in Sydney, managed by Dr. Robert Coenraads, to begin developing a market for their gemstones. Dr. Coenraads has developed a classification system for the various colors of corundum (yellow through green, to blue, and parti-colors) that they produce. The faceted rubies and pink sapphires are graded into six color categories (red no. 1 and pink nos. 1–5) and four quality ranges (1–4; “clean” to heavily included). The company continues to cut and stockpile its stones in preparation for a major marketing campaign. As of August 2001, around 5,000 grams of ruby had been recovered during the exploration program, and about half of this was of cutting quality (R. Coenraads, pers. comm.).

Studies by Dr. Sutherland have shown that two types of corundum coexist in this vast region (see F. L. Sutherland et al., “Origin of chromium-colored gem corundums, Australia,” *Gemmologists Handbook*, International Gemmological Congress, 1999, pp. 37–39; G. Webb, “Gemmological features of rubies and sapphires from the Barrington volcano, eastern Australia,” *Australian Gemmologist*, Vol. 19, 1997, pp. 471–475). One type is chromium-bearing and is related to a metamorphic or metasomatic corundum-sapphirine-spinel source. The colors of these rubies and sapphires include red/pink through purple to violetish blue, and even pure blue. The other, smaller population consists of blue to blue-green sapphires that are related to a magmatic sapphire-bearing source. Sapphires of this type exhibit the typical surface corrosion features of corundum transported as xenocrysts in alkali basalts. This magmatic-type gem corundum is typical of many basalt-related deposits in eastern Australia, but the Barrington Tops area is unusual in that significant quantities of metamorphic-type ruby/sapphire gems are also present. Similar bimodal gem corundum associations have been recognized in other basaltic fields in eastern Australia, as well as in Cambodia (Pailin), Laos, and southern Vietnam. *Shane F. McClure and CPS*

**Renewed mining for rubies in Nanyaseik, northern Myanmar.** Over the past few months, thousands of miners have converged on the Nanyaseik area of northern Myanmar, in a new “gem rush” for ruby and pink sapphires, as well as spinel. The area, also referred to as Nanyar Zeik

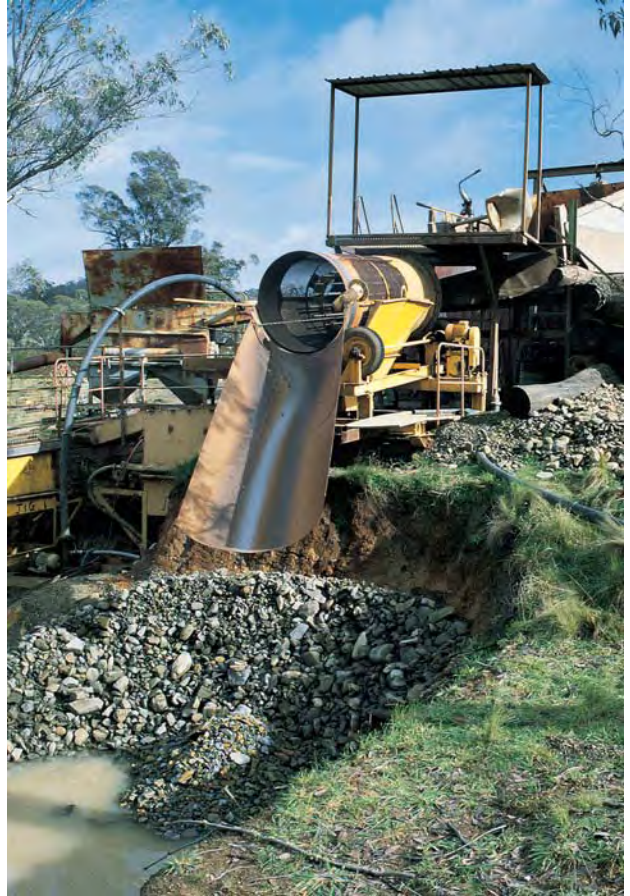


Figure 28. This equipment is used for washing the gem-bearing sediments in the Barrington Tops area of eastern Australia. Photo by Shane F. McClure.

(and various other spellings), is located in the Myitkyina district of Kachin State. This region is well known for the famous jadeite deposits near Hpakan, which are located approximately 30 km west of Nanyaseik. Rubies from this area have been described previously (see, e.g., H. Htun and G. E. Harlow, “Identifying sources of Burmese rubies,” Fall 1999 *Gems & Gemology*, pp. 148–149), but past production has been rather small and sporadic.

Thick vegetation and forests of tall trees have been cleared so that pits could be excavated to reach the gem-bearing alluvial layer (figure 29). The miners use traditional Burmese mining techniques: First, they dig a “lebin,” or square pit, and then they hoist the soil and gem-bearing material to the surface using a rope and a bucket. Washing of the gravels and initial processing of the ruby rough is performed on-site. Although most of the newly mined ruby is reportedly small, good-quality crystals up to 8–10 ct also have been found.

Overall, the faceted rubies appear very similar to Mogok material. The color typically ranges from pink and purple-pink to dark red, and the stones are usually very clean. During a recent visit to Bangkok, one of the contributors (CPS) examined 25 high-quality rubies that reportedly came from Nanyaseik. Observation with a microscope revealed planar and swirled internal growth structures. These non-heated rubies also had long, iridescent rutile needles as well as small “nests” of short rutile needles. Other mineral inclusions consisted of colorless calcite, rounded crystals of



Figure 29. The Nanyaseik area of northern Myanmar is producing ruby and pink sapphire, as well as spinel, from alluvial diggings such as this. The gem-bearing gravel has been hoisted to the surface from the pit on the lower left, and is being washed by the miners. Photo courtesy of Frederico Barlocher.

light yellow sphene, and dark orange rutile. All of the mineral inclusions were identified visually, based on features that are diagnostic of their appearance in Burmese rubies. EDXRF analyses of the Nanyaseik rubies revealed trace-element contents that are similar to those recorded for rubies from Mogok, with relatively high levels of vanadium and lower concentrations of iron, titanium, and gallium.

CPS and George Bosshart  
Gübelin Gem Lab  
Lucerne, Switzerland

Figure 30. "Spider" quartz has been mined in the Antsirabe region of central Madagascar for the past few years. The crystals shown here weigh 52.05 and 26.62 ct, and the faceted stone weighs 12.48 ct; courtesy of John I. Koivula and photo by Maha Tannous. The inset shows the interesting display created by the needle-like inclusions. Photomicrograph by John I. Koivula; magnified 10x.



"Spider" quartz. An attractive variety of colorless quartz with interesting inclusions has been mined in the Antsirabe region of central Madagascar for the past few years (figure 30). It contains small radiating sprays of black needles that measure up to a few millimeters across (again, see figure 30). The appearance of these inclusions has prompted the dealers to call it "Spider" quartz or "Microstar." Denis Gravier of Le Minéral Brut, St. Jean-le-Vieux, France, provided several specimens to this contributor in the hope that our research laboratory could identify the inclusions.

We broke open several rough samples and examined the fractures with a JEOL 5800 scanning electron microscope (SEM). One of the fractures revealed protruding needle-like crystals, up to 10  $\mu\text{m}$  across (figure 31), that corresponded to an underlying "spider" inclusion. The chemical composition was measured with the EDX spectrometer of the SEM, although only a semi-quantitative analysis was possible because of the small size of the needles and the lack of a polished surface perpendicular to the beam. Nevertheless, we obtained several consistent analyses. These revealed that, in addition to oxygen (about 60 atomic percent, determined by stoichiometry), manganese was abundant (about 27 at.%), followed by barium (a little less than 4 at.%), iron (about 3.5 at.%), and aluminum (about 2.3 at.%); the remainder (about 3 at.%) consisted of lead and silicon. The major-element composition is consistent with the mineral hollandite,  $\text{Ba}(\text{Mn}^{4+}, \text{Mn}^{2+})_8\text{O}_{16}$ . Lead is probably an impurity in the hollandite, whereas silicon, iron, and aluminum may be contaminants related to the quartz (silicon) or possibly clay-like materials that coat the inclusions.

We confirmed the identification of these inclusions as hollandite by single-crystal X-ray diffraction analysis, using a curved-detector Linel diffractometer. The shape of the needles is consistent with the monoclinic pseudotetragonal crystal habit of hollandite. EF

Figure 31. This scanning electron micrograph of a broken piece of "Spider" quartz from Madagascar shows the fine needle-like inclusions that were identified as hollandite.



**Blue-to-green tourmaline from Nigeria.** In recent years, the Ibadan region of western Nigeria has become an important source of pink and bicolored (pink-green) tourmaline for the gem trade (see, e.g., Winter 1998 Gem News, pp. 298–299). According to Dudley Blauwet (Dudley Blauwet Gems, Louisville, Colorado) and Bill Larson (Pala International, Fallbrook, California), Nigeria recently produced some fine blue-to-green tourmaline (figure 32). Some of the rough appears as clean, elongate “pencils” that do not show evidence of alluvial transport, but alluvial material also is recovered. The first discoveries of these tourmalines were made late last year, from granitic pegmatite deposits. Nigerian dealers of rough have indicated that the mine is located in the Ilorin area of western Nigeria, and production has been sporadic.

Although production figures are not available, shortly before the 2001 Tucson shows Mr. Blauwet saw a parcel of rough that weighed 1,100 grams, and at Tucson he saw another parcel that weighed 400 grams. Most of the tourmaline in these parcels was blue and appeared dark, but some showed attractive colors. From a selection of 110 grams of rough, Mr. Blauwet obtained about 250 carats of faceted stones; most of these ranged from 1 to 7 ct. Pala International participated in the sale of a 3,500 gram parcel of this tourmaline in June 2001, from which two crystals (49.81 and 79.22 ct) were selected for chemical analysis. The saturated blue color shown by these unheated gemmy crystals resembled that of some copper-bearing “Paraíba” tourmaline from northeast Brazil (see also the following entry). EDXRF qualitative chemical analysis at the GIA Gem Trade Laboratory in Carlsbad revealed major amounts of Al, Si, and Fe, as well as traces of Ca, Mn, Zn, Ga, and Sn, in both crystals; however, no copper was detected in either crystal.

**Nigeria as a new source of copper-manganese-bearing tourmaline.** In August 2001, the Gübelin Gem Lab (GGL) received samples of tourmaline from firms in Idar-Oberstein, Germany (Gebrüder Bank, Wild & Petsch, and Paul Wild) that also reportedly were from a new deposit near Ilorin, Nigeria. We were informed by these suppliers that the tourmalines from this deposit are found in a wide range of colors, many of which are similar to those observed in “Paraíba” tourmalines from the São José da Batalha mine in Brazil. According to the suppliers, most of the Nigerian material—like the Brazilian tourmalines—is heat treated; after heat treatment, the majority of the tourmaline is sold in Germany and in Brazil.

The Nigerian tourmalines studied at GGL were submitted by the dealers before heat treatment, and consisted of a 22.98 ct violet gemstone (figure 33), six purplish pink to blue crystal pieces (0.69–1.44 ct; figure 34), and a 3.30 ct bluish green piece. Standard gemological properties obtained for the 22.98 ct stone were typical for gem tourmaline: R.I.— $n_o=1.620$ ,  $n_e=1.638$ ; birefringence—0.018; optic character—uniaxial negative; and inert to short- and long-wave UV radiation. Internal features consisted of the typical liq-

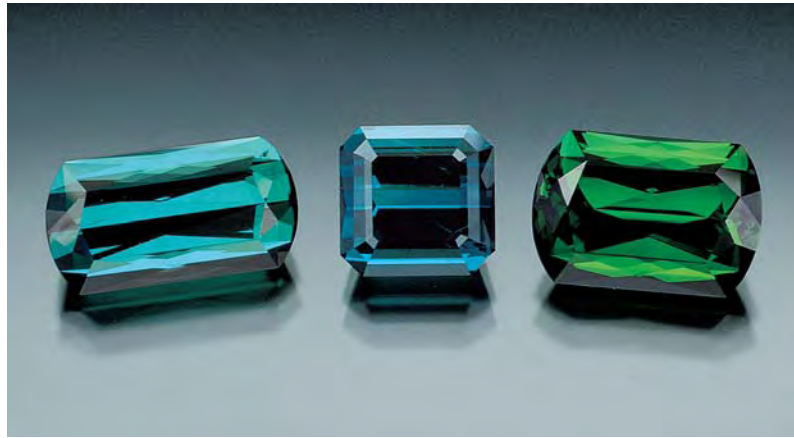


Figure 32. These three blue-to-green faceted gems (9.5, 7.0, and 9.5 ct) show the range of color seen in the tourmaline found recently in the Ilorin area of western Nigeria. Courtesy of Dudley Blauwet; photo by Jeff Scovil.

uid inclusions observed in tourmalines, some of which contained a secondary gas bubble. The gemstone displayed moderately strong pleochroism consisting of purple-violet parallel to the optic axis and slightly grayish violet-blue perpendicular to the optic axis. A distinct color change was visible when the stone was viewed in day- or fluorescent light (violet) and incandescent light (purple).

EDXRF qualitative chemical analysis of the violet gemstone and the purplish pink to blue pieces revealed the presence of copper, as well as manganese, iron, and bismuth, in varying relative intensities. The bluish green slice contained relatively high concentrations of iron and manganese, but no copper was detected.

Copper-manganese-bearing elbaite from Nigeria was

Figure 33. This 22.98 ct copper-manganese-bearing tourmaline comes from a new deposit in Nigeria, also believed to be in the Ilorin area. Some of the gems recovered from this deposit are similar in color to “Paraíba” tourmalines from Brazil. Photo by Franzisca Imfeld.



recently documented by J. W. Zang et al. ("Cu-haltige Elbaite aus Nigeria," *Berichte der Deutschen Mineralogischen Gesellschaft, Beihefte zum European Journal of Mineralogy*, Vol. 13, 2001, p. 202), who reported the source as the Edeko area, near Ilorin in western Nigeria. These authors obtained quantitative chemical analyses of three violet-blue samples (J. Zang, pers. comm., 2001) that are consistent with the results we obtained; using an electron microprobe and laser mass spectrometry, they measured 2.13–2.59 wt.% MnO, 0.51–2.18 wt.% CuO, 0–0.05 wt.% TiO<sub>2</sub>, 0–0.02 wt.% FeO, and 0–0.02 wt.% Bi<sub>2</sub>O<sub>3</sub>, as well as other minor and trace elements. Prior to this new find, cuprian elbaite was known only from the Paraíba and Rio Grande do Norte states in northeast Brazil (see, e.g., E. Fritsch et al., "Gem-quality cuprian-elbaite tourmalines from São José da Batalha, Paraíba, Brazil," Fall 1990 *Gems & Gemology*, pp. 189–205; J. Karfunkel and R. R. Wegner, "Paraiba tourmalines—Distribution, mode of occurrence, and geologic environment," *Canadian Gemmologist*, Vol. 17, No. 4, 1996, pp. 99–106).

Tourmaline mining in the Edeko area is reportedly unorganized, with up to several thousand miners working the area. At this time, the amount of copper-manganese-bearing tourmaline produced from there is not known. Some reports indicate that over 100 kg of Edeko rough have been sent to Idar-Oberstein, but very little of the material is of high quality, and even less has enough copper to attain the intense "Paraíba"-like blue, blue-green, and "turquoise" colors (J. W. Zang, pers. comm., 2001).

CPS, George Bosshart, and Dietmar Schwarz  
Gübelin Gem Lab, Lucerne, Switzerland

Figure 34. These six samples (0.69–1.44 ct) show a range of colors from the new tourmaline deposit in Nigeria. All of them were identified as copper-manganese tourmaline by EDXRF qualitative chemical analysis. Photo by Franzisca Imfeld.



**More on liddicoatite from Nigeria.** A report on an orangy pink crystal of Nigerian liddicoatite in the Summer 2001 GNI section (pp. 152–153) speculated that an untold amount of tourmaline from this country might be liddicoatite, which historically has been known primarily from Madagascar. More liddicoatite now has been identified from Nigeria, this time purplish red.

Last spring, John Patrick of El Sobrante, California, sent two purplish red tourmalines to GNI editor Brendan Laurs for examination after he noticed that they had a slight color shift between incandescent light and an Ott-Lite (which is represented as a "total spectrum light source"). The 8.64 ct oval brilliant and 6.89 ct cushion step cut were purchased about two-and-a-half years ago, and reportedly were mined in the Abuja area in central Nigeria (figure 35). Mr. Patrick also donated a 1.39 ct purplish red tourmaline crystal from the same parcel to GIA, one end of which we polished flat, perpendicular to the c-axis, for analysis.

The three stones were reddish purple when viewed with a daylight-equivalent fluorescent lamp, and their color appeared somewhat more brownish in incandescent light. This color behavior is quite normal, due to the different wavelengths of these two light sources, and it would not be considered a color-change phenomenon. Gemological properties were: R.I.— $n_o=1.621$ ,  $n_e=1.639$ ; birefringence—0.018; S.G.—3.07–3.08; fluorescence—inert to long-wave UV radiation, and inert to very weak greenish yellow to short-wave UV. With the microscope, the oval-cut stone and the crystal revealed strong graining and tiny colorless crystals that appeared isotropic between crossed-polarizers. The grain lines were planar and intersected in angular or triangle-shaped patterns that were centered on the c-axis. Concentrations of graining along each triangular apex appeared in the shape of a Mercedes Benz symbol perpendicular to the c-axis of the crystal, but otherwise there was no evidence of zoning within this homogeneously colored tourmaline. The crystal also contained minute growth tubes parallel to the c-axis, some of which originated from the tiny included crystals.

The polished surface of the crystal was analyzed with an electron microprobe by Drs. William ("Skip") Simmons and Alexander U. Falster at the University of New Orleans, Louisiana, as part of an ongoing research project there on tourmaline composition. There was no systematic chemical zoning in five analyses that traversed a cross-section of the crystal. The sample proved to be liddicoatite, with average concentrations of 2.87 wt.% CaO and 1.44 wt.% Na<sub>2</sub>O. Fluorine (1.35 wt.% F), manganese (0.20 wt.% MnO), and iron (0.09 wt.% FeO) also were detected; the latter two chromophoric elements are the likely cause of the purplish red color. Other elements known to influence the color of tourmaline (i.e., titanium, chromium, and vanadium) were not detected. Unlike the Nigerian liddicoatite reported in the Summer 2001 GNI section, this crystal contained very little bismuth—an average of only 0.03 wt.% Bi<sub>2</sub>O<sub>3</sub>. Traces of zinc (up to 0.09 wt.% ZnO), magnesium (up to 0.05 wt.% MgO), and potassium (up to 0.03 wt.% K<sub>2</sub>O) also



Figure 35. These 8.64 ct (left) and 6.89 ct (right) tourmalines were reportedly mined in the Abuja area of central Nigeria. The purplish red color is seen here as viewed with a daylight-equivalent fluorescent lamp. A crystal of identical color from the same parcel proved to be liddicoatite. Courtesy of John Patrick; photos by Maha Tannous.

were found in some analyses, whereas barium, lead, and chlorine were not detected.

## SYNTHETICS AND SIMULANTS

**Laboratory-grown orange-to-yellow “langasite.”** Langasite is a transparent piezoelectric silicate of lanthanum and gallium ( $\text{La}_3\text{Ga}_5\text{SiO}_{14}$ ) that is grown by the Czochralski method for technological applications. It has no natural counterpart. The name *langasite* is derived from its chemical components (La, Ga, and Si); it should not be confused with the unrelated natural mineral *langisite*, (Co,Ni)As. Langasite is one of about 100 compounds with the  $\text{Ca}_3\text{Ga}_2\text{Ge}_4\text{O}_{14}$  structure that were first grown in Russia in the early 1980s (see B. V. Mill et al., “Synthesis, growth and some properties of single crystals with the  $\text{Ca}_3\text{Ga}_2\text{Ge}_4\text{O}_{14}$  structure,” 1999 Joint Meeting EFTF – IEEE IFCS, *Extended Abstracts*, pp. 829–834). The high refractive indices, high dispersion, and hardness (reported as 6.6 on the Mohs scale) of langasite make it suitable for use as a gem material. It is currently produced in Russia, Japan, Korea, France, and the U.S., and is used in wireless and cellular communications and cable television. The color of langasite can vary, depending on growth conditions and added dopants. We know that orange to yellow crystals are grown in Russia, Japan, and France (see S. Uda and O. Buzanov, “Growth of 3-inch langasite crystal with clear faceting,” *Journal of Crystal Growth*, Vol. 211, 2000, pp. 318–324), and colorless crystals are reportedly produced in the U.S. (Prof. Y. Pisarevsky, pers. comm., 2001).

GIA recently used both standard and advanced gemological techniques to examine nine samples of langasite from Russia (see, e.g., figure 36). Three of the samples were faceted (4.59, 4.98, and 56.80 ct), and four were crystal fragments or oriented sections (up to 81.99 ct or  $23.6 \times 19.8 \times 13.2$  mm). Detailed results of this examination will be published in *Vestnik Gemmolgii* (*Gemology Herald*; T. Lu et al., “Langasite—A new man-made orange-to-yellow gem material,” Vol. 1, No. 2, 2001, in press), a new journal of the Gemmological Society of Russia in Moscow. The samples ranged from orange to yellow, with the larger samples having the greatest color saturation. The coloration was uniform, with no color banding observed. Moderate pleochroism (light yellow/orange) was seen with a polar-

iscope. All samples yielded a specific gravity (measured hydrostatically) of 4.65. The refractive indices of langasite are over-the-limits of a standard refractometer. However, on a sample of orange Russian langasite, Prof. Y. Pisarevsky (Institute of Crystallography Russian Academy of Sciences, Moscow, Russia) used the prism method to determine R.I. values of  $n_o = 1.9099$  and  $n_e = 1.9213$  (with 546 nm light), a birefringence of 0.0114, and high dispersion (0.035) with green and red dispersive colors.

None of the samples exhibited any twinning or fracturing. We observed triangular-shaped solid inclusions (oriented in linear arrays) in one faceted sample, and a large number of two-phase inclusions in the form of parallel needles in another faceted sample. The rough samples with crystal faces showed growth striations in oblique orientation to the optic axis direction.

Using a handheld spectroscope, we did not observe any absorption bands in the samples; nor did we observe any visible luminescence when they were held over the spectroscope lamp. All the samples were inert to short- and long-wave UV radiation.

The visible spectra (250–850 nm) of five orange-to-yellow samples showed gradually decreasing absorption from 350 to about 580 nm, and no absorption features from about 580 to 850 nm. The infrared spectra displayed a broad band centered at  $5436\text{ cm}^{-1}$ , and weak sharper bands at  $3405$ ,  $2921$ , and  $2847\text{ cm}^{-1}$ . The Raman spectra showed peaks at  $5280$ ,  $5246$ ,  $3472$ , and  $3223\text{ cm}^{-1}$ ; a broad peak centered at  $4612\text{ cm}^{-1}$ ; and weak peaks at  $3574$ ,  $2654$ ,  $2628$ ,  $737$ , and  $704\text{ cm}^{-1}$ . EDXRF spectra showed the expected major elements (lanthanum, gallium, and silicon); no trace elements were detected. The color of the samples was stable when heated to  $250^\circ\text{C}$ . No data have been reported on the cause of the yellow to orange color.

Faceted pieces of this langasite could resemble other transparent orange or yellow gem materials. However, the properties of langasite permit easy identification by a trained gemologist with standard gemological instruments. The high refractive indices distinguish langasite from sapphire and spinel, and its double refraction differentiates it from optically isotropic gems such as diamond, cubic zirconia, YAG (yttrium aluminum garnet), and GGG (gadolinium gallium garnet).

The gem material that most easily could be confused



Figure 36. These two faceted samples of the synthetic material “langasite” ( $\text{La}_3\text{Ga}_5\text{SiO}_{14}$ ) were grown in Russia by the Czochralski method. They weigh 56.80 and 4.59 ct. Photo by Maha Tannous.

with langasite is zircon. However, characteristic absorption lines seen with the desk-model spectroscope can separate the two materials. Also, the infrared and Raman spectra, as well as the EDXRF chemical analysis, of langasite and zircon are quite distinct. In addition, the crystal morphology of zircon is tetragonal, whereas langasite (which is trigonal) is grown in the form of hexagonal-shaped crystals.

Langasite-type compounds have received much attention in the optoelectronics industry. Several varieties have been grown as single crystals by the Czochralski method

Figure 37. This laboratory-grown 5.45 ct rectangular step cut ( $11.1 \times 6.9 \times 5.1$  mm) was represented as “langasite.” Chemical analysis of the sample revealed a composition that is consistent with a theoretical formula of  $\text{SrLaGa}_3\text{O}_7$ , which differs from that of langasite,  $\text{La}_3\text{Ga}_5\text{SiO}_{14}$ . Photo by Alain Cossard.



(again, see Mill et al., 1999), and their gemological properties are likely to vary from what is reported here.

Taijin Lu and JES  
GIA Research  
tlu@gia.edu

Vladimir S. Balitsky  
Institute of Experimental Mineralogy  
Russian Academy of Science  
Chernogolovka, Russia

**Laboratory-grown pink  $\text{SrLaGa}_3\text{O}_7$ , a material related to “langasite.”** Pierre Vuillet of Villards d’Heria, France, provided this contributor with a light pink 5.45 ct rectangular step cut represented as “langasite” by a crystal grower from the French Alps (who reported the chemical formula as  $\text{SrLaGa}_4\text{O}_7$ ). Although the sample is light pink in daylight (figure 37), this color changes to light yellow with exposure to strong incandescent light. Unlike an alexandrite effect, however, the color change is not instantaneous—it takes several minutes. But like the alexandrite effect, the change in color is reversible. With a calibrated Sarasota Instruments reflectometer, a refractive index of approximately 1.82 could be measured. Observation with a polariscope revealed a fairly strong birefringence, but this could not be measured with the reflectometer due to the resolution (approximately  $\pm 0.02$ ) of the instrument. The sample was optically uniaxial, but no pleochroism could be seen, perhaps because of the very light color. The specific gravity was very high, at about 5.25. The sample fluoresced an intense green to long-wave UV radiation, and a weaker green to short-wave UV. The handheld spectroscope revealed a line in the blue region at about 485 nm and a doublet in the green region around 525 nm. There were many groups of inclusions, including whitish “breadcrumbs” and short cylindrical tubes that were interrupted in places and in a few instances originated at larger “breadcrumb” inclusions. Also observed were what looked like negative crystals, and a few small, irregular yellowish masses.

Analysis with the energy-dispersive X-ray spectrometer of a JEOL 5800 scanning electron microscope revealed the following chemical composition (measured in atomic percentage): 24.74 at.% gallium, 8.36 at.% strontium, 8.57 at.% lanthanum, and 58.34 at.% oxygen (determined by stoichiometry). This is consistent with a theoretical formula of  $\text{SrLaGa}_3\text{O}_7$ , which differs from the formula provided by the manufacturer by one less gallium atom per formula unit.

To investigate the origin of the pink color, a UV-visible absorption spectrum was recorded with a Unicam UV4 spectrophotometer in the range 350–700 nm. A number of sharp lines and doublets—with the major ones at 365, 380, 485–488, 520–523 and 648–653 nm—were superimposed on an absorption continuum that rose slowly toward the ultraviolet. This latter absorption may be enhanced by incandescent lighting, which shifts the color of the sample toward yellow over a period of minutes. These absorption features are consistent in general shape and position with those seen with the handheld spectroscope. They are

typical for erbium ( $\text{Er}^{3+}$ ) in cubic zirconia (see, e.g., Kammerling et al., "An examination of nontransparent 'CZ' from Russia," Winter 1991 *Gems & Gemology*, pp. 240–246), as is the luminescence behavior. However, the erbium concentration was below the detection limit (which is estimated at approximately 400 ppm) using our SEM-EDX analytical technique under standard conditions.

Although this material is not langasite, which has a formula of  $\text{La}_3\text{Ga}_5\text{SiO}_{14}$ , its composition suggests that it could be part of the langasite family of compounds (see B. V. Mill et al., 1999, cited in the previous entry). EF

**An unusual "crystal" of synthetic ruby from Sri Lanka.** In December 1999, a friend of this contributor purchased a 9.56 ct specimen in Sri Lanka that was represented as ruby. The sample looked like a typical broken bipyramidal crystal with waterworn surfaces, and showed a saturated red color (figure 38). Examination with a handheld spectroscope revealed a typical ruby spectrum. With strong back-lighting, straight parallel zones perpendicular to the perceived optic-axis direction could be seen with difficulty; these appeared to result from the presence of inclusions.

The rough yielded a well-proportioned 4.17 ct pear shape. Prominent, eye-visible zoning appeared to be caused by dense concentrations of the "silk" inclusions that are typical of ruby (figure 39). When viewed with a microscope, however, slightly curved zones of tiny gas bubbles were seen. Between the zones of small bubbles were larger bubbles, some with a long attached channel (figure 40). Also present were abundant, curved hollow cavities that were very similar to the "trichites" seen in many tourmalines.

The gas bubbles proved that this sample was a flame-fusion synthetic ruby. However, this fake crystal was unusual in that it was fashioned from low-quality synthetic material containing abundant bubbles. While most gem

Figure 38. This 9.56 ct broken bipyramidal "crystal" was actually manufactured from low-quality flame-fusion synthetic ruby. Photo by Jaroslav Hyrsl.



Figure 39. The 4.17 ct pear-shaped synthetic ruby cut from the "crystal" shown in figure 38 appears to contain zones of "silk," which give it a natural appearance to the unaided eye. Photo by Jaroslav Hyrsl.

dealers are suspicious of high-quality rough *without* inclusions, few expect to see clever imitations of rough crystals made from lower-quality synthetics. Such mistakes can be very costly. Jaroslav Hyrsl

**A rare medieval sapphire imitation.** Gemstone imitation is an ancient practice, and some historic examples are very clever. One such imitation was recently documented by this contributor during a gemological examination of the medieval Ardennes cross at the German National Museum in Nuremberg. The gem materials in the cross were identified by a combination of optical properties (using a microscope, dichroscope, spectroscope, color filters, and sometimes a refractometer), as well as UV fluorescence, thermal properties, and (in rare instances) hardness.

The wooden cross measures 73 cm tall and 45 cm wide, and is covered by dozens of polished gems; one arm is

Figure 40. When examined with a microscope, the streaks of "silk" were revealed to be slightly curved zones of gas bubbles, which proved the ruby was synthetic. Photomicrograph by Jaroslav Hyrsl; field of view is 1.7 mm.





Figure 41. A gemological examination of the medieval Ardennes cross revealed red almandine garnet and glass or quartz imitations of more valuable gem materials. The wooden cross measures 73 × 45 cm; one arm is damaged, and the stones and metalwork are missing. Courtesy of Germanisches Nationalmuseum Nürnberg.

damaged and the stones are missing (figure 41). According to art historians, it probably was crafted in France in the second quarter of the ninth century. Most of the gems are set in their original mountings, although some were apparently added during restorations—these have a larger mounting and/or a different cutting style. On the basis of their optical characteristics, the gems were identified as red almandine garnet, green glass, rock crystal, and many unusually large samples that apparently served to imitate sapphires.

Three of the sapphire imitations are blue glass; these contain many gas bubbles and scratches on the surface, and one of them is drilled. Based on the criteria mentioned above, these appear to be replacements for the original gems. In addition, 15 of the large “sapphires”—all of which are believed to be original to the piece—are polished pebbles that have been drilled. They are colorless with a few blue spots (figure 42) and appear similar to Sri Lankan sapphires, which were available in Europe since at least Roman times. Microscopic examination of the colorless portions revealed fractures and two-phase inclusions, as are typical of natural stones. However, the blue spots contained tiny gas bubbles (again, see figure 42). Thermal con-

ductivity testing showed no reaction on the blue spots, but significant conductivity on the colorless areas. The colorless portion of one broken “sapphire” revealed a conchoidal fracture, which is typical of quartz or glass; a careful hardness test made while examining the sample with a microscope supported an identification as quartz, as did the presence of the two-phase inclusions.

These observations suggest that the 15 drilled sapphire imitations consist of quartz pebbles that were dipped into molten blue glass and then drilled and repolished. (Note that “gemstones” in ancient Sri Lanka were commonly used as amulets, and therefore almost all Roman and medieval sapphires are drilled.) These imitations are much more convincing than those made of blue glass, which are common to medieval as well as younger objects. Nevertheless, the gas bubbles seen with the microscope, and the relatively low hardness of the quartz, were key factors in recognizing these imitations.

Jaroslav Hyrsl

## ANNOUNCEMENTS

### CONFERENCES/SHOWS

**GAGTL Gem-A Conference 2001.** The Gemmological Association and Gem Testing Laboratory of Great Britain will host its annual conference on November 4, 2001, at London’s Barbican Conference Centre. Presentations will cover HPHT-treated diamonds, heat treatment of rubies, and more. In conjunction with the conference, one-day GAGTL workshops will focus on pearls (October 31) and amber (November 6). Additional events include a guided tour of the geologic section of the Natural History Museum in London (November 2) and a visit to De Beers (November 5). For further information, visit <http://www.gagtl.ac.uk/gnews.htm>; contact Mary Burland at 44-20-7404-3334 (phone), 44-20-7404-8843 (fax); or e-mail [gagtl@btinternet.com](mailto:gagtl@btinternet.com).

**SimDesign 2001.** The *1st Brazilian Symposium of Jewelry Design and Gemology* will take place November 29–December 1 at the Marina da Glória Convention Center in Rio de Janeiro. The event will provide networking opportunities for designers, jewelers, and gemologists. For more, visit <http://www.simdesign2001.com.br> or e-mail [info@simdesign2001.com.br](mailto:info@simdesign2001.com.br).

**Australian Diamond Conference.** On December 4–5, 2000, this conference will take place in Scarborough, Perth, Western Australia. The program will feature presenters from several diamond explorers, as well as major industry analysts. A pre-conference tour of the Argyle diamond mine will occur on December 1. Contact Eleanor Dix at 61-8-9321-0355 (phone), 61-8-9321-0426 (fax), or e-mail at [elle@louthean.com.au](mailto:elle@louthean.com.au).

**Visit *Gems & Gemology* staff in Tucson.** *Gems & Gemology* editors Alice Keller, Brendan Laurs, and Stuart Overlin will join Subscriptions manager Debbie Ortiz at





Figure 42. Among the sapphire imitations in the medieval Ardennes cross were 15 drilled and polished pieces such as the 2.4-cm-long example shown on the left. The light-colored area crossing the length of the stone in the center is a drill hole. On the right, note the tiny gas bubbles in the blue glass areas, as well as the two-phase inclusions in the colorless portion, which was tentatively identified as quartz (field of view is 8.0 mm wide). Photos by Jaroslav HyrsI.

the *Gems & Gemology* booth in the Galleria section (middle floor) at the Tucson Convention Center for the AGTA show, February 6–11, 2002. Stop by to ask questions, share information, or just say hello. And take advantage of the many back issues—and special prices—we’ll be offering, including a limited number of out-of-print issues that we recently acquired.

Following the AGTA show, the Tucson Gem and Mineral Show will take place on February 14–17. The theme of the show and of the 23rd Annual Mineralogical Symposium (February 16) will be *African Minerals*.

## EXHIBITS

**Jewels of the Nizam.** The famed gem and jewelry collection of the Nizam of Hyderabad, valued at \$1.27 billion, is now on display to the public. The exhibit was inaugurated on August 29, 2001 by Indian prime minister Atal Bihari Vajpayee at the National Museum in New Delhi. The Indian government purchased the 173-piece collection from the trust of the last Nizam, as the feudal princes of the western Indian state of Hyderabad were known, after years of negotiations. The Nizams governed Hyderabad from 1712 until 1948, a year after the end of British colonial rule of India. After the last Nizam’s death in 1967, the collection—which includes the 185 ct Jacob diamond as well as emeralds, pearl necklaces, and gem-encrusted turbans—was housed in the Reserve Bank of India in Mumbai. Beginning in November, the exhibition will be on display for six weeks at the Salar Jung Museum in Hyderabad. Visit <http://www.nationalmuseumindia.org>, or contact Mr. U. Das at 91-011-3018415 (phone) or [rdchoudh@ndf.vsnl.net.in](mailto:rdchoudh@ndf.vsnl.net.in).

**Gem museum in Sri Lanka.** In March 1999, a new gem and mineral museum opened to the public in Mount Lavinia, Sri Lanka. Undertaken by lapidary and collector

Gamini Zoysa, the museum houses rare and unusual gemstones, organic gem materials, and specimens displaying optical phenomena from Sri Lanka and other countries. Also featured is a large collection of postage stamps depicting gemstones. Call 94-1-726796 or e-mail [mincraft@slt.lk](mailto:mincraft@slt.lk).

**Pearls at the American Museum of Natural History.** A comprehensive exhibition on pearls will take place at the American Museum of Natural History in New York until April 14, 2002. *Pearls* will then travel to Chicago’s Field Museum, where it will be on view from June 28, 2002, through January 5, 2003. The exhibition showcases pearls and pearl-forming mollusks, including white and black pearls from marine *Pinctada* oysters of Japan and Polynesia, freshwater pearls from mussels found in the United States and China, pink conch “pearls” from the Caribbean Queen conch, and more. A section on the decorative use of pearls will feature a wide range of jewelry and *objets d’art*. Visit [www.amnh.org](http://www.amnh.org), or call (212) 769-5100.

## ERRATA

1. In the Summer 2001 article on Chinese freshwater cultured pearls by S. Akamatsu et al., line five of the abstract on p. 96 should have read “Zhejiang Province” (of which Hangzhou city is the capital). We thank Dr. Tian Lianguang for this correction.
2. In the abstract on synthetic corundum and spinel from Skawina, Poland (Summer 2001, p. 170), the  $Al_2O_3$  that does not occur naturally and does not have a trigonal structure should have been reported as  $\gamma-Al_2O_3$ , not  $\alpha-Al_2O_3$ . The material described in the last sentence of the abstract also is  $\gamma-Al_2O_3$ . We thank Dr. W. Wm. Hanneman for bringing this error to our attention.

## EDITORS

Susan B. Johnson  
Jana E. Miyahira-Smith

### Gemstones—Quality and Value, Vol. 3: Jewelry

By Yasukazu Suwa, 144 pp., illus., publ. by Sekai Bunka Publishing, Tokyo, 2001. US\$95.00\*

This beautifully illustrated and designed book helps explain “the factors that determine the quality of jewelry” in a way that most readers will understand and appreciate. Mr. Suwa accomplishes this by separating the book into two main sections. In the first, “Gemstone-Oriented Jewelry,” he examines 26 individual pieces of jewelry and explains the features that make each one unique and desirable. He then focuses on specific aspects of each jewel in an educational format that teaches the reader what to look for in similar jewelry. For example, the chapter on a “band-type emerald and diamond ring” explains why the diamonds are set in platinum while the emerald is set in gold (because each metal flatters the color of the particular stone). Mr. Suwa further adds that the emerald in the ring is from Zambia and is untreated. In the next few pages of the chapter, he moves into a more general discussion of treated vs. untreated emeralds and the versatility of band rings.

The second section, “The Quality of Jewelry,” is especially informative for those unfamiliar with the jewelry trade. Here Mr. Suwa reviews quality, value, and price. He also takes the reader through design conception, choice of materials, fabrication, evaluation of the jewelry’s condition (porosity, solder marks, etc.), remodeling, and recirculation (resale). Diagrams illustrate various jewelry parts. The book finishes with a chapter on trends and traditions, and a useful jewelry glossary.

As a reference, this volume accomplishes much. The areas discussed are well illustrated and organized, and a convenient section on “How to Use This Book” is included. Rather than just deal with a particular type of setting, stone, or style, *Gemstones: Quality and Value* achieves distinction by taking actual pieces of jewelry and teaching the reader how to evaluate them. As the author clearly states, the book is not a technical manual. However, it does succeed as an overview. At the very least, it will give the reader a deep appreciation for jewelry of quality.

JANA E. MIYAHIRA-SMITH  
*Gemological Institute of America*  
Carlsbad, California

### Mogôk: Valley of Rubies & Sapphires

By Ted Themelis, 270 pp., illus., publ. by A & T Publishing, Los Angeles, 2000. US\$89.00

This reviewer has anxiously awaited Ted Themelis’s Mogok book for more than two years. When I saw a copy at the 2001 Las Vegas JCK show, I knew that my long wait was justified. From the pleasing dust jacket through the plethora of maps, drawings, and photographs both old and new, it was obvious that the author’s love for Mogok and Burma (now Myanmar) had been transferred to the pages of this book. This hardcover book measures 22 × 29 cm (8.6 × 11.4 inches), and has more than 500 illustrations.

Chapter 1 covers the history of Burma. As complicated as that history might be, Mr. Themelis manages to make it both understandable and

accurate. Sidebars of interesting legends, together with the pictures and graphics, hold the reader’s attention even through complex dynastic names and tongue-twisting transliterations from Burmese into English.

In the following three chapters, Mr. Themelis plunges directly into the cultural melting pot that is Mogok, covering the town’s varied lifestyles, religions, cuisines, and superstitions. While some readers may find certain details unnecessary, many of them relate back to the gems themselves.

Gem trading from early times to the present day is covered in chapter 5, and chapter 6 examines how the lapidaries of Burma and Mogok have changed over the years, with influence from Indian, British, and most recently Thai lapidaries. An interesting explanation of why Burmese cutters leave extra weight on their stones is provided (i.e., not just for higher weight yield, but also so subsequent buyers can improve the stone if they desire).

Chapter 7 covers notable rubies and sapphires from Mogok, and includes a wonderful story on a major piece of rough that eventually produced a 25.55 ct faceted ruby. However, the tables that list major stones produced from 1630 to 1999 contain many stories with little substance or substantiation. For example, an item on page 229 reads: “1928. A 437-carat blue sapphire was found in an unspec-

*\*This book is available for purchase through the GIA Bookstore, 5345 Armada Drive, Carlsbad, CA 92008. Telephone: (800) 421-7250, ext. 4200; outside the U.S. (760) 603-4200. Fax: (760) 603-4266.*

ified area of Mogok. It was valued at over £11,000." Even though mystery and intrigue are a big part of the gem business, items such as this still leave the reader wishing for more solid information.

"Burmese Court Regalia" is the subject of chapter 8, with an interesting account of how so many valuable palace rubies and other gems disappeared the night of November 28, 1885, when the British occupied Mandalay. The British returned several items, but retained others.

Chapter 9 contains numerous examples of Burmese jewelry, in both traditional and modern settings. Concluding the book is a four-page selected bibliography, a one-page glossary, and an index.

*Mogok* lacks information on geology, mineralogy, and specific mining areas, as well as pictures of rough. According to the author, however, these topics will be covered in the second volume, which this reviewer eagerly awaits.

This book's main flaws are those found in many self-published productions. It lacks professional editing and polish. Numerous errors in spelling, grammar, and traditional publishing symbols are found throughout the book. Many photos and plates lack credit information (e.g., p. 203), and many statements lack references (e.g., pp. 12–13). These diminish the value of a book that is aimed, at least in part, at an academic audience. Another serious defect is seen in the photo reproduction. All of the book's photos should have been sharpened in the pre-press stage, and virtually all have unnatural color casts.

However, such distractions are minor when compared to the overall value of the work. Since his first visit to Mogok in 1996, Mr. Themelis has immersed himself in everything Burmese and, especially, Mogok. This included travel to the British Library in London, private libraries, various museums, and, of course, the area itself. The author's impassioned love of Mogok provides insights not found in any other modern book on this region. *Mogok—Valley of Rubies* e

*Sapphires* is a must for every gemologist's library. It captures all aspects of Mogok's gem and jewelry industry—the history, romance, intrigue and, most importantly, the enchantment of a truly enchanted land.

WILLIAM F. LARSON  
*Pala International*  
*Fallbrook, California*

### Southwest Silver Jewelry

By Paula A. Baxter, 212 pp., illus., publ. by Schiffer Publishing, Atglen, PA, 2001. US\$49.95

When an author writes about a subject he or she loves, it really reaches the reader. Such is the case with this beautiful book, which examines and pays tribute to the first century of Navajo and Pueblo metal jewelry making in the American Southwest. The historical information is enlightening, and is complimented by the high-quality presentation and numerous large-format photos that illustrate the evolution of this jewelry.

Telling a story that starts in the 1860s, the author points out that the use of silver for jewelry was a relatively recent development for Native Americans. Metals were not considered to be "spiritual" materials, but the natives loved the pale luster of silver because it reminded them of the moon. Early work involved the melting of coins to make practical items (such as buttons and belt buckles) and objects for personal adornment. When these items were seen by the white settlers and Native Americans both locally and from other regions, a commercial market slowly began to develop. This book recounts the fascinating tale of how ingenious Native Americans created tools out of available materials after learning skills from blacksmiths and Mexican silversmiths, and how each tribe branched off to create a unique style that continues to evolve.

Silversmithing production steadily expanded during the "first phase" (1868–1900) of Southwestern Indian jewelry. At first, the techniques were crude due to the tools available, but as

lapidary work developed and skills were perfected, more complex designs began to appear. Stones first appeared in the silver jewelry around the 1880s, usually as a single polished center-piece mounted in a bezel. The first gems used were small pieces of local garnets, turquoise, malachite, or shell. Since the supply of turquoise was initially scarce, traders imported Persian turquoise to meet demand. By 1900, however, new mines in the southwestern U.S. yielded plentiful supplies. Photos in the book show the transition from simple early designs to beautiful and intricate works of modern art.

The book also helps readers distinguish the work of the Navajo, Zuni, and Hopi tribes. It clearly explains terms such as *old pawn* vs. *dead pawn*, and it includes tips for collecting, a list of prestigious pre-1970 Indian artists, and a value reference guide. The pricing guide is understandably vague, since most of the hand-wrought items are unique and their age or origin is frequently difficult to determine. Nevertheless, this guide provides a good starting point for establishing values. Readers will learn to better recognize authentic Indian jewelry and to appreciate the art and designs, which are ever-changing but at the same time are always returning to—and honoring—their past. The enthusiasm of the author is infectious, and leaves the reader wanting to take a trip to the Southwest in search of silver treasures.

MARY MATHEWS  
*Gemological Institute of America*  
*Carlsbad, California*

### Jewelry Wax Modeling— A Practical Guide for the Jewelry Model Maker

By Adolfo Mattiello, 161 pp., illus., publ. by Du-Matt Corp., Guttenberg, NJ, 1999. US\$38.95\*

This is an excellent book for someone who wants to get started or learn more about the art of wax carving. Descriptions of 11 ring projects are

designed to take the reader from the very basics to the very advanced. At the beginning of each project is a beautiful painted rendering of the design, accompanied by photos of the actual wax at different stages. The in-depth, step-by-step instructions—with nicely done graphics and measurements—make the lessons very easy to follow and understand.

This guide is filled with many unique and time-saving tricks and tips. In addition, it includes a few tool modifications that will help the reader achieve higher levels of craftsmanship.

Many of the projects contain stone-setting styles that involve skills that are considered rather advanced, such as pavé work and channel setting with baguettes and round stones. It would be helpful to have some previous stone-setting skill and experience. If you do not, the author recommends that you do the prep work for the stone setting, finish the ring in metal, and then seek the assistance of a good stone setter. This should be seen as a challenge rather than a discouragement.

With patience and determination, the reader can learn a great deal from this book.

LARRY LAVITT  
*Gemological Institute of America*  
Carlsbad, CA

### Western Queensland Opals— Exploration and Geoscience Data Sets

*CD-ROM, Queensland Government Department of Mines and Energy, 2000, free of charge [e-mail: lcranfield@dme.qld.gov.au].*

Geographic information systems (GIS) provide a new, powerful way to look at spatial data such as geology, gem and mineral occurrences, and land status. This CD-ROM provides an extensive set of data for opal occurrences in the Cretaceous sedimentary rocks of western Queensland, Australia. Also included are several short HTML (Web browser) files that summarize the contents of the CD, introduce opal in western Queensland, note sapphire and chrysoprase occurrences in Queensland, and give related information on noncommercial collecting (fossicking) regulations. The text on opals is a few pages long, with only two illustrations, but, unfortunately, it is not integrated into the GIS data sets. The latter are quite extensive, with information on geology, structure, opal occurrences, land status, regional geophysics, and topography.

The CD is simple to use. It opens immediately with a Web browser running under Windows 95 or higher (in

my case, Windows 98 under Virtual PC on a Macintosh). The GIS data sets are in ESRI ArcView and MapInfo formats, which are suited to regular GIS users. In addition, a stand-alone viewer, ArcExplorer, is included along with easy-to-follow instructions.

As a geologist and teacher, I found the data sets and background quite interesting, but the information on opals is rather thin. This CD would be of interest to those prospecting in or visiting western Queensland opal districts. On the other hand, it has little to offer for those primarily interested in the gemology or detailed geology of these occurrences. Nevertheless, the Queensland Department of Mines and Energy is to be commended for publishing this CD-ROM; there is a coming revolution in the use of electronic publication with incorporation of approaches such as GIS that simply cannot be done in print.

MARK D. BARTON  
*Department of Geosciences*  
University of Arizona, Tucson

**Correction:** The Summer 2001 Book Reviews section listed the retail price of *The Practical Guide to Jewelry Appraising* by Cos Altobelli as \$49.95. This price is for AGS members only. The actual retail price is \$64.95.


# GEMS & GEMOLOGY

## TWENTY YEAR INDEX: 1981–2000

*GEMS & GEMOLOGY's TWENTY YEAR INDEX, your indispensable reference guide to the 1981–2000 issues, is now available. Search the index by subject or author to locate the articles, Lab Notes, and Gem News entries of interest to you.*

Printed copies are on sale for only \$9.95 in the U.S. (\$14.00 elsewhere). Download the index **FREE OF CHARGE** from the G&G website, [www.gia.edu/gandg](http://www.gia.edu/gandg). Or receive a free index by purchasing any three years of back issues.

To order your printed copy of the **TWENTY YEAR INDEX**, mail in the Index order card in this issue or contact Subscriptions Manager **Debbie Ortiz** at [dortiz@gia.edu](mailto:dortiz@gia.edu), or call toll-free 800-421-7250 ext. 7142. Outside the U.S. and Canada, call 760-603-4000, ext. 7142.



Back issues are also available.  
Visit [www.gia.edu/gandg](http://www.gia.edu/gandg)

# Gemological ABSTRACTS

# 2001

## EDITOR

**A. A. Levinson**  
University of Calgary  
Calgary, Alberta, Canada

## REVIEW BOARD

**Anne M. Blumer**  
Bloomington, Illinois

**Jo Ellen Cole**  
GIA Museum Services, Carlsbad

**R. A. Howie**  
Royal Holloway, University of London

**Jeff Lewis**  
University of New Orleans, Louisiana

**Taijin Lu**  
GIA Research, Carlsbad

**Wendi M. Mayerson**  
GIA Gem Trade Laboratory, New York

**Kyaw Soe Moe**  
GIA Gem Trade Laboratory, Carlsbad

**Joshua Sheby**  
GIA Gem Trade Laboratory, New York

**James E. Shigley**  
GIA Research, Carlsbad

**Jana E. Miyahira-Smith**  
GIA Education, Carlsbad

**Maha Tannous**  
GIA Gem Trade Laboratory, Carlsbad

**Rolf Tatje**  
Duisburg University, Germany

**Lila Taylor**  
Santa Barbara, California

**Paige Tullos**  
GIA Gem Trade Laboratory, Carlsbad

**Sharon Wakefield**  
Northwest Gem Lab, Boise, Idaho

**Philip G. York**  
GIA Education, Carlsbad

## COLORED STONES AND ORGANIC MATERIALS

**Chinese pearls: Their culturing and trading.** Guo T., *Australian Gemmologist*, Vol. 20, No. 11, 2000, pp. 486–490.

Chinese freshwater cultured pearls are playing an increasingly important role in the industry. In the 1960s, the cultivation was done primarily by individual families or indigenous farmers. In recent years, however, pearl culturing has shifted to large, modernized farms and the use of different mollusks, resulting in large quantities of a highly desirable product. In 1999, global production of cultured pearls was estimated at 1,262 tons, with Chinese freshwater cultured pearls making up 1,000–1,200 tons of that amount. Most of the farms are located along the banks of the Chang Jiang (Yangtze) River, where more than 400,000 people are engaged in the pearling industry. After 2–5 years of propagation and 1–3 years of cultivation, the implanted mussels produce jewelry-grade cultured pearls in a range of shapes (mostly off-round and baroque) and colors; most undergo color treatment before being sold. Luster ranges from poor to excellent, with larger cultured pearls (over 10 mm in diameter) typically showing low luster.

In the last two decades, the coastline of the Guangxi Province (Hepu and nearby areas) in southern China, including Hainan Island, has been used for the culturing of saltwater pearls. Natural pearls have been known from these areas since the Qin and Han Dynasties (221 BC to 221 AD). About 15–20 tons of Chinese Akoya cultured pearls were produced in 1999. The Beihai Municipal Bureau of Technical and Quality Supervision has dictated standards for Chinese Akoya pearl cultivation, with the objective of improving quality. These standards include specifications for the condition and depth of the

*This section is designed to provide as complete a record as practical of the recent literature on gems and gemology. Articles are selected for abstracting solely at the discretion of the section editor and his reviewers, and space limitations may require that we include only those articles that we feel will be of greatest interest to our readership.*

*Requests for reprints of articles abstracted must be addressed to the author or publisher of the original material.*

*The reviewer of each article is identified by his or her initials at the end of each abstract. Guest reviewers are identified by their full names. Opinions expressed in an abstract belong to the abstracter and in no way reflect the position of Gems & Gemology or GIA.*

*© 2001 Gemological Institute of America*

water, characteristics of the basket in which the seeded mussels are housed, techniques for implantation, and minimum cultivation times. Some of the large saltwater farms are attempting to improve the quality of their cultured pearls by implementing crossbreeding, low-density farming, and better processing technology. In size and quality, Chinese Akoya cultured pearls still do not match their Japanese counterparts, which sell for significantly more. Chinese Akoyas also are routinely color treated: bleached and then dyed. MT

**Emerald deposits—A review.** D. Schwarz and G. Giuliani, *Australian Gemmologist*, Vol. 21, No. 1, 2001, pp. 17–23.

Emerald is relatively rare because its chromophoric elements, Cr and V, are not typically associated with Be. Sources of Cr and V are mafic-ultramafic igneous rocks and black shales, whereas Be occurs in granitic magmas, black shales, and metamorphic rocks. The principal mechanism responsible for emerald crystallization is fluid–rock interaction, which allows the combination of these geochemically incompatible elements.

Most emerald deposits are associated with granitic intrusions and their related hydrothermal processes; examples include most African and Brazilian deposits, as well as those in the Ural Mountains of Russia. A second type of emerald formation is not directly related to granitic intrusions, but rather results from the circulation of fluids along regional tectonic structures (thrust faults and shear zones), as at Santa Terezinha in Brazil and the Swat Valley in Pakistan. The famous Colombian emerald deposits have a unique formation through the thermochemical reduction of evaporitic sulfate brines, with organic matter from the surrounding black shales participating in the reactions. RAH

**The factors for restricting quality of Chinese pearl.** Y. Deng and K. Yuan, *Journal of Guilin Institute of Technology*, Vol. 21, No. 1, 2001, pp. 6–12 [in Chinese with English abstract].

This article summarizes the results of research on Chinese saltwater cultured pearls of various grades, from different localities. Basic gemological properties were determined, and analytical data were obtained using (1) X-ray diffraction to determine mineral composition, and (2) ICP-AES (inductively coupled plasma–atomic emission spectroscopy) to determine trace elements and organic components present in these cultured pearls. The density of high-quality cultured pearls from Hepu (Guangxi Province) was 2.76 g/cm<sup>3</sup>, whereas low-quality cultured pearls had a density of 2.69 g/cm<sup>3</sup>. Although Chinese saltwater cultured pearls are composed predominantly of aragonite crystals, significant calcite (10%–45%) is also present. As is the case for most pearls (both natural and cultured), the c-axes of the aragonite crystals are oriented radially from the center of the cultured pearls. Studies of

the mineral composition, colors and their distribution, impurities, and internal growth features of Chinese saltwater cultured pearls revealed that these features could be correlated to different growth environments. TL

**Gem tourmaline chemistry and paragenesis.** W. B. Simmons, K. L. Webber, A. U. Falster, and J. W. Nizamoff, *Australian Gemmologist*, Vol. 21, No. 1, 2001, pp. 24–29.

Gem tourmalines from six pegmatite mining areas were studied by electron microprobe (no actual analyses are given). The samples were from Transbaikalia (Siberia, Russia), central Madagascar (Antandrokomby and Fianarantsoa/Anjanabonoina), Paraíba (Brazil), and the U.S. (Dunton, Maine, and the Himalaya mine in California). All were found to be dominantly elbaite or liddicoatite, with the darker varieties having a minor schorl component. Y-site chemistry correlated strongly with color and appeared to be influenced by the chemistry of the parent pegmatites. X-site vacancies were <0.3 atoms per formula unit (apfu).

The principal chromophores in the study samples were identified as Fe, Mn, Ti, and Cu. The pink and green tourmalines from Transbaikalia were essentially elbaite, but yellow zones in these crystals revealed a substantial liddicoatite component and elevated levels of Ti and Mn. Samples from Fianarantsoa/Anjanabonoina were liddicoatite. The Antandrokomby tourmalines belonged to the schorl-elbaite series, with significant Mg and Ca; they revealed the lowest Y-site Al content as well. The Maine and California tourmalines also were schorl-elbaite, with the lighter-colored gem varieties approaching end-member elbaite. The Paraíba tourmalines were elbaite, colored a vivid blue by Cu (0.1–0.3 apfu) in the Y-site. RAH

**The genetic relation between good-quality jadeite and microstructure.** K. Yuan and Y. Deng, *Journal of Guilin Institute of Technology*, Vol. 21, No. 1, 2001, pp. 1–5 [in Chinese with English abstract].

This well-illustrated article summarizes recent studies relating the quality of jadeite to microstructural characteristics that result from various geologic processes. Low-quality jadeite is correlated to cataclastic textures (characterized by bending and breaking) that are produced by severe mechanical stresses during metamorphism. Good-quality material is associated with mylonitic textures, which are characterized by intense microbrecciation and shearing. The highest-quality jadeite forms via “dynamic recrystallization” under conditions of low temperature, with strong shear stress and high strain velocity accompanying ductile deformation. Such jadeites have a fine-grained texture and good transparency. Green in jadeite is caused by the release of Cr from associated or included chromite grains; the intensity of the color appears to be related to the degree and type of structural deformation. TL

**Jade: Occurrences and metasomatic origin.** G. E. Harlow and S. S. Sorensen, *Australian Gemmologist*, Vol. 21, No. 1, 2001, pp. 7–10.

A brief review is given of the nephrite and jadeite varieties of jade and their occurrence. Nephrite, the more common variety, is formed via contact metasomatism of dolomite by magmatic fluids (at <550°C), or of silicic rocks by serpentinite-derived fluids (~100° to ~400°C) in ophiolites at moderate to low pressure (<2 kbar?). Jadeite is much rarer and forms only in subduction-related serpentinites along major fault zones at 200°–400°C and at high pressure (>5–6 kbar). Thus, most jade deposits record events at convergent plate margins that involve fluid interactions in and around serpentinitizing peridotite. RAH

**Micro-analytical study of the optical properties of rainbow and sheen obsidians.** C. Ma, J. Gresh, G. R. Rossman, G. C. Ulmer, and E. P. Vicenzi, *Canadian Mineralogist*, Vol. 39, 2001, pp. 57–71.

Samples of Mexican obsidian that exhibit “sheen” or “rainbow” optical properties were studied by a combination of micro-analytical (e.g., scanning electron microscope) and microscopic (e.g., thin-section) techniques to explain the cause of these phenomena.

The sheen (single color, usually a velvety “silver” or “gold”) is attributed to the presence of gas- and glass-filled flow-aligned areas in the obsidian. These areas have different chemical (e.g., lower SiO<sub>2</sub>) and optical (e.g., lower refractive index) properties compared to the matrix. The difference in R.I. (by as much as 0.04) leads to optical interference, hence sheen, along the interfaces between the two glasses.

There are two types of rainbow obsidian, so-called because of the bands of various colors ranging from red through purple. Both are trachytic, in that they have sub-parallel elongate crystallites in the groundmass. One type contains rods of hedenbergite (a clinopyroxene), and the other has rods of feldspar. The two types are mutually exclusive; they do not occur together. The matrix glasses of the two types have nearly identical and uniform refractive indices and composition, so the rainbow effect is not attributed to these parameters. However, the differences in R.I. between the matrix and the crystallites in both types of rainbow obsidian result in the scattering of white light. Thus, the arrays of crystallites—and in particular their sizes and shapes—serve to produce a thin-film interference, which is the preferred explanation for the rainbow effect. AAL

**Origin of gem corundums from basaltic fields.** F. L. Sutherland and D. Schwarz, *Australian Gemmologist*, Vol. 21, No. 1, 2001, pp. 30–33.

Gem corundum is widely formed as xenocrysts in basaltic rocks; that is, the crystals form deep in the earth and are “picked up” from that environment by the basaltic magma that carries them to the surface. Such corundum

has been recorded from six continental regions, within 15 countries, involving some 40 main basalt fields—which this article tabulates, along with their ages of eruption. Two corundum suites are differentiated: (1) blue, green, and yellow color-zoned “magmatic” sapphires that are thought to have formed by igneous crystallization in the earth’s crust or mantle; and (2) variously colored “metamorphic” sapphires and rubies from deep-seated metamorphic source rocks. Magmatic suites (which make up 60% of the basaltic sapphires) dominate over mixed magmatic/metamorphic suites (25%) and metamorphic suites (15%). Zircon found in the same deposits yield U–Pb isotope formation ages that are presumed to be the ages of sapphire crystallization. These ages are usually close to those determined for the associated basalts. RAH

**Production and colour changing treatment of Chinese cultured pearl.** L. Li, *Singaporean Gemologist*, Vol. 8, No. 1, 2001, pp. 11–14.

Recently, Chinese pearl farmers and dealers have been experimenting with various aspects of cultured pearl production, not just the shape of the final product and the material used for nuclei (e.g., wax, aluminum), but also color manipulation. There are two fundamental types of color treatment: dyeing and gamma-ray irradiation. Also mentioned is a new “lasering” technique, which produces dark “peacock” green and purple colors.

A short description of methods for detecting dye treatment is provided. These include: (1) color distribution (e.g., color patches on the surface, or concentration of color in and near the drill hole); (2) fluorescence (treated-colored samples typically show anomalous fluorescence or are inert); (3) Raman spectrometry (the presence of specific weak peaks); and (4) chemical testing (alcohol/acetone removes some dyes). Irradiation may turn the cultured pearls green, black, “silver,” dark red, or “bronze.” It may also increase the sample’s susceptibility to fracturing just below the surface and around the drill hole. A slight decrease in S.G. and hardness may also occur in irradiated freshwater cultured pearls. JS

**Raman spectra of nacre from shells of main pearl-culturing mollusk in China.** G. Zhang, X. Xie, and Y. Wang, *Spectroscopy and Spectral Analysis*, Vol. 21, No. 2, 2001, pp. 193–196 [in Chinese with English abstract].

Cultured pearls in China are grown using four types of mollusks: *Pinctada martensii*, *Pinctada maxima*, and *Pteria penguin* (saltwater); and *Hyriopsis cumingi* (freshwater). Aragonite is the main mineral component of the nacre (mother-of-pearl) in shells from all four mollusks. Raman spectrometry was used to study the organic components in nacre from each mollusk.

The Raman bands related to organic components were different in the nacre from each species. Organic material was not observed in the nacre of *Pinctada max-*

*ima*. Two bands resulting from a carotenoid were clearly identified in the nacre of *Pinctada martensii* and *Hyriopsis cumingi*, and the number of C=C double bonds in the molecular structure of this carotenoid was predicated to be 10 based on the position of the Raman bands. A number of complicated Raman bands were observed in the nacre of *Pteria penguin*; these bands are possibly caused by metalloporphyrin compounds. There is a close relationship between the color of the nacre and the relative concentrations of carotenoid and inferred metalloporphyrin compounds in the nacre layers. TL

## DIAMONDS

**Diamants [Diamonds].** *Le Règne Minéral*, No. 38, 2001, 66 pp. [in French, with some English abstracts].

The fabulous diamond exhibition at the Muséum National d'Histoire Naturelle in Paris (March 10–July 31, 2001) inspired the French mineral collector's magazine *Le Règne Minéral* to dedicate a special issue to this gem in cooperation with the creators of the exhibition.

The first article, "Le diamant, l'orchidée du règne minéral," by R. De Ascensão Guedes, surveys the mineralogical properties of diamond and shows why diamonds hold a unique position in the mineral kingdom. The focus lies on crystal structures and forms, which are illustrated by several diagrams as well as crystal drawings from Dana (1871), Goldschmidt (1911), and others.

Next, "Naissance et voyages du diamant" (R. de Ascensão Guedes and J.-C. Goujou) describes diamond geology: the structure of the earth's interior, conditions and processes of diamond formation, transport to the surface, and types of diamond deposits. This article also includes a comprehensive listing, with short descriptions, of diamond deposits worldwide.

In "Le diamant et ses paradoxes," J.-C. Goujou describes the paradoxical nature of the diamond world. This article contrasts graphite vs. diamond, the cubic crystal system vs. diamond's variety of forms, and old diamonds vs. young host rocks, but it is mostly concerned with the contrast between diamond as the paragon of riches and luxury vs. the poverty and sociopolitical problems in many mining areas. The result is a description of the mining histories and present-day situations in Angola, Democratic Republic of Congo (formerly Zaire), Guinea, Liberia, and Sierra Leone.

Three more articles (B. Cairncross—"Les diamants d'Afrique du Sud, du Botswana et de Namibie"; G. B. Webb and F. L. Sutherland—"Les gisements diamantifères Australiens"; J. Cassedanne—"Le diamant au Brésil") present detailed descriptions of some important African, Australian, and Brazilian diamond deposits.

The final article, "Contrebande de diamants: affaire Schreiber, Dakar" (J. E. Dietrich), tells the story of 18,000 carats of rough diamonds that were seized as contraband at Dakar's Yoff Airport in 1956, but had to be returned to their owner in spite of the obvious crime—an episode used by Ian Fleming in his book *The Diamond Smugglers*.

The issue is well illustrated, with many fine color photographs of diamonds and diamond mining. RT

**Diamond from the Guaniamo area, Venezuela.** F. V. Kaminsky, O. D. Zakharchenko, W. L. Griffin, D. M. DeR. Channer, and G. K. Khachatryan-Blinova, *Canadian Mineralogist*, Vol. 38, 2000, pp. 1347–1370.

The Guaniamo region is an important placer diamond mining area in Venezuela—an estimated 25–30 million carats may have been produced since 1968—but the diamonds have never been studied scientifically. This comprehensive report, based on more than 5,000 diamond crystals and fragments from placer and kimberlite sill deposits, characterizes the diamonds in terms of morphology, abundance and aggregation state of nitrogen, mineral inclusions, and carbon isotopic composition.

About 50% of the crystals were resorbed dodecahedra; octahedra were the next most abundant form. Most of the diamonds were colorless, but 55%–90% showed some radiation-induced areas of pigmentation. About 20% of the diamonds had very low nitrogen contents (<250 ppm; type II); the remainder belonged to the transitional type IaAB, with B>A. The mineral inclusions in 86% of the samples (77 were studied) had eclogitic affinity represented by garnet, omphacite, rutile, ilmenite, and pyrrhotite. Inclusions of peridotitic affinity were represented by garnet, chromian spinel, and olivine. Values of  $\delta^{13}\text{C}$  ranged from  $-3.2\text{‰}$  to  $-28.7\text{‰}$ , but most of the diamonds were isotopically light ( $\delta^{13}\text{C}$  less than  $-10\text{‰}$ ), which is also typical of an eclogitic origin. The high proportion of diamonds with eclogitic characteristics, and several features of the mineral inclusions, show striking parallels to diamonds from the Argyle mine in Australia. Both deposits occur in cratons that have had extensive Proterozoic tectonothermal activity. The authors believe that the Guaniamo placer diamond deposits are of local origin and were derived from the kimberlite sills rather than having been recycled from the ancient Roraima sediments in the area, as has been previously suggested. AAL

**Diamonds from Myanmar and Thailand: Characteristics and possible origins.** W. L. Griffin, T. T. Win, R. Davies, P. Wathanakul, A. Andrew, I. Metcalfe, and P. Cartigny, *Economic Geology*, Vol. 96, No. 1, 2001, pp. 159–170.

Alluvial diamonds (262 samples) from two localities in Myanmar (Theindaw and Momeik) and one in Thailand (Phuket), for which there are no obvious rocks in the area that might serve as the primary source, were studied in order to determine their origin. This detailed investigation found similarities in the physical features of the diamonds from both countries—that is, their color (mostly yellow through brown), morphology (mostly rounded and resorbed), and surface features (lamination lines reflecting plastic deformation). The inclusions (e.g., olivine, chromite, pyrope) are primarily of peridotitic origin.



Carbon isotope values ( $\delta^{13}\text{C}$  mostly between  $-3\%$  and  $-8\%$ ) are also consistent with a peridotitic origin. Nitrogen aggregation studies indicate a long residence and/or deformation at mantle temperatures; the association of the diamonds with a corrosive magma is evidenced by their resorbed shapes. Extensive abrasion and abundant brown spots due to radiation damage suggest appreciable surface transport.

These alluvial diamonds (as well as others in Sumatra, Indonesia, which were not studied) are found in the Sibumasu geological terrane, which is believed to have separated from the ancient Gondwana supercontinent in Early Permian time (about 275 million years ago). At the time, Gondwana also included Australia. The diamonds are also closely associated with certain glacial-marine sediments of slightly younger age that came from western Australia. Hence, it is suggested that these Southeast Asian diamonds were derived from primary kimberlite sources in northwestern Australia, or within the Sibumasu terrane itself. However, the predominantly peridotitic nature of both the inclusions and the carbon isotope data rule out the Argyle lamproite as the primary source because of its eclogitic paragenesis. AAL

**Irradiation-induced structure development in type Ia diamond.** T. D. Ositinskaya, V. N. Tkach, and G. P. Bogatyreva, *Journal of Superhard Materials*, Vol. 22, No. 1, 2000, pp. 56–60.

Four types of diamonds (natural type Ia, type IaA, and type IaA/B, and synthetic type IIa) were subjected to set doses of intense electron irradiation. Cathodoluminescence (CL) spectroscopy revealed three distinct zones in the irradiated type Ia diamond. The zone 1 spectrum was characterized by peaks at 389 and 575 nm; it strongly resembled the spectrum derived from the irradiated synthetic type IIa diamond. The spectrum of zone 2 was most similar to that of the irradiated type IaA/B diamond, which contains a less intense peak at 575 nm along with peaks at 415, 484.5, and 490.7 nm. Zone 3 was characterized by peaks at 484.5, 490.7, and 511.5 nm, as well as three prominent peaks at 415, 430, and 439 nm that were not observed in other spectra. The most prominent peaks in the irradiated type IaA diamond were at 484.5, 490.7, 503.5, and 575 nm. These observations indicate that CL spectroscopy may be useful for studying the genesis of irradiation-induced defects in mixed diamond types. Troy Blodgett

## GEM LOCALITIES

**Brazilian gem provinces.** C. P. Pinto and A. C. Pedrosa-Soares, *Australian Gemmologist*, Vol. 21, No. 1, 2001, pp. 12–16.

The principal Brazilian colored gems are aquamarine, alexandrite, emerald, tourmaline, topaz, amethyst, agate, and opal. The main deposits are related to pegmatites

and pneumatolitic-hydrothermal fluids in mafic-ultramafic rocks, hydrothermal fluids in metasediments, and volcanogenic concentrations in continental basalt flows. The main pegmatitic provinces are situated in Neoproterozoic mobile belts affected by intense granitic intrusion and mineralization. The Be-bearing gems (aquamarine, beryl, chrysoberyl, and alexandrite) are mainly related to these granitic intrusions, which are 500–520 million years old. Gem-quality tourmaline occurs in pegmatites that are related to S-type granites (derived from the partial melting of sedimentary rocks). Emerald occurs in ultramafic schist in the vicinity of granitic bodies. The quartz-family gems are related to hydrothermal veins in quartzose rocks, or are found as druses in Mesozoic basalt flows. RAH

**Clinopyroxene–corundum assemblages from alkali basalt and alluvium, eastern Thailand: Constraints on the origin of Thai rubies.** C. Sutthirat, S. Saminpanya, G. T. R. Droop, C. M. B. Henderson, and D. A. C. Manning, *Mineralogical Magazine*, Vol. 65, No. 2, 2001, pp. 277–295.

A clinopyroxene xenocryst with an inclusion of ruby, found in alkali basalt from the Late Cenozoic Chanthaburi-Trat volcanic rocks of eastern Thailand, was chemically similar to clinopyroxene inclusions in rubies from nearby alluvial gem deposits. This suggests a common origin for both minerals. The clinopyroxene is fairly sodic, highly aluminous, and magnesian; sapphirine and garnet also occur as inclusions in the alluvial rubies. Thermodynamic calculations constrain the temperature of clinopyroxene + corundum crystallization to between  $800^\circ$  and  $1150^\circ\text{C} \pm 100^\circ\text{C}$ . Other equilibria indicate a pressure of crystallization of 10–25 kbar, implying depths of formation between 35 and 88 km. The rubies are presumed to have crystallized in rocks of mafic composition (i.e., garnet clinopyroxenites or garnet pyroclastics) within the upper mantle. RAH

**Einmalige Tropfsteinbildungen aus Argentinien: Rhodochrosit-Stalaktiten [Unique stalactite formations: Rhodochrosite from Argentina].** W. Lieber, *Lapis*, Vol. 25, No. 11, 2000, pp. 13–20 [in German].

This lavishly illustrated article describes the well-known Capillitas deposits near Andalgalá, Catamarca Province, Argentina, where rhodochrosite occurs as stalactites more than 5 m (16 feet) long and up to 50 cm (20 inches) in diameter. The growth conditions of rhodochrosite are compared to those of “normal” calcite/aragonite stalactites. Chemical data are presented for the different bands or layers of rhodochrosite. The stalactites formed at  $150^\circ$ – $200^\circ\text{C}$  (whereas calcite stalactites develop below  $25^\circ\text{C}$ ). Contrary to the commonly held belief that the stalactites formed within the last 700 years, the authors suggest that they are actually 50,000–500,000 years old. RT

**The geology of Australian opal deposits.** I. J. Townsend, *Australian Gemmologist*, Vol. 21, No. 1, 2001, pp. 34–37.

Australian opal is mainly hosted in Cretaceous sedimentary rocks of the Great Artesian Basin. Silica, derived from weathering, forms micro-spheres that are deposited in a regular array. Most opaline silica is common opal, or potch, and does not show a play of color. Opal is often found associated with lineaments or faults, which provide passageways for the movement of groundwater; these have proved useful in locating opal at Lightning Ridge in New South Wales. A climate of alternating wet and dry periods is important in creating a rising and falling water table; the silica is deposited when it is concentrated in solution by a receding water table, forming opal in a variety of host materials. RAH

**The geology, mineralogy and rare element geochemistry of the gem deposits of Sri Lanka.** C. B. Dissanayake, R. Chandrajith, and H. J. Tobschall, *Bulletin of the Geological Society of Finland*, Vol. 72, No. 1–2, 2000, pp. 5–20.

Nearly all the gem-bearing formations of Sri Lanka are located in the central high-grade metamorphic terrain of the Highland Complex. The gem deposits are classified as sedimentary, igneous, and metamorphic, but sedimentary deposits are dominant. The most important gems include corundum, chrysoberyl, beryl, spinel, topaz, zircon, tourmaline, garnet, and sphene.

Analysis of trace elements in sediments from three gem fields (Ratnapura, Elahera, and Walawe Ganga) revealed that some of these sediments are considerably enriched in certain elements compared to their average crustal abundances. Sediments from Walawe Ganga are anomalously enriched in the high-field-strength and associated elements, particularly Zr, Hf, W, and Ti. This is attributed to the presence of accessory zircon, monazite, and rutile in the heavy-mineral fraction, which may constitute up to 50% (by weight) of the sediment. The geochemical enrichment of some trace elements is taken to indicate that highly differentiated granites and associated pegmatites provided the source material for these sedimentary deposits. RAH

**Oriented inclusions in spinels from Madagascar.** K. Schmetzer, E. Gübelin, H.-J. Bernhardt, and L. Kiefert, *Journal of Gemmology*, Vol. 27, No. 4, 2000, pp. 229–232.

Lamellar and needle-like inclusions found in six faceted bluish gray spinels (0.15 to 0.50 ct) from southern Madagascar are described. The samples were purchased two years prior to the discovery (in 1998) of the deposits at Ilakaka; their exact origin is unknown. Chemical analyses were performed on the inclusions in three samples, and Raman spectra were obtained from several included crystals in two samples. These data established that the lamel-

lar inclusions are enstatite,  $MgSiO_3$ . The inclusions are oriented parallel to dodecahedral {110} directions in the host spinels. According to the authors, enstatite in this oriented relationship within spinel has not been previously reported. The gemological properties of the samples were normal for spinel, and the UV-Vis absorption spectra were typical for spinels containing iron. WMM

**Tourmaline and aquamarine deposits from Brazil.** J. César-Mendes, H. Jort-Evangelista, and R. Wegner, *Australian Gemmologist*, Vol. 21, No. 1, 2001, pp. 3–6.

Brazil is one of the world's largest producers of gem-quality aquamarine and tourmaline, which are found in granitic pegmatites both in the Oriental Province (>500 gem pegmatites) in the states of Minas Gerais, Bahia, and Espírito Santo, and in the Northeastern Province (>50 gem pegmatites) in the states of Ceará, Paraíba, and Rio Grande do Norte. Aquamarine occurs in pegmatites that have undergone only slight geochemical differentiation; it is associated with mica, K-feldspar, and quartz. Tourmaline (green, blue, and pink-red, but always rich in the elbaite component) occurs mainly in rare-element-bearing pegmatites with lepidolite, albite, tantalite, and morganite; it varies in composition depending on its position within the pegmatite. RAH

## INSTRUMENTS AND TECHNIQUES

**Nuclear microscopic studies of inclusions in natural and synthetic emeralds.** K. N. Yu, S. M. Tang, and T. S. Tay, *X-Ray Spectrometry*, Vol. 29, No. 2, 2000, pp. 178–186.

Micro-proton-induced X-ray emission (micro-PIXE) spectra were obtained from 56 natural emeralds from Colombia, Pakistan, Zambia, Brazil, and 26 synthetic emeralds from eight manufacturers using flux and hydrothermal growth techniques. These spectra were used to study mineral and other types of inclusions (such as flux residues) as well as chemical variations that could be correlated to color zoning.

Five flux-grown synthetic emeralds (Chatham) and one hydrothermal (Lechleitner) sample yielded nearly featureless spectral data; such was not the case for the natural stones. Color zoning in the natural emeralds correlated to concentrations of Cr, V, and Fe, although in one Colombian sample the concentration of Fe did not fit this pattern. Chlorine was detected in both the natural and hydrothermal synthetic emeralds. Previous work has suggested a correlation between Cr and Cl in synthetic emeralds, possibly due to the use of  $CrCl_3 \cdot 6H_2O$  to supply Cr as a coloring agent, but this association was not observed in this study. Mineral inclusions of calcite, dolomite, chromite, magnetite, pyrite, and several types of mica and feldspar were identified in the natural emeralds. The asso-

ciation of the minerals sphalerite or wurtzite (both ZnS) with pyrite in Zambian emeralds is presented as a new discovery. The authors conclude that the (non-destructive) micro-PIXE method has great potential for studying emeralds. Further cataloging of chemical and inclusion features for natural stones from known localities, as well as for synthetic emeralds grown by various methods, could allow the identification of provenance or growth method with this technique in the future. JL

**PIXE/PIGE characterisation of emeralds using an external micro-beam.** T. Calligaro, J.-C. Dran, J.-P. Poirot, G. Querré, J. Salomon, and J. C. Zwaan, *Nuclear Instruments and Methods in Physics Research B*, Vol. 161–163, 2000, pp. 769–774.

An improved method of PIXE/PIGE (proton-induced X-ray/Gamma-ray emission) was employed to examine a suite of reference emeralds from 12 countries to characterize provenance characteristics based on chemistry, and then use that database in the examination of one piece each of Gallo-Roman (3rd century AD) and Visigothic (7th century AD) emerald jewelry. A micro-beam feature of the instrumentation allowed the emeralds to be analyzed while still mounted in the jewelry.

Hellenistic and Roman writings suggest that emerald sources at that time existed in what are now Egypt, Afghanistan, and Russia's Ural Mountains. The emeralds in the ancient jewelry examined here have chemical compositions comparable to samples analyzed from Austria and Egypt. The authors advocate further research to expand the database, and the usefulness of this method as a nondestructive tool in gemological investigations is noted. JL

**Precious precision.** *Mazal U'Bracha*, Vol. 16, No. 131, March 2001, pp. 52–53.

A high-tech Israeli company (Bental Industries Ltd.) is manufacturing an innovative cutting machine, the Crown Jewel Diamond Spindle. A variable speed, 2.7 horsepower motor operates at 900–5,000 RPM and requires no special electrical capabilities. It has an instant-response, programmable speed controller with digital display. The great advantage of this equipment is that it allows the diamond cutter to change from polishing to brushing (i.e., final finishing) instantaneously as the machine switches to a different speed. Previously, such a change would be a time-consuming process or the cutter would have to use a different machine that runs at a slower speed. AAL

**Presidium Moissanite Tester™.** T. Linton and K. Hunter, *Australian Gemmologist*, Vol. 20, No. 11, 2000, pp. 483–485.

The Presidium Moissanite Tester senses the small forward-leakage of current (based on the electrical property of capacitance) in synthetic moissanite, which is a semiconductor. Other synthetic moissanite detectors current-

ly on the market are based on "breakdown voltage," the voltage that overcomes resistance to an insulator causing current to flow.

In the authors' evaluation, the instrument detected all synthetic moissanite specimens, reporting them as a bright red window display accompanied by an audible "beep." Stones other than synthetic moissanite, including diamond, illuminated the green "TEST" lamp. False (positive) synthetic moissanite readings were recorded in several circumstances, such as when the tip of the probe touched metal (including metal mounts on the instrument case) and when a P-type semiconductor (germanium transistor) was tested. An industrial-quality black diamond that was electrically conductive also gave a synthetic moissanite response. However, the overall evaluation of the Presidium Moissanite Tester was very favorable. MT

**What's new in gem testing instruments: The Brewster-Angle Meter.** T. Linton, K. Hunter, A. Cumming, N. Masson, and G. Pearson, *Australian Gemmologist*, Vol. 20, No. 10, 2000, pp. 428–431.

Brewster's Law states that when an incident monochromatic ray is reflected from a smooth, non-metallic surface (e.g., a gemstone), and the angle between the reflected and refracted rays in the specimen is 90°, then the reflected ray will be polarized in the plane of the reflecting surface. The angle of incidence of the monochromatic ray (Brewster's angle) required to achieve the polarization of the reflected ray, however, will vary with the index of refraction of the reflecting substance. Specifically, the tangent of Brewster's angle is equal to the R.I. of the reflecting substance. The Brewster-Angle Meter measures Brewster's angle, so that the R.I. of the gemstone can be calculated.

The instrument, which weighs 1.49 kg, is equipped with a miniature 670 nm laser (the monochromatic source) and a filter to determine the maximum polarization of the reflected ray; it is powered by two AA batteries. Gems with Brewster's angles ranging from 55° to 73° can be measured (read from a scale on an outside drum) and then converted (see mathematical relationship above) to refractive indices within the broad range of 1.43–3.30. This instrument does not require toxic optical contact liquids, as do critical-angle refractometers. The greatest potential of this highly rated instrument is for use with both unset and set gemstones (although jewelry with claws that protrude above the surface cannot be tested), as well as synthetics and imitations, that have R.I. values greater than 1.81 and, therefore, are beyond the capability of the standard refractometer. MT

## JEWELRY RETAILING

**Pearls: Branding.** *Jewellery New Asia*, No. 203, July 2001, pp. 74–83 passim.

This collage of brief articles focuses on three branding campaigns for cultured pearls: by Mikimoto, Perle Utopia,

and Golay. Mikimoto, a name known worldwide, has developed a new approach to bring "fashion to jewelry." Working with well-known designers such as Vera Wang, Mikimoto is expanding its image as a creator of classic jewelry to a purveyor of fashion-forward jewelry. In the future, the Mikimoto image may even include the use of cultured pearls directly on high-fashion clothing or the creation of clothing lines to match their cultured pearl jewelry.

The second article in the section reviews the building of brand identity through recognizable designs. Gemindustria Gaia Ferrando SpA markets jewelry by its own designers under the Perle Utopia brand. Gaia also works with other well-known jewelry designers, such as the Spanish firm Carrera y Carrera and New York's Henry Dunay. This unique jewelry is sold under the designer's name with acknowledgment that the cultured pearls are from Perle Utopia, strengthening consumer awareness of the brand. The third article discusses how Golay, while not intending to create a brand, has been promoting a recognizable "quality label" on strands of cultured pearls, with consumers responding positively.

JEM-S

**Successful strategies for selling pearls.** V. Gomelsky, *National Jeweler*, Vol. 45, No. 7, April 1, 2001, pp. 52, 54–55.

Promotions, whether in-store or in the community, are a proven strategy for retailers to boost their sales of cultured pearls. These events require significant planning, which includes everything from collecting inventory from suppliers to recruiting speakers for presentations. One successful approach is for retailers to appeal to their customers' desire for exclusivity by explaining the rarity of large, lustrous, round cultured pearls that are blemish-free, and the time-consuming effort involved in assembling strands of fine cultured pearls. The Cultured Pearl Information Center recommends that retailers start planning their promotions well in advance of an event. Their guidelines are:

- Three months prior: Develop the concept.
- Two months prior: Find suppliers and begin to organize marketing materials, which may include newspaper ads, public relations campaigns, invitations, and radio spots.
- One month to three weeks prior: Start running ads, send out invitations, and make catering arrangements.
- Two weeks to one week prior: Educate the staff about the event, make follow-up phone calls to invite guests, and prepare store decorations.
- Two to three weeks following the event: Maintain contact with clients who attended the promotion.

When properly executed, promotions are an excellent means of educating clients, as well as establishing and cultivating relationships that keep them coming back.

MT

## PRECIOUS METALS

**Cookson Precious Metals launches new gold alloy.**

*Jewellery in Britain [JIB]*, Vol. 5, January 2000, p. 5.

Enduragold is a new alloy developed by Cookson Precious Metals that reportedly offers better strength, hardness, wearability, and consistency of color than equivalent gold alloys. It has tested successfully in the production of gate-bracelets, torque bangles, hooped earrings, Creole earrings, lockets, pendants, wedding rings, set rings, chains, and findings. Cookson believes the properties of their product will benefit manufacturers through enhanced performance, fewer returns, and higher customer satisfaction. Working with this metal is different from working with the usual gold alloys, mainly in the order of production. Therefore, manufacturers will need to consult Cookson for details of the manufacturing process. Enduragold is available in 9K, 10K, 14K, and 18K yellow, and 9K white. The chemical composition of the alloy was not divulged.

PT

**A stable blue silver is developed.** *Jewellery News Asia*, No. 201, May 2001, p. 36.

Silver jewelry can be changed from white through different colors to black by means of a chemical dipping process that causes oxidation. The key to the color change is the duration of the oxidation process. Sunny Pang has developed a new technique that enables the oxidation time to be extended up to 40 minutes with special (unspecified) chemicals. Extending the time allows certain colors to stabilize and become permanent; for example, it takes 10–15 minutes to turn white silver into blue silver. Brown, charcoal gray, and black have also been achieved by the new method. Since oxidation is a surface treatment, and the resultant color can be worn or scratched off, the technique is best applied to jewelry such as earrings or pendants. Mr. Pang has also achieved different colors with 14K gold-silver alloy electroformed and electroplated jewelry.

PT

## SYNTHETICS AND SIMULANTS

**Characterization of a new Chinese hydrothermally grown**

**emerald.** Z. Chen, J. Zeng, K. Cai, C. Zhang, and W. Zhou, *Australian Gemmologist*, Vol. 21, No. 2, 2001, pp. 62–66.

The examination of five crystals of a new Chinese hydrothermal synthetic emerald produced in Guilin (Guangxi Province) is reported. These crystals, which have a slightly bluish green color, showed a strong red reaction to the Chelsea filter and a moderate red fluorescence to long-wave UV radiation. Electron-microprobe analyses recorded much lower chlorine (0.06–0.25 wt.% Cl) and higher alkali (1.09–1.30 wt.% Na<sub>2</sub>O) contents than in other synthetic emeralds. Refractive indices are reported as  $n_e = 1.569$ – $1.571$  and  $n_o = 1.572$ – $1.578$ , and specific gravity as ranging from 2.68 to 2.73. Two-phase (liquid-vapor) inclusions were noted. The infrared spectra of these crystals in the 3500–3800 cm<sup>-1</sup> region showed only a single peak at 3701

cm<sup>-1</sup>, but in the 5000–5500 cm<sup>-1</sup> region there were three strong peaks, which is characteristic of synthetic emeralds (natural emeralds show only two). RAH

**Synthesis of yttria-stabilized zirconia crystals by skull-melting method.** W.-S. Kim, I.-H. Suh, Y.-M. You, J.-H. Lee, and C.-H. Lee, *Neues Jahrbuch für Mineralogie, Monatshefte*, No. 3, 2001, pp. 136–144.

Of the three known zirconium oxide (ZrO<sub>2</sub>) polymorphs, the cubic form is the only one of interest to gemologists because of its widespread use as a diamond simulant. Crystals large enough for gem purposes are best produced by the skull-melting method. Cubic zirconia (CZ) is stable at room temperature only if at least 7 mol.% yttria (Y<sub>2</sub>O<sub>3</sub>) is added during the growth process, but this amount does not result in gem-quality material.

The authors carried out several CZ growth experiments and studied the physical properties of the resulting crystals. To obtain gem-quality, transparent colorless crystals, the addition of 25 wt.% Y<sub>2</sub>O<sub>3</sub> is necessary for stabilization, as well as 0.04 wt.% Nd<sub>2</sub>O<sub>3</sub> to remove the yellow color. The authors also performed X-ray powder diffraction analyses and a single-crystal neutron diffraction analysis to refine the crystal structure of yttria-stabilized CZ. The Y stabilizer atoms randomly occupy the Zr sites, resulting in displacement of oxygen atoms from their ideal positions in the crystal structure. RT

## TREATMENTS

**Are treatments killing the romance of gems?** S. Robertson, *Jewelers' Circular Keystone*, Vol. 171, No. 6, June 2000, pp. 238–240, 242, 244.

Certain treatments (enhancements) are well accepted in the industry and by the public—for example, the heat treatment of tanzanite to develop its blue color, and the oiling of emeralds to enhance their apparent clarity. Yet today many colored stones and cultured pearls in the marketplace have been treated in some way, often to a greater extent than most people (including jewelers) realize. Bicolored (blue and red) corundum from Mong Hsu (Myanmar) may be heated twice, first to make the stone entirely red and a second time to fill fractures, so that it can subsequently be sold as “fine ruby.” Akoya cultured pearls may be bleached, dyed, and waxed to produce brightness and overtones seldom found in nature.

Modern treatments raise the important ethical and legal question of how one defines “too much treatment,” and what the obligations are with regard to disclosure. There is still no agreement on what constitutes excessive treatment, and there is a tendency to disclose only what is visible at 10× magnification. Yet many significant enhancements (e.g., the residues of fluxes or glasses in partially healed or open fractures) may be visible only with higher magnification. Therefore, meaningful disclosure cannot be based on magnification alone, and the use of some arbitrary magnification only heightens the pub-

lic's suspicion. The use of excessive treatments and the absence of full disclosure have reached the point that the future of the colored stone industry is threatened. AMB

**Treated and synthetic gem materials.** J. E. Shigley, *Current Science*, Vol. 79, No. 11, 2000, pp. 1566–1571.

Both treated and synthetic gems are encountered frequently in today's jewelry marketplace. In some cases, the appearance and gemological properties of these materials correspond closely to those of valuable natural gems. This often results in identification difficulties for jewelers, especially those who lack modern gemological training and/or advanced testing equipment. This article reviews the major treated and synthetic gems, as well as the methods (both standard and advanced) for their identification.

The history and techniques of gem synthesis are outlined. A table of major synthetics (diamond, beryl, chrysoberyl, corundum, opal, and quartz) differentiates between melt and solution methods of synthesis. How these synthetic gems are produced in the laboratory is explained. The routine treatment of some natural gems, such as topaz and aquamarine, is mentioned.

The author differentiates between the more common commercial synthetics, such as those produced by flame fusion, and so-called “luxury” synthetics, such as the more expensive hydrothermal- and flux-grown rubies and sapphires. An underlying theme is that even with advanced testing methods, the accurate identification of some of the treated and synthetic gems on the market today can be difficult. Modern technology will likely produce new treatments and synthetics, thus requiring ongoing development of gem testing methods and identification criteria. LT

**High-pressure, high-temperature treatment of natural diamonds and their recognition from the point of view of two patent registrations by General Electric.** K. Schmetzer, *Goldschmiede Zeitung*, Vol. 99, July 2001, p. 75 [in German; English translation at [www.gz-online.com](http://www.gz-online.com)].

The use of high-pressure, high-temperature (HPHT) conditions for changing the color of natural, normally brown diamonds has been well documented over the past two years. However, detection of these color-altered diamonds remains problematic. Recent publication of disclosure documents submitted by General Electric in support of two in-process international patent registrations may provide additional insight into this controversial subject.

One document (WO01/14050A1, published March 1, 2001) describes the HPHT treatment of brown and other poorly colored diamonds. According to Dr. Schmetzer, the proposed method is parallel to one described in patent documentation submitted in the late 1970s by General Electric for desaturating the yellow color of synthetic or natural type Ib diamonds. The current document details the HPHT transformation of natural brown type Ia diamonds to a yellowish green to greenish yellow hue.

A second document (WO01/33203A1, published May 10, 2001) illustrates a method for detecting HPHT-treated diamonds based on photoluminescence criteria. The fundamental premise: Absence of the 490.7 nm photoluminescence line—generally present in natural type I and type II diamonds—indicates a 95% probability of HPHT treatment. While other articles cited by Dr. Schmetzer indicate a similar approach to HPHT detection, he also refers to at least one study that raises some questions about the reliability of the 95% accuracy claim in this patent document. SW

## MISCELLANEOUS

**American Watch Guild makes time for excellence.** W. G. Shuster, *Jewelers' Circular Keystone*, Vol. 171, No. 11, November 2000, pp. 176–177.

Using the American Gem Society and its ethical principles as a model, a group of authorized retailers of fine watches have banded together to form a modern-day guild. The new American Watch Guild (AWG, headquartered in Hewlett, New York) will bring together authorized retailers, service providers, and manufacturers of timepieces who are committed to excellence in both sales and service. Members can be identified by means of AWG decals and plaques. The guild is making itself known through exhibitions of fine timepieces, charitable activities, and a scholarship fund.

The need for such a guild stems from marketing practices that are unacceptable to ethical, professionally trained jewelers. Such practices include: gray marketing (sales by unauthorized dealers), transshipping (sales by authorized dealers to unauthorized vendors), counterfeiting, and the proliferation of Internet vendors who sell genuine timepieces without authorization. AAL

**America's largest parking lot.** C. Wolinsky, *National Geographic*, Vol. 199, No. 1, January 2001, pp. 124–128.

The population of Quartzsite, Arizona swells from 2,300 year-round residents to more than a million at its winter peak in January. Although this article concentrates on the flea-market atmosphere of mid-winter Quartzsite, gem and mineral people know it as the show that precedes Tucson, and unusual lapidary material is likely to appear there first. Just don't expect many amenities—Quartzsite is mostly a dry-camping location, with many visitors staying in recreational vehicles. Mary L. Johnson

**The De Beers story: A new cut on an old monopoly.** N. Stein, *Fortune*, Vol. 143, No. 4, February 19, 2001, pp. 186–206 passim.

This article reviews the recent history of De Beers and examines its future in the 21st century diamond market based on an inside view of the company and visits to mining operations in southern Africa. Early on the author expresses his concern about the motives for the company's

recent business moves and poses the question: Why would a company voluntarily give up control of the world diamond supply after 100 years, move to a new open world market of diamonds, and develop a "Supplier of Choice" strategy?

It becomes clear that De Beers had little choice but to rethink the way it was doing business to thrive in the future. During the 1990s, De Beers saw its market share of world rough diamond sales fall from 85% to 65% and its stockpile of rough diamonds increase to US\$5 billion. This was due to three major factors: the collapse of the Soviet Union in 1991, Argyle's termination of its contract with De Beers in 1996, and the rise of new diamond producers—especially Canada. All these entities sell at least a major portion of their diamonds outside the cartel. Further, the investment community voiced its concern as De Beers's stock plummeted to \$12/share in the late 1990s. Hence, a new strategy was necessary that would work in a significantly more competitive market.

A cornerstone of the new De Beers is the development of brand names such as "Forevermark" to stimulate consumer demand. The new plan creates the "Supplier of Choice" category of sightholder who is able to build strong brands independently or by teaming up with other companies. Hence, the new breed of sightholders will be fewer in number than in the past, but they will be the financially strongest manufacturer with the best retail marketing skills. "The cartel of many will be transformed into an equally powerful cartel of the few." The article reminds the reader that for this plan to succeed, De Beers must allay the fears of antitrust regulators in the U.S. and abroad. PY

**Tahiti sets up pearl ministry.** *Jewellery News Asia*, No. 200, April 2001, pp. 1, 44.

The French Polynesian government has created a ministry devoted entirely to cultured pearls. Initial goals of this ministry will be to:

1. Revise the existing industry classification chart so that the rejects category will be expanded.
2. Set up a standard for nacre thickness to prevent immature or thinly coated cultured pearls from reaching the market.
3. Ensure that customs controls will prevent inferior-quality cultured pearls from leaving the country.

These measures, aimed at boosting wholesale prices and consumer confidence, were announced amid the negative publicity generated by the influx of low-quality Tahitian cultured pearls in the world market. The creation of the ministry has been well received by Tahiti's pearl culturing industry. In fact, the industry had been requesting government intervention to help secure the long-term future of pearl farming in the area. The President of French Polynesia, Gaston Flosse, will serve as the head of the new ministry. JEM-S